Am J Transl Res 2017;9(10):4652-4672
www.ajtr.org /ISSN:1943-8141/AJTR0058983

Original Article

Bardoxolone methyl (CDDO-Me or RTA402) induces cell cycle arrest, apoptosis and autophagy via PI3K/Akt/mTOR and p38 MAPK/Erk1/2 signaling pathways in K562 cells

Xin-Yu Wang[1,2,3*], Xue-Hong Zhang[3,4*], Li Peng[2], Zheng Liu[5], Yin-Xue Yang[6], Zhi-Xu He[7], Hong-Wan Dang[1,2*], Shu-Feng Zhou[3,8]

[1]Institute of Clinical Pharmacology, General Hospital of Ningxia Medical University, Yinchuan, Ningxia Hui Autonomous Region, China; [2]Department of Pharmacy, General Hospital of Ningxia Medical University, Yinchuan, Ningxia Hui Autonomous Region, China; [3]Department of Pharmaceutical Sciences, College of Pharmacy, University of South Florida, Tampa, FL, USA; [4]Department of Pediatrics, General Hospital of Ningxia Medical University, Yinchuan, Ningxia Hui Autonomous Region, China; [5]Department of Neurosurgery, General Hospital of Ningxia Medical University, Yinchuan, Ningxia Hui Autonomous Region, China; [6]Department of Colorectal Surgery, General Hospital, Ningxia Medical University, Yinchuan, Ningxia Hui Autonomous Region, China; [7]Guizhou Provincial Key Laboratory for Regenerative Medicine, Stem Cell and Tissue Engineering Research Center & Sino-US Joint Laboratory for Medical Sciences, Guizhou Medical University, Guiyang, Guizhou, China; [8]Department of Bioengineering and Biotechnology, College of Chemical Engineering, Huaqiao University, Xiamen, Fujian 361021, China. [*]Equal contributors.

Received June 7, 2017; Accepted September 14, 2017; Epub October 15, 2017; Published October 30, 2017

Abstract: Chronic myeloid leukemia (CML) treatment remains a challenge due to drug resistance and severe side effect, rendering the need on the development of novel therapeutics. CDDO-Me (Bardoxolone methyl), a potent Nrf2 activator and NF-κB inhibitor, is a promising candidate for cancer treatment including leukemia. However, the underlying mechanism for CDDO-Me in CML treatment is unclear. This study aimed to evaluate the molecular interactome of CDDO-Me in K562 cells using the quantitative proteomics approach stable-isotope labeling by amino acids in cell culture (SILAC) and explore the underlying mechanisms using cell-based functional assays. A total of 1,555 proteins responded to CDDO-Me exposure, including FANCI, SRPK2, XPO5, HP1BP3, NELFCD, Na^+,K^+-ATPase 1, etc. in K562 cells. A total of 246 signaling pathways and 25 networks regulating cell survival and death, cellular function and maintenance, energy production, protein synthesis, response to oxidative stress, and nucleic acid metabolism were involved. Our verification experiments confirmed that CDDO-Me down-regulated Na^+,K^+-ATPase α1 in K562 cells, and significantly arrested cells in G_2/M and S phases, accompanied by remarkable alterations in the expression of key cell cycle regulators. CDDO-Me caused mitochondria-, death receptor-dependent and ER stress-mediated apoptosis in K562 cells, also induced autophagy with the suppression of PI3K/Akt/mTOR signaling pathway. p38 MAPK/Erk1/2 signaling pathways contributed to both apoptosis- and autophagy-inducing effects of CDDO-Me in K562 cells. Taken together, these data demonstrate that CDDO-Me is a potential anti-cancer agent that targets cell cycle, apoptosis, and autophagy in the treatment of CML.

Keywords: Chronic myeloid leukemia, CDDO-Me/Bardoxolone methyl, K562 cells, SILAC, cell cycle, apoptosis, autophagy, Na^+,K^+-ATPase α1

Introduction

Chronic myeloid leukemia (CML) is one of a group of diseases called chronic myeloproliferative disorders that also include chronic granulocytic leukemia, myelofibrosis/osteomyelosclerosis, polycythemia vera, and idiopathic thrombocythemia [1, 2]. These diseases have overlapping clinical and molecular features, characterized by the unrestrained expansion of pluripotent hematopoietic stem cells. With a low incidence of 0.6 to 2 cases per 100,000

adults, CML accounts for ~15% of all newly diagnosed cases of leukemia in adults [3, 4]. The estimated number of new cases of CML is 8950 (representing 0.5% of all new cancer cases and 13.8% of all new leukemia cases) and there would be 1080 deaths due to CML in the United States (US) in 2017 (https://seer.cancer.gov/statfacts/html/cmyl.html). More than 95% of CML patients have a distinctive and characteristic cytogenetic abnormality, the Philadelphia chromosome (Ph^+) arising from the translocation t(9;22)(q34;q11.2) which involves the *ABL1* gene in chromosome 9 and the *BCR* gene in chromosome 22, resulting in a fused *BCR-ABL* gene encoding the constitutively active BCR-ABL of p210 or sometimes p185 that is necessary and sufficient for initiating CML [5-8]. The BCR-ABL transcript is continuously active with no dependence on other cellular signaling proteins. In turn, BCR-ABL activates a cascade of critical proteins controlling the cell cycle and accelerates cell division and proliferation. BCR-ABL also inhibits DNA repair, resulting in genomic instability and making the cell more susceptible to developing further genetic abnormalities [5-7]. With more understanding of the nature of BCR-ABL as the pathologic basis of CML and its action as an overactive tyrosine kinase, targeted biological therapies that specifically inhibit the activity of BCR-ABL have been developed in the past 20 years [9-12]. These tyrosine kinase inhibitors (TKIs) can induce complete remissions in CML and change the clinical course of CML. The first of these TKIs was imatinib mesylate (trade names: Gleevec and Glivec), which was approved by the US Food and Drug Administration (FDA) in 2001, and has been considered the standard of care for more than a decade. Imatinib inhibited the progression of 65-75% of CML patients, but approximately 20-30% patients developed resistance and/or intolerance to imatinib [13]. To overcome drug resistance and to increase clinical response, second generation TKIs targeting BCR-ABL and other oncogenic tyrosine kinases have been developed. The first, dasatinib, a more potent inhibitor of BCR-ABL, was approved in 2007 by the US FDA to treat CML patients who were either resistant to or intolerant of imatinib. Nilotinib and dasatinib were then approved by the FDA for first-line therapy of Ph^+ CML in 2010. Both dasatinib and nilotinib are highly effective in newly diagnosed CML patients as well as those who fail imatinib. In 2012, radotinib was approved in South Korea only for use in CML patients resistant to or intolerant of imatinib. Another second generation TKI, bosutinib, received FDA approval in 2012 for the treatment of adult patients with Ph^+ CML with resistance, or intolerance to prior therapy [14]. Second generation TKIs have been demonstrated to induce better and faster clinical responses compared to imatinib and are highly effective in patients resistant to and/or intolerant to imatinib and are extremely active against all the resistant BCR-ABL1 mutations, with the exception of T3151 [14]. However, no survival advantage has been seen in CML patients [11, 13]. Ponatinib is a third generation TKI, which causes response in both early and advanced phases of CML and those bearing any resistant mutations, specifically T315I [15]. The successful implementation of above TKIs for the treatment of CML remains a flagship for molecularly targeted therapy in cancer. However, some patients still did not respond to these TKIs due to primary or secondary resistance to such therapy and some patients developed severe adverse effects [12, 16]. Although mutations in the *BCR-ABL* gene have proven to be the most prominent mechanism of resistance to TKIs, other mechanisms dependent on BCR-ABL activity or supporting oncogenic properties of the leukemic cells independent of BCR-ABL signaling have been documented [17]. Clearly, there is a strong need to develop more efficacious and safer drugs for CML therapy when all TKI fail for the treatment.

Oleanolic acid is naturally occurring triterpenoids that have been used in traditional medicine for centuries, showing antioxidant, antibacterial, antifungal, anticancer, and antiinflammatory activities [18]. To further improve their pharmacological efficacy, a series of novel derivatives have been synthesized, such as 2-cyano-3,12-dioxooleana-1,9(11)-dien-28-oic acid (CDDO), CDDO-imidazolide (CDDO-Im), the methyl amide of CDDO (CDDO-Ma), and CDDO methyl ester (CDDO-Me, also named as bardoxolone methyl, RTA402, TP-155 and NSC713200) (**Figure 1A**) [19]. These synthetic triterpenoids are potent inhibitors of the *de novo* synthesis of inflammatory enzymes such as inducible nitric oxide synthase (iNOS) and inducible cyclooxygenase 2 (COX-2) [20]. CDDO-Me is a promising candidate for prevention and treat-

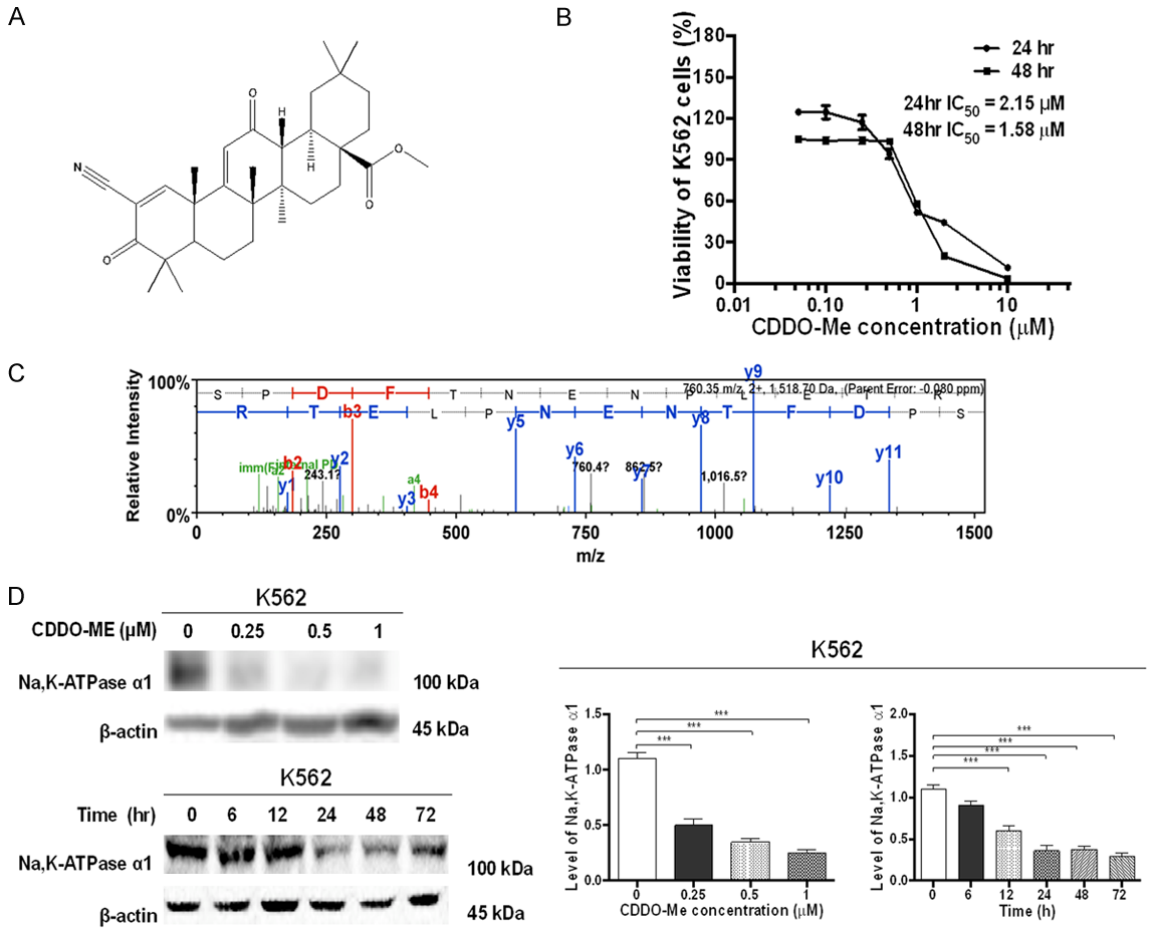

Figure 1. Cytotoxicity of CDDO-Me on K562 cells and the regulating effect on Na^+,K^+-ATPase α1 expression. A. The chemical structure of CDDO-Me. B. Viability of K562 cells as examined by the MTT assay. C. Mass spectrum of Na^+,K^+-ATPase α1 quantified and identified by the SILAC-based proteomics assay. D. Representative blots and bar graphs showing the level of Na^+,K^+-ATPase α1, when cells were treated with CDDO-Me at 0.25, 0.5, and 1 μM for 24 h or 0.5 μM for 72 h, then the protein samples were subject to Western blot assay. Data are expression as mean ± SD of three independent experiments. $^{***}P<0.005$ by one-way ANOVA.

ment of cancer, which protects cells from oxidative stress at nanomolar concentrations, whereas exhibits cytotoxicity against various cancer cells at micromolar concentrations [21, 22]. CDDO-Me is more potent than CDDO in anticancer and cancer-preventive activities and in the activation of Kelch-like erythroid cell-derived protein with CNC homology-associated protein 1/nuclear factor (erythroid-derived 2)-like 2/antioxidant response element (Keap1/Nrf2/ARE) pathway [23, 24], which is involved in cytoprotection in the presence of excessive electrophiles or oxidative stress. Binding of CDDO-Me to Keap1 disrupts its critical cysteine residues, leading to the release of Nrf2, which hinders its ubiquitination and finally leads to stabilization and nuclear translocation of NF-κB. In the nucleus, Nrf2 activates the transcription of phase 2 response genes, leading to a coordinated antioxidant and anti-inflammatory response [24]. As a potent Nrf2 activator and NF-κB inhibitor, the therapeutic effects of CDDO-Me has been tested in Phase III for chronic kidney disease [25]. The antitumor effect of CDDO-Me has been demonstrated in different cancers by inhibition of proliferation and induction of apoptosis [26]. Moreover, preclinical studies have shown that CDDO-Me induced tumor regression in xenografted-mouse models [27-29]. It was evaluated in a few Phase I clinical trials for advanced solid tumor or lymphoid malignancy and showed good tolerance [30, 31]. Notably, Samudio et al. [32] reported that CDDO-Me induced cytotoxicity in

imatinib-resistant CML cells. However, the underlying mechanisms of the anticancer effects of CDDO-Me in the treatment of CML are not fully understood.

Mass spectrometry-based proteomics is increasingly applied in a quantitative formatto investigate changes in protein abundances in biological samples, often based on labeling of samples with stable isotopes that are introduced chemically or metabolically. Stable-isotope labeling by amino acids in cell culture (SILAC) is a powerful and increasingly popular approach for quantitative proteomics studies [33-36]. In the SILAC method, two cell populations are cultured in the presence of heavy or light amino acids (typically lysine and/or arginine), one of them is subject to a perturbation (e.g. drug exposure), and then both are combined, processed, and analyzed. Incorporation of the "heavy" amino acid occurs through cell growth, protein synthesis, and turnover. SILAC allows "light" and "heavy" proteomes to be distinguished by mass spectrometry while avoiding any chemical derivatization and associated purification. SILAC can be applied to systemically assess global protein profile, evaluate the target network of drugs, estimate drug toxicity, and find new biomarkers for the diagnosis and treatment of cancers [35, 37, 38]. In this study, we evaluated the SILAC-based proteomic response of human CML K562 cells to CDDO-Me exposure and examined its effects on cell proliferation, cell cycle distribution, apoptosis, and autophagy in K562 cells.

Materials and methods

Chemicals and reagents

CDDO-Me (purity >98%) and JC-1 mitochondrial membrane potential assay kit were obtained from Cayman Chemical Inc. (Ann Arbor, MI, USA). MK-2206 was purchased from Selleckchem Inc. (Houston, TX, USA). SB202190, Alexa Fluor 488-conjugated secondary antibodies, 6-diamidino-2-phenylindole (DAPI) and Dulbecco's modified Eagle's medium (DMEM)/F12 (1:1) were bought from Invitrogen Inc. (Carlsbad, CA, USA). $^{13}C_6{}^{15}N_4$-L-arginine, L-arginine, $^{13}C_6$-L-lysine, L-lysine, DMEM/F12 for the SILAC study, 4-(2-hydroxyethyl) piperazine-1-ethanesulfonic acid (HEPES), ethylenediaminetetraacetic acid (EDTA), ribonuclease (RNase A), propidium iodide (PI), dimethyl sulfoxide (DMSO), fetal bovine serum (FBS), dialyzed FBS, Dulbecco's phosphate buffered saline (PBS), and 2-(4,5-dimethylthiazol-2-yl)-2,5-diphenyltetrazolium bromide (MTT) were sourced from Sigma-Aldrich Inc. (St Louis, MO, USA). The annexin V: phycoerythrin (PE) apoptosis detection kit was obtained from BD Biosciences Inc. (San Jose, CA, USA). The Cyto-ID® Autophagy detection kit was bought from Enzo Life Sciences Inc. (Farmingdale, NY, USA). The caspase-3 colorimetric assay kit was purchased from R&D Systems Inc. (Minneapolis, MN, USA). The FASP™ protein digestion kit was obtained from Protein Discovery Inc. (Knoxville, TN, USA). The Pierce™ bicinchoninic acid (BCA) protein assay kit, radioimmunoprecipitation assay buffer (RIPA), skim milk and Western blotting substrate were obtained from Thermo Fisher Scientific Inc. (Hudson, NH, USA). The polyvinylidene difluoride (PVDF) membrane was purchased from Bio-Rad Inc. (Hercules, CA, USA). U0126 and primary antibody against human β-actin were obtained from Santa Cruz Biotechnology Inc. (Dallas, TX, USA). The rest of antibodies for signaling proteins related to cell cycle, apoptosis, and autophagy were all sourced from Cell Signaling Technology Inc. (Beverly, MA, USA).

Cell line and cell culture

The human chronic myeloid leukemia K562 cell line was obtained from American Type Culture Collection (Manassas, VA, USA) and cells were cultured in DMEM/F12 medium supplemented with 10% heat-inactivated FBS at 37°C in a 5% CO_2/95% air humidified incubator. CDDO-Me was dissolved in DMSO as stock solution of 50 mM. The stock solution was freshly diluted with culture medium at a final concentration of 0.05% DMSO (v/v). The control cells were treated with 0.05% DMSO only.

Cell viability

The effect of CDDO-Me on cell viability of K562 cells was examined using the MTT assay. Briefly, K562 cells were seeded in 96-well culture plates at a density of 9×10^3 cells/well overnight, then treated with CDDO-Me at concentrations ranging from 0.05 to 10 μM for 24 or 48 h. Ten mL of MTT solution (5 mg/mL) was added into each well for another 4 h incubation. Then the solution was aspirated and 100 mL of DMSO was added into each well. After shaking

for 10 min, the absorbance of the plate was measured at wavelengths of 560 nm (MTT formazan) and 670 nm (background) using a Synergy™ H4 Hybrid microplate reader (BioTek, Winooski, VT, USA). The half maximal inhibitory concentration (IC_{50}) value was calculated using the relative viability over CDDO-Me concentration curve by GraphPad Prism 6.0 (GraphPad Software Inc., La Jolla, CA, USA).

Quantitative proteomics

A SILAC-based approach was used to identify the molecular targets of CDDO-Me in K562 cells as previously described [39, 40]. In brief, K562 cells were cultured in DMEM/F12 medium (for SILAC) with (heavy) or without (light) stable isotope labeled amino acids ($^{13}C_6$ L-lysine and $^{13}C_6{}^{15}N_4$ L-arginine) and 10% dialyzed FBS. After treatment with 0.5 μM CDDO-Me for 24 h, cellular proteins were collected for the subsequent digestion and desalting. Five mL of the peptide mixtures in 0.1% formic acid were subject to hybrid linear ion trap-Orbitrap (LTQ Orbitrap XL, Thermo Scientific Inc., Hudson, NH, USA) for liquid chromatography-tandem mass spectrometry (LC-MS/MS) analysis. The peptide SILAC ratio was calculated using MaxQuant version 1.2.0.13 (Max Planck Institute of Biochemistry, Munich, Germany). And the proteins were identified using Scaffold 4.3.2. The pathway was analyzed using ingenuity pathway analysis (IPA, www.ingenuity.com) from QIAGEN Inc. (Redwood City, CA, USA).

Determination of cell cycle distribution

The effect of CDDO-Me on the cell cycle distribution of K562 cells was determined by flow cytometry as previously described [41]. After treatment with CDDO-Me at concentrations of 0.25, 0.5, and 1 μM for 24 h, K562 cells were harvested, washed by PBS and fixed in 70% ethanol at -20°C overnight. Then, the cells were resuspended in 1 mL PBS containing 1 mg/mL RNase A and 50 μg/mL PI in dark at room temperature for 30 min. A total number of 1×10^4 cells were subject to cell cycle analysis using a flow cytometer with CellQuest™ software (Becton Dickinson Immunocytometry Systems, San Jose, CA, USA).

Determination of cellular apoptosis

The effect of CDDO-Me on the apoptosis of K562 cells was evaluated using the annexin V:PE apoptosis detection kit as previously described [21, 41]. In short, the cells were collected after CDDO-Me treatment at different concentrations over 24 h, or evaluated for different time intervals, and resuspended and incubated in 100 μL 1 × binding buffer containing 5 mL annexin V:PE and 5 μL 7-amino-actinomycin D (7-AAD) in the dark at room temperature for 15 min. The number of apoptotic cells was analyzed by flow cytometer (Becton Dickinson Immunocytometry Systems, San Jose, CA, USA) within 1 h.

Determination of caspase 3 activity

Caspase 3 activity was determined using the caspase 3 colorimetric assay kit following the manufacturer's instructions. Briefly, K562 cells were harvested and lysed on ice for 1 h. Cell lysates were placed in 96-well plates and then 100 mL reaction buffer (containing DTT) was added. The plates were incubated at 37°C for 1 h and the caspase activity was determined using a Synergy™ H4 Hybrid microplatereader (BioTek Inc.) at 380 nm (excitation wavelength) and 440 nm (emission wavelength).

Immunofluorescence

For the immunofluorescence assay, cells were fixed with fresh 4% formaldehyde in PBS for 10 min at room temperature, and subsequently penetrated with 0.25% Triton X-100 for 5 min and blocked with 5% BSA for 30 min. The samples were incubated with primary antibodies (1:500 dilution) at 4°C overnight. Then the cells were incubated for 1 h with the Alexa Fluor 488 goat anti-rabbit secondary antibodies (1:500 dilution) conjugated to FITC and stained with DAPI. Finally, the specimens were analyzed with a TCS SP2 laser scanning confocal microscope (Leica, Wetzlar, Germany).

Mitochondrial membrane potential ($\Delta\psi_m$) changes in apoptosis

The mitochondrial membrane potential changes in apoptosis of K562 cells induced by CDDO-Me treatment was assayed using JC-1 following the manufacturer's instructions. JC-1 exists either as a green fluorescent monomer at depolarized membrane potential with low $\Delta\psi_m$ or as a red fluorescent J-aggregate at hyperpolarized membrane potential with high $\Delta\psi_m$. Briefly, K562 cells were cultured in 6-well plate. After

Table 1. Top 5 network functions regulated by CDDO-Me in K562 cells

ID	Associated network functions	Score
1	RNA post-transcriptional modification, protein synthesis, & cancer	55
2	Protein synthesis, gene expression, & RNA post-transcriptional modification	49
3	RNA post-transcriptional modification, cell morphology, & cellular assembly and organization	44
4	Connective Tissue disorders, developmental disorder, & hereditary disorder	44
5	Gene expression, protein synthesis, & amino acid metabolism	43

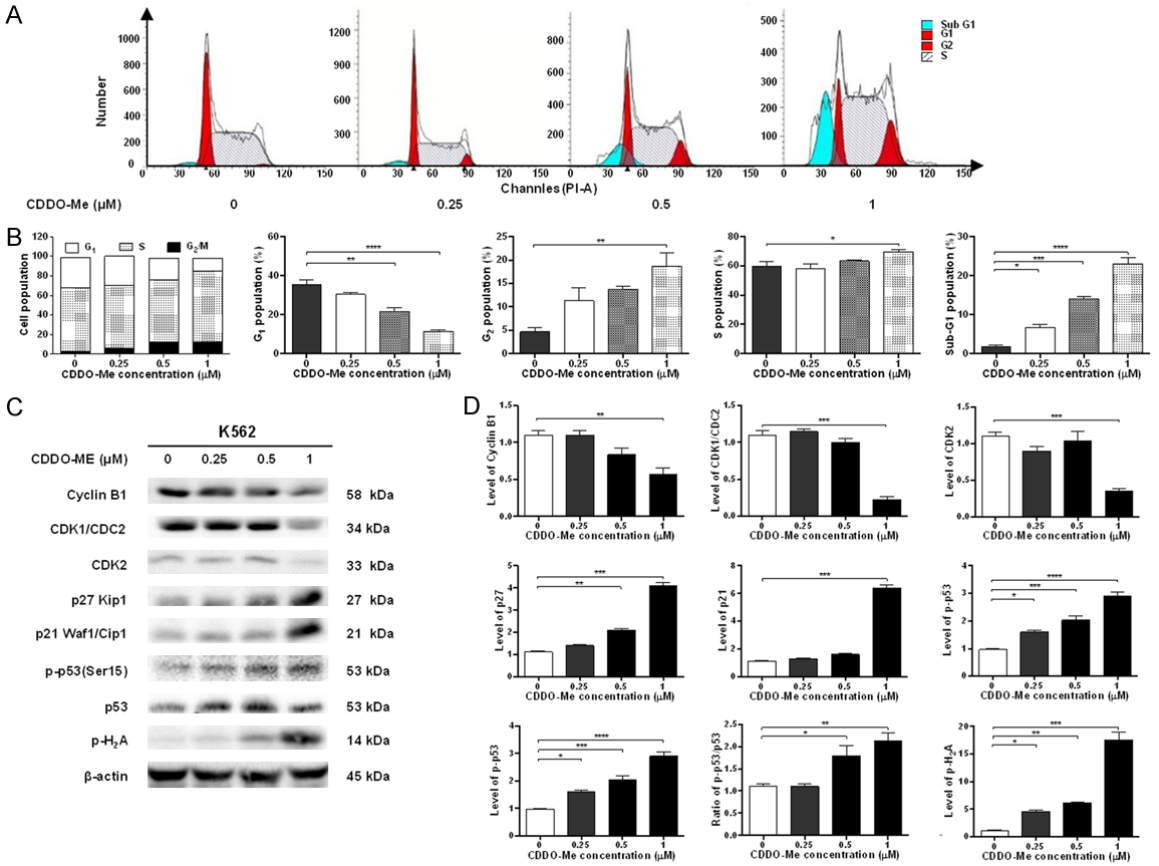

Figure 2. CDDO-Me induces cell cycle arrest in G_2/M and S phases and modulates key cell cycle regulators in K562 cells. The cells were incubated with CDDO-Me at 0.25, 0.5, and 1 μM for 24 h. (A) The flow cytometric histograms showing the cell cycle arresting effect of CDDO-Me in K562 cells. (B) Bar graphs showing a concentration-dependent cell cycle arresting effect of CDDO-Me in K562 cells. (C) Representative blots and (D) bar graphs showing the expression of cyclin B1, CDK1/CDC2, CDK2, p27 Kip1, p21 Waf1/Cip1, p-p53 (Ser15), p53, p-H2A and β-actin. Data are expression as mean ± SD of three independent experiments. $^{*}P<0.05$, $^{**}P<0.01$, $^{***}P<0.005$, and $^{****}P<0.001$ by one-way ANOVA.

CDDO-Me treatment, cells were loaded with culture medium containing 10 μmol/L JC-1 for 20 min at 37°C. The fluorescence was analyzed using a TCS SP2 laser scanning confocal microscope. Healthy cells with mainly JC-1 J-aggregates can be detected with fluorescence settings designed to detect rhodamine (excitation/emission = 540/570 nm). Apoptotic cells with mainly JC-1 monomers can be detected with settings designed to detect FITC (excitation/emission = 488/535 nm).

Determination of cellular autophagy

The effect of CDDO-Me on the autophagy of K562 cells was detected by flow cytometry as previously described [21, 41]. In brief, cells were collected after CDDO-Me treatment at dif-

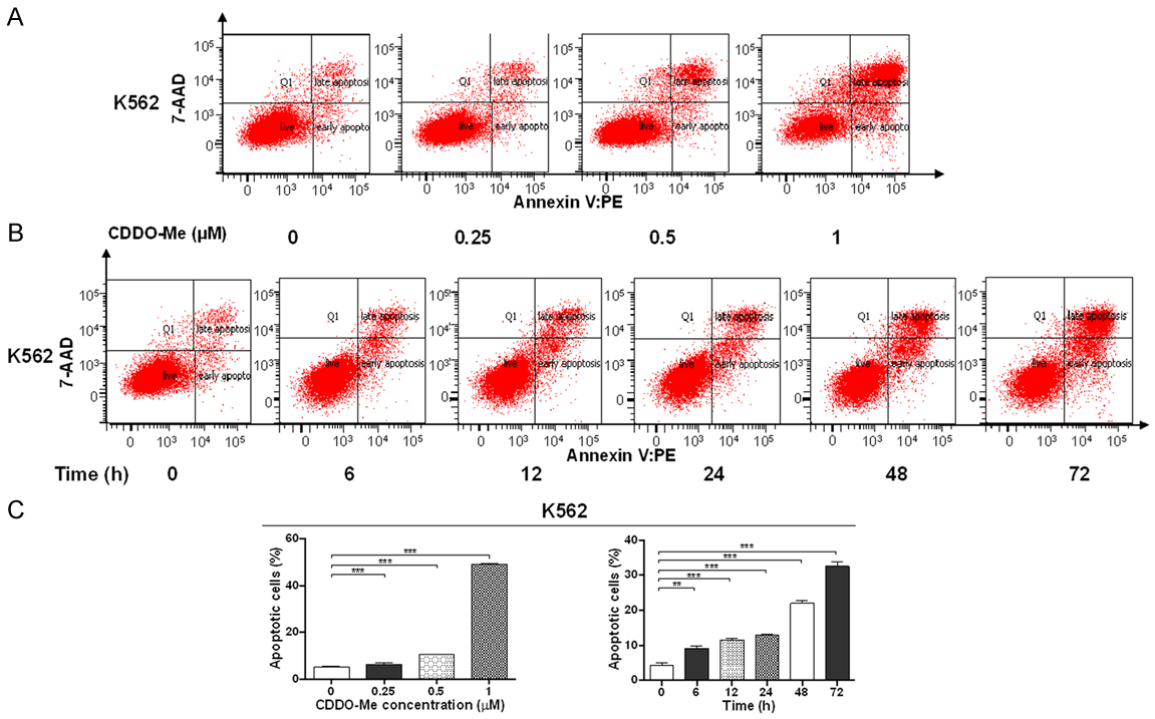

Figure 3. CDDO-Me induces apoptosis in K562 cells. A. Representative flow cytometric plots of apoptotic K562 cells when treated with CDDO-Me at 0.25, 0.5, and 1 μM for 24 h. B. Representative flow cytometric plots of apoptotic K562 cells when treated with CDDO-Me at 0.5 μM over 72 h. C. Bar graphs showing the percentage of apoptotic cells when treated with CDDO-Me at 0.25, 0.5, and 1 μM for 24 h, or 0.5 μM over 72 h. Data are expression as mean ± SD of three independent experiments. $^{**}P<0.01$, and $^{***}P<0.005$ by one-way ANOVA.

ferent conditions and resuspended in 250 mL of assay buffer containing 5% FBS. Following with the addition of 250 mL of the diluted Cyto-ID® Green stain solution, cells were incubated at room temperature in the dark for 20 min, then cells were collected and washed with 1 × assay buffer. The percentage of autophagy cells was analyzed using the green (FL1) channel of a flow cytometer (Becton Dickinson Immunocytometry Systems, San Jose, CA, USA).

Western blotting assay

The expression levels of targeted proteins were determined using Western blotting assay. Protein samples were collected in the RIPA buffer (50 mmol HEPES at pH 7.5, 150 mmol NaCl, 10% glycerol, 1.5 mmol $MgCl_2$, 1% Triton-X 100, 1 mmol EDTA at pH 8.0, 10 mmol sodium pyrophosphate, 10 mmol sodium fluoride) containing the protease inhibitor and phosphatase inhibitor cocktails, and centrifuged at 3,000 × *g* for 10 min at 4°C. Nuclear and cytoplasmic protein were separated using NE-PER® Nuclear and Cytoplasmic Extraction Reagents as previously described [21, 41]. Protein concentrations were determined using the BCA assay and 20 μg samples were resolved by sodium dodecyl sulfate polyacrylamide gel electrophoresis (SDS-PAGE) sample loading buffer and electrophoresed on 7-12% SDS-PAGE mini-gel after thermal denaturation at 95°C for 5 min. Proteins were transferred onto PVDF membrane at 400 mA for 2 h at 4°C. Membranes were probed with indicated primary antibody overnight at 4°C and then blotted with respective secondary anti-mouse or anti-rabbit antibody. Visualization was performed using Bio-Rad ChemiDoc™ XRS system with an enhanced chemiluminescence kit. The blots were analyzed using Image Lab 3.0 (Bio-Rad) and the protein level was normalized to the matching densitometric value of β-actin or histone H3.

Statistical analysis

Data are presented as the mean ± standard deviation (SD). The comparisons of multiple groups were tested by one-way analysis of variance (ANOVA) followed by Tukey's multiple comparison procedure. $P<0.05$ was conside-

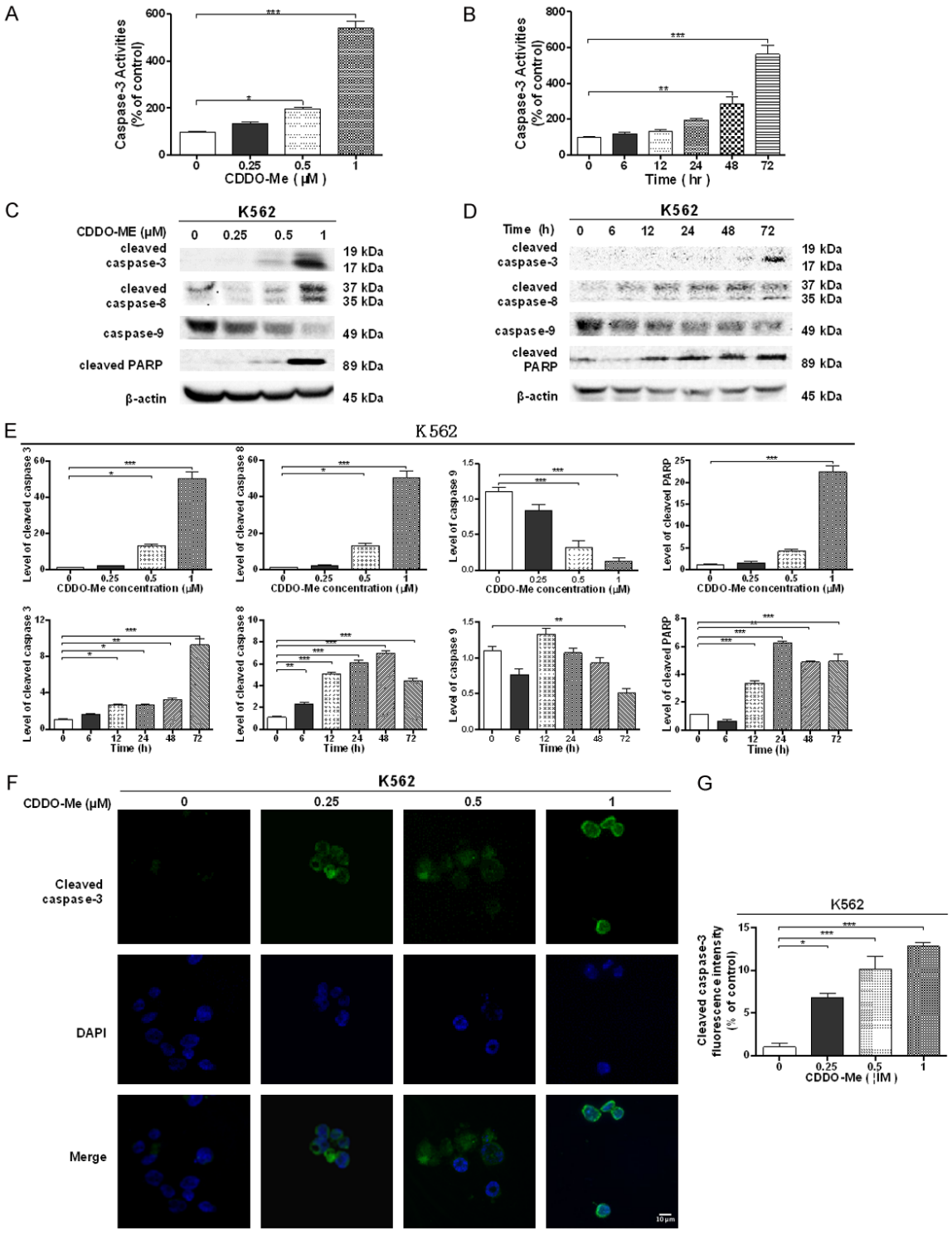

Figure 4. CDDO-Me induces caspases and PARP cleavage in K562 cells. (A) Activation of caspase 3 in K562 cells induced by CDDO-Me. Cells were treated with or without CDDO-Me at 0.25, 0.5, and 1 μM for 24 h. (B) The time course of activation of caspase 3 in K562 cells induced by CDDO-Me. Cells were treated with 0.5 μM CDDO-Me for various periods of time. (C) Representative blots of caspases and cleaved PARP, and K562 cells were incubated with CDDO-Me at different concentrations for 24 h. (D) Representative blots of caspases and cleaved PARP, and K562 cells were incubated with 0.5 μM CDDO-Me over 72 h. (E) Bar graphs showing the expression level of the proteins above mentioned. (F) Representative Immunofluorescence staining the expression levels of cleaved caspase 3. (G) Bar graph showing quantitation results from (F). Data are expression as mean ± SD of three independent experiments. $^{*}P<0.05$, $^{**}P<0.01$, and $^{***}P<0.005$ by one-way ANOVA.

red to be statistically significant. The experiments were performed at least three times independently.

Results

Proteomic response to CDDO-Me treatment in K562 cells

SILAC-based proteomics assay was firstly performed to examine proteomic responses to CDDO-Me treatment in K562 cells. A total number of 1,555 protein molecules was identified in response to CDDO-Me treatment, of which 657 proteins expression level were up-regulated and 898 ones were down-regulated (Table S1). These proteins include FANCI, SRPK2, XPO5, HP1BP3, NELFCD, TH1L, HMGA1, ZC3HC1, PCK2, SOD1, GSR, etc. Interestingly, we observed a reduction of Na^+,K^+-ATPase α1 expression.

Subsequently, the identified proteins were subject to the IPA analysis. The results showed that 246 signaling pathways (Table S2), and 25 networks of signaling pathways and cellular functions (Table S3 and **Table 1**) responded to CDDO-Me in K562 cells. The signaling pathways involved included G_1 and G_2 checkpoint regulation pathways, mTOR signaling pathway, PI3K/Akt signaling pathway, Erk/MAPK signaling pathway, Nrf2-mediated oxidative stress response pathway, unfolded protein response (UPR) pathway, mitochondrial dysfunction signaling pathway, and apoptosis signaling pathway. The networks involved have important roles in pathophysiological functions and the development of cancer, diabetes, Alzheimer's disease, and chronic inflammatory diseases (**Table 1**). In aggregate, the IPA results have demonstrated that CDDO-Me modulates various molecular proteins and signaling pathways, including cell cycle, response to oxidative stress, apoptosis, and autophagy, eventually, leading to cell proliferation inhibition and deathin K562 cells. To validate the proteomic results, we next investigated the effects of CDDO-Me on cell cycle distribution, apoptosis, and autophagy and the role of key signaling pathways.

CDDO-Me inhibits the proliferation of K562 cells

We evaluated the effect of CDDO-Me on the viability of K562 cells using the MTT assay. The cell viability was markedly decreased when exposed to CDDO-Me at concentrations from 0.05 to 10 μM (**Figure 1B**). The IC_{50} values were 2.15 and 1.58 μM for 24 and 48 h incubation with CDDO-Me, respectively. The results show that CDDO-Me significantly inhibits the proliferation of K562 cells.

CDDO-Me suppresses Na^+,K^+-ATPase α1 expression in K562 cells

Compelling evidence shows that Na^+,K^+-ATPase has a role in cancer development and is a potential target for cancer therapy [42]. As our proteomic data revealed the reduction of Na^+,K^+-ATPase α1 expression in response to CDDO-Me treatment (**Figure 1C**), we verified this effect using Western blotting assay. Consistently, CDDO-Me concentration- and time-dependently decreased Na^+,K^+-ATPase α1 expression level in K562 cells (P<0.005, **Figure 1D**). These results suggest that CDDO-Me may target Na^+,K^+-ATPase α1 to exhibit the cancer cell killing effect.

CDDO-Me induces K562 cell cycle arrest

Since the IPA pathway analysis results showed that CDDO-Me had effects on G_2/M and G_1/S checkpoint regulation (Table S2 and Figure S1), we examined the cell cycle distribution of K562 cells when treated with CDDO-Me at different concentrations. The data showed that CDDO-Me hampered cell cycle progression by arresting cells at G_2/M and S phases (**Figure 2A** and **2B**). When treated with CDDO-Me at 1 μM for 24 h, the percentage of K562 cells arrested at G_2 and S phases ascended from 4.7% to 18.7% (P<0.01) and 59.7% to 69.3% (P<0.05), respectively, with concomitant decrease in G_1 phase from 35.3% to 11.3% (P<0.001). In addition, CDDO-Me treatment markedly increased the number of sub-G_1 cells in a dose-dependent manner, which reflected the proportion of apoptotic cells in K562 cells.

Next, we further tested the effect of CDDO-Me on the expression levels of several key regulators in cell cycle checkpoints. As shown in **Figure 2C** and **2D**, compared with the control cells, there was a significant decrease in the expression of cyclin B1, CDK1/CDC2 and CDK2 when treated with 1 μM CDDO-Me for 24 h. In contrast, the level of p27 Kip1 was elevated 2.1- and 4.2-fold when cells were treated with

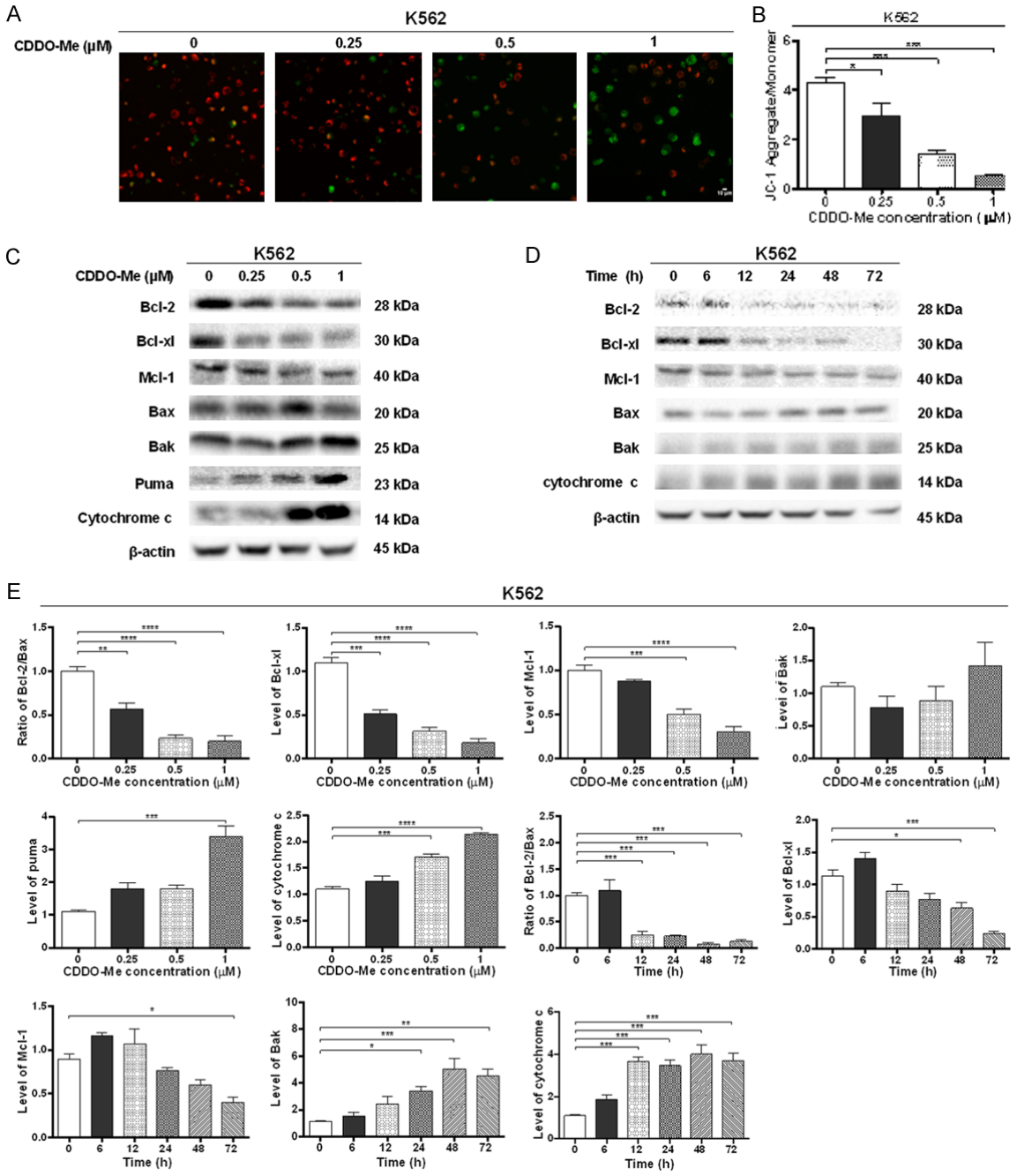

Figure 5. CDDO-Me induces mitochondrial dysfunction by regulating the expression of Bcl-2 family proteins in K562 cells. (A) Representative fluorescence microscopy images of K562 cells treated with 0.25, 0.5, and 1 μM CDDO-Me for 24 h, and stained with the JC-1 dye. (B) Bar graph showing quantitation results from (A). (C) Representative blots of Bax, Bak, Bcl-2, Bcl-xL, Mcl-1, and cytochrome C, when K562 cells were exposed to CDDO-Me at 0.25, 0.5, and 1 μM for 24 h. (D) Representative blots of caspases and cleaved PARP, and K562 cells were incubated with 0.5 μM CDDO-Me over 72 h. (E) Bar graphs showing the expression level of the proteins above mentioned. Data are expression as mean ± SD of three independent experiments. $^{*}P<0.05$, $^{**}P<0.01$, and $^{***}P<0.005$ by one-way ANOVA.

0.5 and 1 μM CDDO-Me for 24 h, respectively ($P<0.01$ or 0.005, **Figure 2C** and **2D**), and p21 Waf1/Cip1 level was up-regulated 6.7-fold when cells were exposed to 1 μM CDDO-Me ($P<0.005$, **Figure 2C** and **2D**). Moreover, there was a concentration-dependent increase in p-p53 (Ser15) and p53 levels, resulted in a 1.7-, 2.3-, and 2.6-fold increase in the ratio of p-p53 (Ser15)/p53 ($P<0.05$, **Figure 2C** and **2D**) with 0.25, 0.5, and 1 μM CDDO-Me for 24 h,

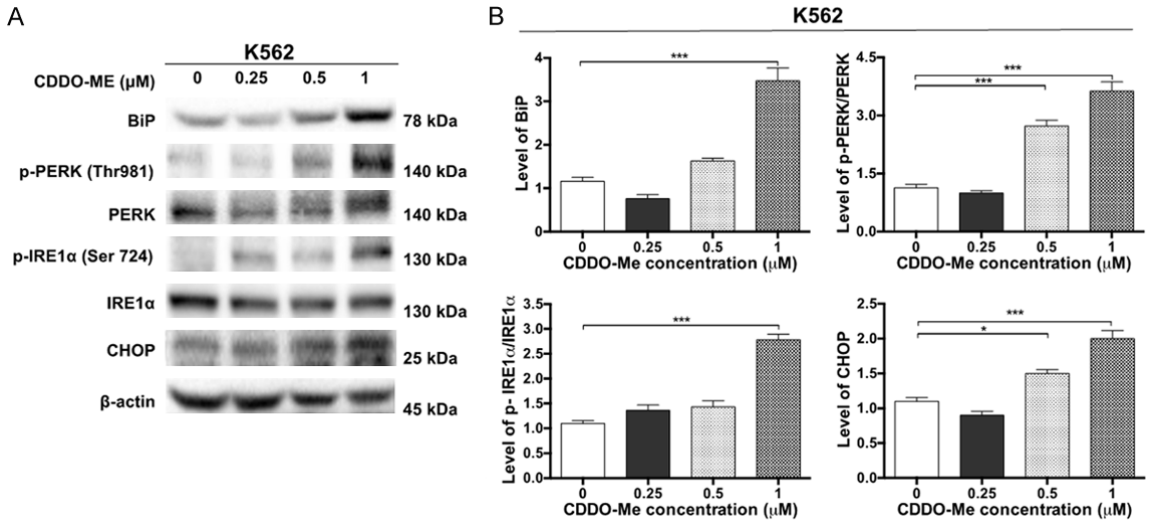

Figure 6. CDDO-Me induces UPR in K562 cells. K562 cells were treated with CDDO-Me at 0.25, 0.5, and 1 μM for 24 h. A. Representative blots of Bip, p-PERK, PERK, p-IRE1α, IRE1α, CHOP, and β-actin. B. Bar graphs showing the ratio of p-PERK/PERK and p-IRE1α/IRE1α, the expression of Bip and CHOP. Data are expression as mean ± SD of three independent experiments. $^{*}P<0.05$ and $^{***}P<0.005$ by one-way ANOVA.

respectively. Meanwhile, we detected level of p-H_2A, a DNA damage marker associated with G_2/M phase, was elevated with treatment of CDDO-Me in K562 cells (**Figure 2**). In aggregate, the results indicate that CDDO-Me alters the cell cycle distribution and induces G_2 and S phase arrest with DNA damage, contributing to its anticancer effect in K562 cells.

CDDO-Me induces apoptosis of K562 cells via both extrinsic and intrinsic pathways

After observation of a clear increase in the number of sub-G_1 cells, we next examined the effect of CDDO-Me on apoptosis of K562 cells. CDDO-Me concentration- and time-dependently induced apoptosis of K562 cells (**Figure 3**). Incubation of cells with 0.25, 0.5, and 1 μM CDDO-Me for 24 h, the percentage of apoptotic cells (early plus late apoptosis) up-regulated from 5.3% to 6.3%, 10.5%, and 49.1%, respectively ($P<0.005$, **Figure 3A** and **3C**). When cells were exposed to 0.5 μM CDDO-Me for 6, 12, 24, 48, and 72 h, the percentage of apoptotic cells elevated from 4.3% to 9.1%, 11.5%, 12.9%, 21.9% and 32.5%, respectively ($P<0.01$ or 0.005, **Figure 3B** and **3C**).

Following this, we further investigated the underlying mechanisms for the pro-apoptotic effect of CDDO-Me in K562 cells. Caspase 3 is a critical executioner of apoptosis, which can be cleaved and activated in apoptosis. **Figure 4A** and **4B** showed that CDDO-Me remarkably induced a dose- and time-dependent elevation in casepase3 activity. Besides, activation of caspase 3 was further confirmed by Western blotting and immunofluorescence assays (**Figure 4C-G**). PARP is one of the main cleavage targets of caspase 3, and the cleavage of PARP facilitates cellular disassembly and serves as a marker of cells undergoing apoptosis [43]. Our study also showed that the level of cleaved PARP increased significantly (**Figure 4C-E**) after cells were treated with CDDO-Me.

Extrinsic death receptor pathway and the intrinsic mitochondrial-mediated pathway are two main routes leading to apoptosis with the involvement of different caspases [43]. In this study, exposure of K562 cells to CDDO-Me led to an activation of caspases 8 and 9 (**Figure 4C-E**) in a dose- and time-dependent manner, indicating that both intrinsic and extrinsic pathways are involved in CDDO-Me-induced apoptosis in K562 cells.

CDDO-Me induces mitochondrial dysfunction of K562 cells involving the Bcl-2 family

Mitochondria plays a key role in the regulation of apoptosis, which can integrate the apoptotic signals originating from both extrinsic and intrinsic apoptosis pathways [44]. As our pro-

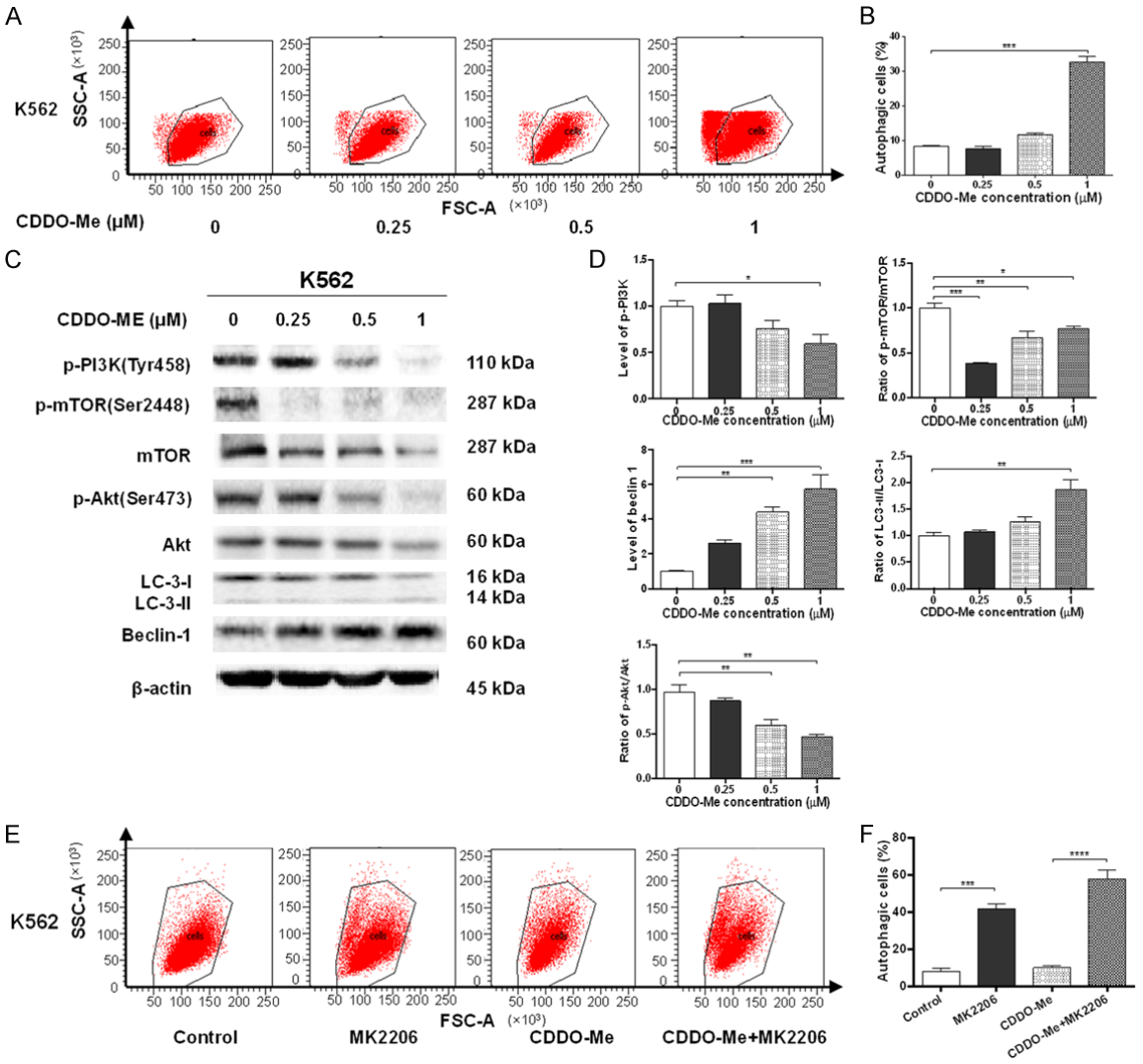

Figure 7. CDDO-Me induces autophagy of K562 cells via PI3K/Akt/mTOR signaling pathway. K562 cells were treated with CDDO-Me at 0.25, 0.5, and 1 μM for 24 h. A. Representative flow cytometric plots of autophagic K562 cells. B. Bar graphs showing the percentage of autophagy cells. C. Representative blots of phosphorylated PI3K, Akt, mTOR, and the expression of PI3K, Akt, mTOR, beclin 1, LC3-I, and LC3-II. D. Bar graphs showing the ratio of p-mTOR/mTOR, p-Akt/Akt, LC3-II/LC3-I, and the level of p-PI3K and beclin 1. E. K562 cells were pretreated with 10 μM MK2206, and then incubated in the presence or absence of 0.5 μM CDDO-Me for 24 h. The treated cells were analyzed by flow cytometry. F. Bar graphs showing the percentage of autophagy cells. Data are expression as mean ± SD of three independent experiments. $^{*}P<0.05$, $^{**}P<0.01$, and $^{***}P<0.005$ by one-way ANOVA.

teomics data indicated that mitochondrial dysfunction was a critical signaling pathway responding to CDDO-Me exposure (Table S2 and Figure S2), we detected mitochondrial membrane potential changes using JC-1 as a molecular probe in K562 cells. As shown in **Figure 5A**, cells exhibited red fluorescence in the control group, whereas CDDO-Me exposure increased the portion of K562 cells with green fluorescence exclusively, indicating loss of mitochondrial membrane potential. Ratios of JC-1 aggregates/monomeric was reduced by 31%, 67%, and 88%, when cells were exposed to CDDO-Me at 0.25, 0.5, and 1 μM, respectively ($P<0.05$, **Figure 5B**). These results demonstrate that CDDO-Me dose-dependently induces a significant reduction or loss of mitochondrial membrane potential due to membrane disruption.

The disruption of the mitochondrial membrane function results in the release of the cyto-

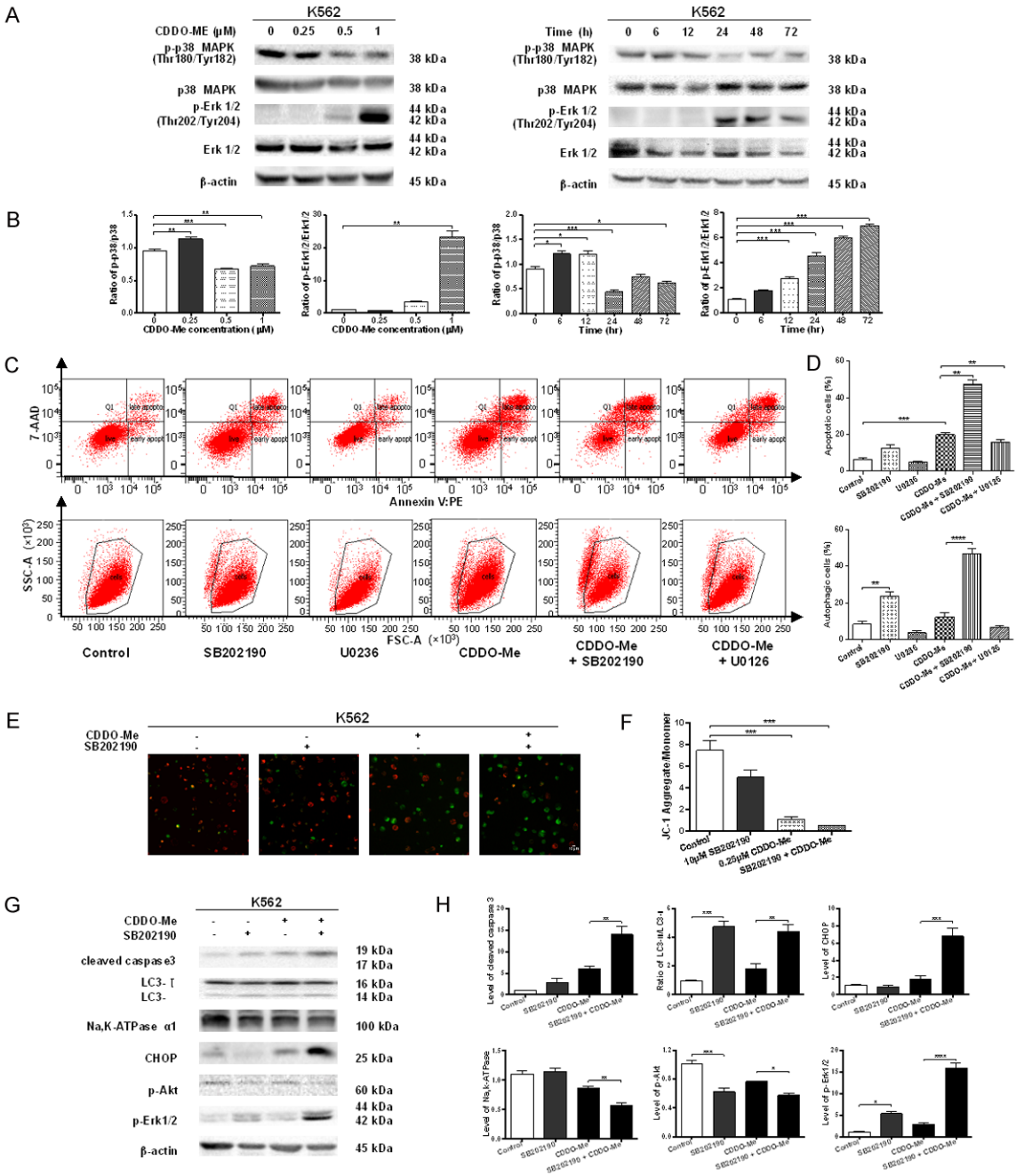

Figure 8. p38 MAPK and Erk1/2 play roles in CDDO-Me-induced apoptosis and autophagy in K562 cells. (A) K562 cells were treated with CDDO-Me at 0.25, 0.5, and 1 μM for 24 h or at 0.5 μM over 72 h. Representative blots of phosphorylated p38 MAPK, Erk1/2, p38 MAPK, andp-Erk1/2. (B) Bar graphs showing the ratio of p-p38/p38 and p-Erk1/2/Erk1/2. (C) Representative flow cytometric plots. (D) Bar graphs showing apoptotic and autophagic K562 cells. Cells were pretreated with 10 μM SB202190 or 10 μM U0126, then incubated with CDDO-Me for 24 h. (E) Representative fluorescence microscopic images. (F) Bar graphs showing K562 cells pretreated with 10 μM SB202190, then incubated with CDDO-Me for 24 h, and stained with JC-1. (G) Representative blots and (H) bar graphs of the expression of cleaved caspase 3, LC-3, Na^+,K^+-ATPase α1, CHOP, p-Akt, and p-Erk1/2. Data are expression as the mean ± SD of three independent experiments. $^*P<0.05$, $^{**}P<0.01$, $^{***}P<0.005$, and $^{****}P<0.001$ by one-way ANOVA.

chrome c, which is coupled to the activation of caspase 9, and the mitochondrial permeability is regulated by the Bcl-2 family [45]. As such, we next evaluated the level of cytochrome c and selected pro-survival and pro-apoptotic Bcl-2 family proteins by Western blotting assay.

As shown in **Figure 5C** and **5E**, the cytosolic level of cytochrome c was increased 1.6- and 2.1-fold in response to the treatment with 0.5 and 1 μM CDDO-Me, respectively (P<0.005). Also, CDDO-Me significantly decreased the Bcl-2 level, while only slightly increasing Bax level. As a consequence, the ratio of Bcl-2/Bax was decreased (**Figure 5C** and **5E**). Compared with the control, there was a 57%, 76%, and 80% reduction in Bcl-xl level when treated with 0.25, 0.5, and 1 μM CDDO-Me, and a 61% and 79% decline in Mcl-1 level when incubated with 0.5 and 1 μM CDDO-Me, respectively (P<0.001, **Figure 5C** and **5E**). Conversely, the expression level of puma was raised 3-fold by incubation with 1 μM CDDO-Me (P<0.005, **Figure 5C** and **5E**), and the expression of Bak was slightly affected.

Following this, we tested the expression of cytochrome c and selected Bcl-2 family proteins over 72 h. In comparison with the control cells, there was a marked increase in the cytosolic level of cytochrome c, and a remarked decrease in the ratio of Bcl-2/Bax, when cells were exposed to CDDO-Me at 0.5 μM for 12, 24, 48, and 72 h (**Figure 5D** and **5E**). The level of anti-apoptosis proteins, both Bcl-xl and Mcl-1, were down-regulated. Interestingly, CDDO-Me treatment led to a significant up-regulation in the level of Bak over 72 h. Collectively, these results reveal that CDDO-Me dose- and time-dependently induces mitochondrial dysfunction in K562 cells through Bcl-2 family, leading to apoptosis.

CDDO-Me triggers endoplasmic reticulum (ER) stress involving UPR signaling in K562 cells

Na^+,K^+-ATPase inhibitors have gained increasing interest for its anticancer potential and Na^+,K^+-ATPase inhibitor activates UPR signaling, which may provide a further explanation for the anticancer effect [42, 46, 47]. As shown by the IPA pathway analysis (Table S2 and Figure S3) on the alteration of the UPR signaling response to CDDO-Me exposure in K562 cells, we examined the expression level of the UPR proteins. In comparison with the control group, CDDO-Me significantly increased the level of Bip and the ratio of p-PERK/PERK and p-IRE1α/IRE1α, indicating a triggered ER stress (**Figure 6A**, **6B**). It is known that excessive and prolonged ER stress triggers apoptosis [48]. Notably, the expression of CHOP is dramatically up-regulated with increasing concentrations of CDDO-Me for 24 h (**Figure 6**). Taken together, CDDO-Me triggers ER stress involving UPR signals, contributing to CDDO-Me-elicited apoptosis.

CDDO-Me induces autophagy of K562 cells via inhibition of the PI3K/Akt/mTOR signaling pathway

To further study the anticancer mechanisms of CDDO-Me on K562 cells, we investigated the effect of CDDO-Me on autophagy of K562 cells. As shown in **Figure 7A** and **7B**, there was a 3.9-fold increase in the autophagic cells when treated with 1 μM CDDO-Me for 24 h (P< 0.005), without significant change at lower concentrations of CDDO-Me. As two important markers of vesicle expansion and formation during autophagic process, LC3 and beclin 1 were determined. As expected, CDDO-Me treatment increased LC3-II level, while decreasing LC3-I level. Correspondingly, the ratio of LC3-II/LC3-I was tripled at 1 μM CDDO-Me (P<0.01, **Figure 7C** and **7D**). Also, the expression level of beclin 1 was elevated 3.0- and 4.2-fold when cells were incubated with CDDO-Me at 0.5 and 1 μM for 24 h, respectively (P<0.01 or 0.005, **Figure 7C** and **7D**). These results indicate that CDDO-Me exerts a promoting effect on autophagy of K562 cells.

We further explored the possible mechanisms for the autophagy-inducing effect of CDDO-Me in K562 cells. The IPA canonical pathway analysis showed that mTOR signaling as well as upstream PI3K/Akt signaling were critical for the effect of CDDO-Me on K562 cells (Table S2, Table S3 and Figure S4). Thus, we examined the level of proteins in PI3K/Akt/mTOR pathways using Western blotting assay. After exposure of the cells to 1 μM CDDO-Me for 24 h, the level of p-PI3K (Tyr458) dropped by 30% (P<0.05, **Figure 7C** and **7D**). Similarly, the ratio of p-Akt/Akt was decreased by 30% and 51% when treated with CDDO-Me at 0.5 and 1 μM for 24 h, respectively (P<0.01, **Figure 7C** and **7D**). Additionally, CDDO-Me significantly down-regulated the phosphorylation level of mTOR at Ser2448, but only slightly affected the level of total mTOR, resulting in 62%, 30% and 21% decrease in the ratio of p-mTOR/mTOR when incubated with CDDO-Me at 0.25, 0.5, and 1

μM, respectively (P<0.005, **Figure 7C** and **7D**). These results show that suppression of PI3K/Akt/mTOR pathway contributes to CDDO-Me-induced autophagy in K562 cells.

In order to further testify the role of PI3K/Akt/mTOR pathway in CDDP-Me-induced autophagy in K562 cells, we subsequently employed 10 μM MK-2206 (anAkt inhibitor and a blocker of autophagosome formation) to examine the autophagy of K562 cells. As shown in **Figure 7D** and **7E**, co-incubation of CDDO-Me with MK-2206 remarkably enhanced the autophagy-inducing effect of CDDO-Me in K562 cells, with the percentage of autophagic cells being elevated from 8.1% to 58.2% (P<0.001). It indicates that PI3K/Akt/mTOR play an important role in CDDO-Me-induced autophagy in K562 cells.

p38 MAPK and Erk1/2 play roles in CDDO-Me-induced apoptosis and autophagy in K562 cells

p38 MAPK and Erk1/2 play a vital role in the regulation of cell death and cell growth. Therefore, we determined p38 MAPK and Erk1/2 signals in response to CDDO-Me treatment.We observed that CDDO-Me suppressed p38 MAPK signaling but enhanced Erk signaling in K562 cells, evidenced by the reduction in the ratio of p-p38 MAPK/p38 MAPK and increase in p-Erk1/2/Erk1/2 (**Figure 8A** and **8B**). Following the observation on the regulatory effect of CDDO-Me on p38 MAPK and Erk1/2 signaling pathway, we explored the roles of p38 MAPK and Erk1/2 in the cancer cell killing effect of CDDO-Me in K562 cells, and examined apoptosis and autophagy by flow cytometry simultaneously. As shown in **Figure 8C** and **8D**, incubation with SB202190 (a selective p38 MAPK inhibitor and autophagy inducer) alone for 24 h led to a 2.0-fold elevation (P<0.01) in the percentage of autophagic cells compared to the control cells. In comparison with cells incubated with CDDO-Me alone, co-incubation with SB202190 significantly enhanced the CDDO-Me-induced apoptosis (2.4-fold, P<0.01, **Figure 8C** and **8D**) and autophagy (3.8-fold, P<0.001, **Figure 8C** and **8D**). On the other hand, pretreatment with U0126 (an Erk1/2 inhibitor) resulted in a 53.3% decline (P<0.01, **Figure 8C** and **8D**) in CDDO-Me-induced apoptosis, while only exhibiting a marginal effect on autophagy in K562 cells.

We further investigate the mechanism for SB202190-enhanced CDDO-Me-induced apoptotic and autophagic effects, the mitochondrial membrane potential change and related protein expression levels were examined. In comparison with the cells treated with CDDO-Me alone, co-incubation CDDO-Me with SB-202190 significantly increased cleaved caspase 3 (2.2-fold), although the alteration in the ratios of JC-1 aggregates/monomeric was not significant (35.7% reduction, P>0.05, **Figure 8E-H**). These changes suggest that SB202190 enhanced CDDO-Me-induced apoptosis via mitochondrial-dependent pathway. Furthermore, in comparison with the cells treated with CDDO-Me only, there was a 3.2-fold increase in CHOP level and a 22.4% decrease in Na^+,K^+-ATPase level when co-treatment with SB202190, indicating that p38 MAPK also influenced Na^+,K^+-ATPase expression and UPR signaling pathway (**Figure 8G** and **8H**). In agreement with the flow cytometric results stated above, exposure of K562 cells to CDDO-Me plus SB202190 remarkably elevated the ratio of LC3-II/LC3-I (**Figure 8G** and **8H**), compared with the control cells receiving CDDO-Me only. Moreover, the level of p-Akt was reduced by 78.8%, whereas the level of p-Erk1/2 was elevated 10.8-fold, in comparison with the cells exposed to CDDO-Me alone (**Figure 8G** and **8H**), suggesting that SB202190 enhanced the effect of CDDO-Me-induced autophagy involving the PI3K/Akt/mTOR pathway. Interestingly, our results also show that CDDO-Me-induced Erk1/2 phosphorylation was increased 10.8-fold by SB202190 (P<0.001, **Figure 8G** and **8H**), which indicates that p38 MAPK exerts an inhibitory effect on CDDO-Me-stimulated Erk1/2 activation. Taken together, there are interactions between CDDO-Me-induced apoptosis and autophagy, involving p38 MAPK/Erk1/2 signaling pathway.

Discussion

Up to now, treatment of CML is still a challenge because of poor response/drug resistance and intolerance in a substantial proportion of patients, thus there is an urgent need to develop new drugs and identify new therapeutic targets for better clinical outcomes. The SILAC-based proteomics approach is a high-throughput quantitative analytical method, which can comprehensively evaluate the effect of a given

compound and recognize its potential molecular targets and related signaling pathways at cellular levels and *in vivo* [33-36]. In order to find the possible molecular targets and mechanisms for the anticancer effects, our earlier studies have employed this technique to disclose the molecular interactome of 5,6-dimethylxanthenone 4-acetic acid (DMXAA, a tumor vascular disrupter) and alisertib (an Aurora kinase A inhibitor) in different cancer cell lines [39, 40, 49, 50]. CDDO-Me is a multi-targeting molecule exerting the potent anticancer effect in the treatment of various types of cancer in preclinical and clinical studies [21, 26]. No studies have reported its proteomic responses in CML cells. In the present study, we evaluated the proteomic responses to CDDO-Me treatment in K562 cells. The results have shown that the responding functional proteins and signaling pathways were mainly involved in cell survival and death, cellular function and maintenance, energy and nutrition metabolism. We have verified that CDDO-Me suppressed Na^+,K^+-ATPase expression, arrested K562 cells in G_2 and S phases, induced marked apoptosis, promoted autophagy, and triggered ER stress.

Na^+,K^+-ATPase is a transmembrane protein complex serving as a central energy-consuming pump to maintain ionic and osmotic balance in cells [51]. It also serves as plasma membrane receptors bound by a family of cardiotonic steroids and signal transducers that can provide a feedback loop between Na^+,K^+-ATPase and the mitochondria [52]. Na^+,K^+-ATPaseis composed of 4 α isoforms (α1, α2, α3 and α4) and 3 β isoforms (β1, β2 and β3); and α1 or α3 isoforms are often overexpressed in cancer whereas the β1 isoform acts as a tumor suppressor [42, 46, 47]. Na^+,K^+-ATPase is a modulator of apoptosis and autophagy in tumor cells [47]. Here, we first reported the down-regulation of Na^+,K^+-ATPase α1 by the treatment of CDDO-Me in human leukemia cells, suggesting that it is a potential novel target protein of CDDO-Me. The mechanism for the anticancer effect of CDDO-Me via targeting Na^+,K^+-ATPase in human leukemia cells deserves further investigations.

It is known that the eukaryotes cell cycle is regulated by cyclins, CDKs and the CDK inhibitors (CKIs). The CDK1-cyclin B1 complexes promote transition and mitosis in G_2/M phase, and the CDK2-cyclin A complexes predominate in Sphase [53, 54]. The CKIs, including p21Waf1/Cip1 and p27Kip1, inhibit the CDK-cyclin activities and prevent cell cycle progression. In this study, we observed a remarkable decrease in cyclin B1, CDK1/CDC2, and CDK2 expression, meanwhile an increase in p21Waf1/Cip1 and p27Kip1 expression, which might explain the G_2 and S phase arrest by CDDO-Me in K562 cells. We also observed CDDO-Me induced an elevation in the level of p53 and p-p53 at Ser15. As a direct p21Waf1/Cip1 upstream target, p53 can lead to either cell cycle arrest and DNA repair or apoptosis [55]. Phosphorylation at Ser15 impairs the ability of MDM2 to bind p53, promoting both the accumulation and activation of p53 in response to DNA damage [56]. Taken together, the proteomic and verification data reveal that CDDO-Me exerts a cell cycle arresting effect *via* regulation of key functional proteins of cell cycle in K562 cells.

Apoptosis is a process of programmed cell death necessary for cell growth, development and maintenance of homeostasis in metazoans associated with G_2/M arrest [43, 57, 58]. Caspases are a family of cysteine proteases and the central regulators in cell apoptosis. In agreement with our previous findings in esophageal squamous cancer cells [21], we observed a concentration- and time-dependent apoptosis induced by CDDO-Me in K562 cells. In this study, enhanced expression level of caspase 9 and cleaved caspase 8 reflected the activation of both intrinsic/mitochondrial-mediated and extrinsic/death receptor pathways, which in turn activated cleavage caspase 3 and PARP and ultimately induced apoptosis. There is a crosstalk between two apoptotic pathways through Bid, which transferred the apoptotic signal from the cell surface to mitochondria [59]. Our proteomics data also showed that CDDO-Me regulated mitochondrial function. Mitochondrial permeabilization is an important cellular event in apoptotic cell death and regulated by Bcl-2 family members, including pro-survival proteins Bcl-2, Bcl-xL,and Mcl-1; pro-apoptotic members Bax, Bak, and “BH3 only” proteins PUMA [60, 61]. We verified the depolarization of mitochondrial membrane potential induced by CDDO-Me in K562 cells and the release of cytochrome c into cytosol and subsequent activation of caspase 9, which might be attributed to down-regulation of Bcl-2/Bax, Bcl-

xL, Mcl-1, and up-regulation of Bak and PUMA. Taken together, our results suggest that CDDO-Me exhibits its apoptotic effects through intrinsic/mitochondrial-mediated as well as extrinsic apoptosis pathways.

In addition to the two major pathways, intrinsic mitochondria-mediated pathway and the extrinsic death receptor-induced pathway, apoptosis can be induced via ER stress [61-64]. When the cellular energy level, the redox state, and Ca^{2+} concentration are perturbed, the ER stress is initiated, triggering the UPR. Interestingly, Jeong et al. [65] reported that CDDO-Me increased intracellular Ca^{2+} concentration. In this study, we observed an up-regulated level of BIP and activated PERK and IREα, indicating that CDDO-Me activates UPR in K562 cells. As well known, BiP is the marker of ER stress, controlling the activation of transmembrane ER stress sensors (PERK, IRE1, and ATF6) through a binding-release mechanism [48, 63, 66]. Our results also displayed that the exposure of K562 cells to CDDO-Me increased the expression of CHOP. Although UPR is a protective factor of cell, if the stress cannot be resolved, it switches from pro-survival to pro-apoptosis [48]. CHOP is a downstream of PERK and IREα, once activated, it can trigger the expression of pro-apoptotic proteins, targeting the Bcl2 family, acting on the mitochondrial membrane to release cytochrome c and initiating the caspase cascade [67, 68]. Similar with our results, Zou et al. [66] have reported that CDDO-Me triggered ER stress, leading to CHOP-mediated apoptosis in lung cancer cells. Our study suggests that UPR signaling is implicated in CDDO-Me-induced apoptosis, although more studied are needed to further validate the UPR-inducing effect in the treatment of CML by CDDM-Me.

Autophagy as type II programmed cell death, extremely affects diverse stages of occurrence and development of cancer with the contribution to overlapped signaling pathways of autophagy, apoptosis and carcinogenesis [64, 69-71]. The PI3K/Akt/mTOR is a central pathway involved in autophagy. The phosphorylation of PI3K activated Akt, then mTOR can integrate upstream activating signals through PI3K/Akt pathway and become phosphorylated form, which negatively regulates autophagy by limiting the inhibitory effect on the ULK1 kinase complex in response to the deprivation of nutrient or stress [72]. CDDO-Me has been found to inhibit proliferation of cancer cells via PI3K/Akt/mTOR signaling pathway by blocking the activation of Akt and downstream targets, including mTOR [22], but the association with autophagy is unclear. In this study, a concentration-dependent autophagy induced by CDDO-Me was observed. In addition, MK2206 was employed and significantly increased the CDDO-Me-induced autophagic cell percentage. Therefore, our results suggest that CDDO-Me-induced autophagy of K562 cells by inhibition of PI3K/Akt/mTOR pathway.

p38 MAPK and Erk1/2, known as the members of MAPK family, play a critical role in the regulation of cell growth, differentiation, and control of cellular responses to cytokines and stress [73]. Erk1/2 and p38 MAPK have opposing effects on cancer cell death, however each of them was involved in stress-induced apoptosis. In the present study, we have observed that CDDO-Me treatment remarkably decreased the phosphorylation of p38 MAPK, contributing to the recent findings that Akt suppresses the activation of p38a by phosphorylation of ASK1 on Ser [74, 75], but increases the phosphorylation of Erk1/2 in K562 cells in concentration- and time-dependent manners. Furthermore, SB202190 significantly enhanced the apoptosis and autophagy induced by CDDO-Me in K562 cells, whereas the reverse regulating effects of U0126 were observed. Interestingly, our results also showed that CDDO-Me-induced Erk1/2 phosphorylation was increased by SB202190, which might be ascribed to a crosstalk between p38 MAPK and Erk1/2 signaling pathways via PP2A. Our results indicate a crosstalk between the autophagic and apoptotic pathways, with a series of key molecules or pathways being synchronized and mediating the complex interplay, including mTOR and UPR signaling pathways, Akt, Erk1/2, and Na^+,K^+-ATPase α1. Herein, CDDO-Me can induce apoptosis and autophagy in a coordinated manner in K562 cells.

Conclusion

The SILAC proteomics and validating cellular studies demonstrate that CDDO-Me inhibits cellular proliferation, induces cell cycle arrest, triggers mitochondria-, death receptor-dependent, and ER stress-mediated apoptosis, and

promotes autophagy by regulating numerous functional proteins and signaling pathways. In particular, the PI3K/Akt/mTOR signaling pathway is involved in autophagy and p38 MAPK/Erk1/2 signaling pathways contributes to apoptosis- and autophagy-inducing effects in K562 cells. Na^+,K^+-ATPase may be a novel target of CDDO-Me. Taken together, CDDO-Me may represent a promising anticancer agent for CML therapy, and further studies are warranted to uncover the biochemical mechanisms.

Acknowledgements

The authors appreciate the financial support from the College of Pharmacy, University of South Florida, Tampa, Florida 33612, USA. This project was supported in part by the Scientific Research Projects for Returned Overseas Scientists of Ningxia Hui Autonomous Region (2016), China. The authors appreciate the sincere help from Dr. Zhi-Wei Zhou, PhD, currently working at UT Southwestern Medical Center at Dallas, TX, for this project.

Disclosure of conflict of interest

None.

Address correspondence to: Dr. Hong-Wan Dang, Institute of Clinical Pharmacology, General Hospital of Ningxia Medical University, Yinchuan, Ningxia Hui Autonomous Region, China. Fax: +86 951 674 3649; E-mail: dhwbeining@163.com; Dr. Shu-Feng Zhou, Department of Bioengineering and Biotechnology, College of Chemical Engineering, Huaqiao University, 668 Jimei Blvd., Xiamen, Fujian 361021, China. Tel: +86 592 616-2288; Fax: +86 592 616-2300; E-mail: szhou@hqu.edu.cn

References

[1] Nangalia J, Grinfeld J and Green AR. Pathogenesis of myeloproliferative disorders. Annu Rev Pathol 2016; 11: 101-126.

[2] Tefferi A. Myeloproliferative neoplasms: a decade of discoveries and treatment advances. Am J Hematol 2016; 91: 50-58.

[3] Global Burden of Disease Cancer Collaboration, Fitzmaurice C, Allen C, Barber RM, Barregard L, Bhutta ZA, Brenner H, Dicker DJ, Chimed-Orchir O, Dandona R, Dandona L, Fleming T, Forouzanfar MH, Hancock J, Hay RJ, Hunter-Merrill R, Huynh C, Hosgood HD, Johnson CO, Jonas JB, Khubchandani J, Kumar GA, Kutz M, Lan Q, Larson HJ, Liang X, Lim SS, Lopez AD, MacIntyre MF, Marczak L, Marquez N, Mokdad AH, Pinho C, Pourmalek F, Salomon JA, Sanabria JR, Sandar L, Sartorius B, Schwartz SM, Shackelford KA, Shibuya K, Stanaway J, Steiner C, Sun J, Takahashi K, Vollset SE, Vos T, Wagner JA, Wang H, Westerman R, Zeeb H, Zoeckler L, Abd-Allah F, Ahmed MB, Alabed S, Alam NK, Aldhahri SF, Alem G, Alemayohu MA, Ali R, Al-Raddadi R, Amare A, Amoako Y, Artaman A, Asayesh H, Atnafu N, Awasthi A, Saleem HB, Barac A, Bedi N, Bensenor I, Berhane A, Bernabe E, Betsu B, Binagwaho A, Boneya D, Campos-Nonato I, Castaneda-Orjuela C, Catala-Lopez F, Chiang P, Chibueze C, Chitheer A, Choi JY, Cowie B, Damtew S, das Neves J, Dey S, Dharmaratne S, Dhillon P, Ding E, Driscoll T, Ekwueme D, Endries AY, Farvid M, Farzadfar F, Fernandes J, Fischer F, G/Hiwot TT, Gebru A, Gopalani S, Hailu A, Horino M, Horita N, Husseini A, Huybrechts I, Inoue M, Islami F, Jakovljevic M, James S, Javanbakht M, Jee SH, Kasaeian A, Kedir MS, Khader YS, Khang YH, Kim D, Leigh J, Linn S, Lunevicius R, El Razek HMA, Malekzadeh R, Malta DC, Marcenes W, Markos D, Melaku YA, Meles KG, Mendoza W, Mengiste DT, Meretoja TJ, Miller TR, Mohammad KA, Mohammadi A, Mohammed S, Moradi-Lakeh M, Nagel G, Nand D, Le Nguyen Q, Nolte S, Ogbo FA, Oladimeji KE, Oren E, Pa M, Park EK, Pereira DM, Plass D, Qorbani M, Radfar A, Rafay A, Rahman M, Rana SM, Soreide K, Satpathy M, Sawhney M, Sepanlou SG, Shaikh MA, She J, Shiue I, Shore HR, Shrime MG, So S, Soneji S, Stathopoulou V, Stroumpoulis K, Sufiyan MB, Sykes BL, Tabares-Seisdedos R, Tadese F, Tedla BA, Tessema GA, Thakur JS, Tran BX, Ukwaja KN, Uzochukwu BSC, Vlassov VV, Weiderpass E, Wubshet Terefe M, Yebyo HG, Yimam HH, Yonemoto N, Younis MZ, Yu C, Zaidi Z, Zaki MES, Zenebe ZM, Murray CJL and Naghavi M. Global, regional, and national cancer incidence, mortality, years of life lost, years lived with disability, and disability-adjusted life-years for 32 cancer groups, 1990 to 2015: a systematic analysis for the global burden of disease study. JAMA Oncol 2017; 3: 524-548.

[4] Torre LA, Bray F, Siegel RL, Ferlay J, Lortet-Tieulent J and Jemal A. Global cancer statistics, 2012. CA Cancer J Clin 2015; 65: 87-108.

[5] Goldman JM. Chronic myeloid leukemia: a historical perspective. Semin Hematol 2010; 47: 302-311.

[6] Mughal TI, Radich JP, Deininger MW, Apperley JF, Hughes TP, Harrison CJ, Gambacorti-Passerini C, Saglio G, Cortes J and Daley GQ. Chronic myeloid leukemia: reminiscences and dreams. Haematologica 2016; 101: 541-558.

[7] Jabbour E and Kantarjian H. Chronic myeloid leukemia: 2012 update on diagnosis, monitoring, and management. Am J Hematol 2012; 87: 1037-1045.
[8] Patnaik MM and Tefferi A. Cytogenetic and molecular abnormalities in chronic myelomonocytic leukemia. Blood Cancer J 2016; 6: e393.
[9] Radich JP and Mauro MJ. Tyrosine kinase inhibitor treatment for newly diagnosed chronic myeloid leukemia. Hematol Oncol Clin North Am 2017; 31: 577-587.
[10] Pasic I and Lipton JH. Current approach to the treatment of chronic myeloid leukaemia. Leuk Res 2017; 55: 65-78.
[11] Rosti G, Castagnetti F, Gugliotta G and Baccarani M. Tyrosine kinase inhibitors in chronic myeloid leukaemia: which, when, for whom? Nat Rev Clin Oncol 2017; 14: 141-154.
[12] Ali MA. Chronic myeloid leukemia in the era of tyrosine kinase inhibitors: an evolving paradigm of molecularly targeted therapy. Mol Diagn Ther 2016; 20: 315-333.
[13] Jabbour E. Chronic myeloid leukemia: First-line drug of choice. Am J Hematol 2016; 91: 59-66.
[14] Molica M, Massaro F and Breccia M. Second line small molecule therapy options for treating chronic myeloid leukemia. Expert Opin Pharmacother 2017; 18: 57-65.
[15] Poch Martell M, Sibai H, Deotare U and Lipton JH. Ponatinib in the therapy of chronic myeloid leukemia. Expert Rev Hematol 2016; 9: 923-932.
[16] Breccia M, Colafigli G, Molica M and Alimena G. Adverse events associated with tyrosine kinase inhibitors for the treatment of chronic myeloid leukemia. Expert Opin Drug Saf 2016; 15: 525-533.
[17] Patel AB, O'Hare T and Deininger MW. Mechanisms of resistance to ABL kinase inhibition in chronic myeloid leukemia and the development of next generation ABL kinase inhibitors. Hematol Oncol Clin North Am 2017; 31: 589-612.
[18] Ryu SY, Oak MH, Yoon SK, Cho DI, Yoo GS, Kim TS and Kim KM. Anti-allergic and anti-inflammatory triterpenes from the herb of prunella vulgaris. Planta Med 2000; 66: 358-360.
[19] Honda T, Honda Y, Favaloro FG Jr, Gribble GW, Suh N, Place AE, Rendi MH, Sporn MB. A novel dicyanotriterpenoid, 2-cyano-3,12-dioxooleana-1,9(11)-dien-28-onitrile, active at picomolar concentrations for inhibition of nitric oxide production. Bioorg Med Chem Lett 2002; 12: 1027-1030.
[20] Liby K, Royce DB, Williams CR, Risingsong R, Yore MM, Honda T, Gribble GW, Dmitrovsky E, Sporn TA and Sporn MB. The synthetic triterpenoids CDDO-methyl ester and CDDO-ethyl amide prevent lung cancer induced by vinyl carbamate in A/J mice. Cancer Res 2007; 67: 2414-2419.
[21] Wang YY, Yang YX, Zhao R, Pan ST, Zhe H, He ZX, Duan W, Zhang X, Yang T, Qiu JX and Zhou SF. Bardoxolone methyl induces apoptosis and autophagy and inhibits epithelial-to-mesenchymal transition and stemness in esophageal squamous cancer cells. Drug Des Devel Ther 2015; 9: 993-1026.
[22] Wang YY, Zhe H and Zhao R. Preclinical evidences toward the use of triterpenoid CDDO-Me for solid cancer prevention and treatment. Mol Cancer 2014; 13: 30.
[23] Yates MS, Tauchi M, Katsuoka F, Flanders KC, Liby KT, Honda T, Gribble GW, Johnson DA, Johnson JA, Burton NC, Guilarte TR, Yamamoto M, Sporn MB and Kensler TW. Pharmacodynamic characterization of chemopreventive triterpenoids as exceptionally potent inducers of Nrf2-regulated genes. Mol Cancer Ther 2007; 6: 154-162.
[24] Dinkova-Kostova AT, Liby KT, Stephenson KK, Holtzclaw WD, Gao XQ, Suh N, Williarrli C, Risingsong R, Honda T, Gribble GW, Sporn MB and Talalay P. Extremely potent triterpenoid inducers of the phase 2 response: correlations of protection against oxidant and inflammatory stress. Proc Natl Acad Sci U S A 2005; 102: 4584-4589.
[25] de Zeeuw D, Akizawa T, Audhya P, Bakris GL, Chin M, Christ-Schmidt H, Goldsberry A, Houser M, Krauth M, Lambers Heerspink HJ, McMurray JJ, Meyer CJ, Parving HH, Remuzzi G, Toto RD, Vaziri ND, Wanner C, Wittes J, Wrolstad D, Chertow GM; BEACON Trial Investigators. Bardoxolone methyl in type 2 diabetes and stage 4 chronic kidney disease. N Engl J Med 2013; 369: 2492-2503.
[26] Shanmugam MK, Dai X, Kumar AP, Tan BK, Sethi G and Bishayee A. Oleanolic acid and its synthetic derivatives for the prevention and therapy of cancer: preclinical and clinical evidence. Cancer Lett 2014; 346: 206-216.
[27] Deeb D, Gao X, Jiang H, Dulchavsky SA and Gautam SC. Oleanane triterpenoid CDDO-Me inhibits growth and induces apoptosis in prostate cancer cells by independently targeting pro-survival Akt and mTOR. Prostate 2009; 69: 851-860.
[28] Jutooru I, Chadalapaka G, Abdelrahim M, Basha MR, Samudio I, Konopleva M, Andreeff M and Safe S. Methyl 2-cyano-3,12-dioxooleana-1,9-dien-28-oate decreases specificity protein transcription factors and inhibits pancreatic tumor growth: role of microRNA-27a. Mol Pharmacol 2010; 78: 226-236.
[29] Ling X, Konopleva M, Zeng Z, Ruvolo V, Stephens LC, Schober W, McQueen T, Dietrich M, Madden TL and Andreeff M. The novel triterpe-

noid C-28 methyl ester of 2-cyano-3,12-dioxoolen-1,9-dien-28-oic acid inhibits metastatic murine breast tumor growth through inactivation of STAT3 signaling. Cancer Res 2007; 67: 4210-4218.

[30] Nagaraj S, Youn JI, Weber H, Iclozan C, Lu L, Cotter MJ, Meyer C, Becerra CR, Fishman M, Antonia S, Sporn MB, Liby KT, Rawal B, Lee JH and Gabrilovich DI. Anti-inflammatory triterpenoid blocks immune suppressive function of MDSCs and improves immune response in cancer. Clin Cancer Res 2010; 16: 1812-1823.

[31] Hong DS, Kurzrock R, Supko JG, He X, Naing A, Wheler J, Lawrence D, Eder JP, Meyer CJ, Ferguson DA, Mier J, Konopleva M, Konoplev S, Andreeff M, Kufe D, Lazarus H, Shapiro GI and Dezube BJ. A phase I first-in-human trial of bardoxolone methyl in patients with advanced solid tumors and lymphomas. Clin Cancer Res 2012; 18: 3396-3406.

[32] Samudio I, Kurinna S, Ruvolo P, Korchin B, Kantarjian H, Beran M, Dunner K Jr, Kondo S, Andreeff M and Konopleva M. Inhibition of mitochondrial metabolism by methyl-2-cyano-3,12-dioxooleana-1,9-diene-28-oate induces apoptotic or autophagic cell death in chronic myeloid leukemia cells. Mol Cancer Ther 2008; 7: 1130-1139.

[33] Tyanova S, Mann M and Cox J. MaxQuant for in-depth analysis of large SILAC datasets. Methods Mol Biol 2014; 1188: 351-364.

[34] Mann M. Fifteen years of stable isotope labeling by amino acids in cell culture (SILAC). Methods Mol Biol 2014; 1188: 1-7.

[35] Geiger T, Wisniewski JR, Cox J, Zanivan S, Kruger M, Ishihama Y and Mann M. Use of stable isotope labeling by amino acids in cell culture as a spike-in standard in quantitative proteomics. Nat Protoc 2011; 6: 147-157.

[36] Ong SE and Mann M. Stable isotope labeling by amino acids in cell culture for quantitative proteomics. Methods Mol Biol 2007; 359: 37-52.

[37] Zanivan S, Maione F, Hein MY, Hernandez-Fernaud JR, Ostasiewicz P, Giraudo E and Mann M. SILAC-based proteomics of human primary endothelial cell morphogenesis unveils tumor angiogenic markers. Mol Cell Proteomics 2013; 12: 3599-3611.

[38] Geiger T, Madden SF, Gallagher WM, Cox J and Mann M. Proteomic portrait of human breast cancer progression identifies novel prognostic markers. Cancer Res 2012; 72: 2428-2439.

[39] Shu LP, Zhou ZW, Zi D, He ZX and Zhou SF. A SILAC-based proteomics elicits the molecular interactome of alisertib (MLN8237) in human erythroleukemia K562 cells. Am J Transl Res 2015; 7: 2442-2461.

[40] Ren BJ, Zhou ZW, Zhu DJ, Ju YL, Wu JH, Ouyang MZ, Chen XW and Zhou SF. Alisertib induces cell cycle arrest, apoptosis, autophagy and suppresses EMT in HT29 and Caco-2 cells. Int J Mol Sci 2015; 17.

[41] Zhou ZW, Li XX, He ZX, Pan ST, Yang Y, Zhang X, Chow K, Yang T, Qiu JX, Zhou Q, Tan J, Wang D and Zhou SF. Induction of apoptosis and autophagy via sirtuin1- and PI3K/Akt/mTOR-mediated pathways by plumbagin in human prostate cancer cells. Drug Des Devel Ther 2015; 9: 1511-1554.

[42] Durlacher CT, Chow K, Chen XW, He ZX, Zhang X, Yang T and Zhou SF. Targeting Na^+/K^+-translocating adenosine triphosphatase in cancer treatment. Clin Exp Pharmacol Physiol 2015; 42: 427-443.

[43] Fuchs Y and Steller H. Programmed cell death in animal development and disease. Cell 2011; 147: 742-758.

[44] van Gurp M, Festjens N, van Loo G, Saelens X and Vandenabeele P. Mitochondrial intermembrane proteins in cell death. Biochem Biophys Res Commun 2003; 304: 487-497.

[45] Gottlieb E, Armour SM, Harris MH and Thompson CB. Mitochondrial membrane potential regulates matrix configuration and cytochrome c release during apoptosis. Cell Death Differ 2003; 10: 709-717.

[46] Alevizopoulos K, Calogeropoulou T, Lang F and Stournaras C. Na^+/K^+ ATPase inhibitors in cancer. Curr Drug Targets 2014; 15: 988-1000.

[47] Felippe Goncalves-de-Albuquerque C, Ribeiro Silva A, Ignacio da Silva C, Caire Castro-Faria-Neto H and Burth P. Na/K pump and beyond: Na/K-ATPase as a nodulator of apoptosis and autophagy. Molecules 2017; 22.

[48] Szegezdi E, Logue SE, Gorman AM and Samali A. Mediators of endoplasmic reticulum stress-induced apoptosis. EMBO Rep 2006; 7: 880-885.

[49] Pan ST, Zhou ZW, He ZX, Zhang X, Yang T, Yang YX, Wang D, Qiu JX and Zhou SF. Proteomic response to 5,6-dimethylxanthenone 4-acetic acid (DMXAA, vadimezan) in human non-small cell lung cancer A549 cells determined by the stable-isotope labeling by amino acids in cell culture (SILAC) approach. Drug Des Devel Ther 2015; 9: 937-968.

[50] Zhu Q, Yu X, Zhou ZW, Zhou C, Chen XW and Zhou SF. Inhibition of Aurora A kinase by alisertib induces autophagy and cell cycle arrest and increases chemosensitivity in human hepatocellular carcinoma HepG2 cells. Curr Cancer Drug Targets 2017; 17: 386-401.

[51] Yan Y and Shapiro JI. The physiological and clinical importance of sodium potassium ATPase in cardiovascular diseases. Curr Opin Pharmacol 2016; 27: 43-49.

[52] Aperia A, Akkuratov EE, Fontana JM and Brismar H. Na^+-K^+-ATPase, a new class of plasma membrane receptors. Am J Physiol Cell Physiol 2016; 310: C491-495.
[53] Grana X and Reddy EP. Cell cycle control in mammalian cells: role of cyclins, cyclin dependent kinases (CDKs), growth suppressor genes and cyclin-dependent kinase inhibitors (CKIs). Oncogene 1995; 11: 211-219.
[54] Morgan DO. Cyclin-dependent kinases: engines, clocks, and microprocessors. Annu Rev Cell Dev Biol 1997; 13: 261-291.
[55] Levine AJ. p53, the cellular gatekeeper for growth and division. Cell 1997; 88: 323-331.
[56] Shieh SY, Ikeda M, Taya Y and Prives C. DNA damage-induced phosphorylation of p53 alleviates inhibition by MDM2. Cell 1997; 91: 325-334.
[57] Taylor RC, Cullen SP and Martin SJ. Apoptosis: controlled demolition at the cellular level. Nat Rev Mol Cell Biol 2008; 9: 231-241.
[58] Green DR, Galluzzi L and Kroemer G. Cell biology. Metabolic control of cell death. Science 2014; 345: 1250256.
[59] Korsmeyer SJ, Wei MC, Saito M, Weiler S, Oh KJ and Schlesinger PH. Pro-apoptotic cascade activates BID, which oligomerizes BAK or BAX into pores that result in the release of cytochrome c. Cell Death Differ 2000; 7: 1166-1173.
[60] Cory S, Huang DC and Adams JM. The Bcl-2 family: roles in cell survival and oncogenesis. Oncogene 2003; 22: 8590-8607.
[61] Nunnari J and Suomalainen A. Mitochondria: in sickness and in health. Cell 2012; 148: 1145-1159.
[62] Banjerdpongchai R, Kongtawelert P, Khantamat O, Srisomsap C, Chokchaichamnankit D, Subhasitanont P and Svasti J. Mitochondrial and endoplasmic reticulum stress pathways cooperate in zearalenone-induced apoptosis of human leukemic cells. J Hematol Oncol 2010; 3: 50.
[63] Pihan P, Carreras-Sureda A and Hetz C. BCL-2 family: integrating stress responses at the ER to control cell demise. Cell Death Differ 2017; 24: 1478-1487.
[64] Song S, Tan J, Miao Y, Li M and Zhang Q. Crosstalk of autophagy and apoptosis: involvement of the dual role of autophagy under ER stress. J Cell Physiol 2017; 232: 2977-2984.
[65] Jeong SA, Kim IY, Lee AR, Yoon MJ, Cho H, Lee JS and Choi KS. Ca2+ influx-mediated dilation of the endoplasmic reticulum and c-FLIPL downregulation trigger CDDO-Me-induced apoptosis in breast cancer cells. Oncotarget 2015; 6: 21173-21192.
[66] Zou W, Yue P, Khuri FR and Sun SY. Coupling of endoplasmic reticulum stress to CDDO-Me-induced up-regulation of death receptor 5 via a CHOP-dependent mechanism involving JNK activation. Cancer Res 2008; 68: 7484-7492.
[67] Chiu SC, Chen SP, Huang SY, Wang MJ, Lin SZ, Harn HJ and Pang CY. Induction of apoptosis coupled to endoplasmic reticulum stress in human prostate cancer cells by n-butylidenephthalide. PLoS One 2012; 7: e33742.
[68] Quick QA and Faison MO. CHOP and caspase 3 induction underlie glioblastoma cell death in response to endoplasmic reticulum stress. Exp Ther Med 2012; 3: 487-492.
[69] Zhu Q, Yu X, Zhou ZW, Zhou C and Chen XW. Targeting Aurora A kinase with alisertib (ALS) induces autophagy and cell cycle arrest and increases chemosensitivity in hepatoblastoma HepG2 cells. Curr Cancer Drug Targets 2016.
[70] Li YC, He SM, He ZX, Li M, Yang Y, Pang JX, Zhang X, Chow K, Zhou Q, Duan W, Zhou ZW, Yang T, Huang GH, Liu A, Qiu JX, Liu JP and Zhou SF. Plumbagin induces apoptotic and autophagic cell death through inhibition of the PI3K/Akt/mTOR pathway in human non-small cell lung cancer cells. Cancer Lett 2014; 344: 239-259.
[71] Ravanan P, Srikumar IF and Talwar P. Autophagy: the spotlight for cellular stress responses. Life Sci 2017; 188: 53-67.
[72] Jung CH, Ro SH, Cao J, Otto NM and Kim DH. mTOR regulation of autophagy. FEBS Lett 2010; 584: 1287-1295.
[73] Sun Y, Liu WZ, Liu T, Feng X, Yang N and Zhou HF. Signaling pathway of MAPK/ERK in cell proliferation, differentiation, migration, senescence and apoptosis. J Recept Signal Transduct Res 2015; 35: 600-604.
[74] He SJ, Shu LP, Zhou ZW, Yang T, Duan W, Zhang X, He ZX and Zhou SF. Inhibition of Aurora kinases induces apoptosis and autophagy via AURKB/p70S6K/RPL15 axis in human leukemia cells. Cancer Lett 2016; 382: 215-230.
[75] Cuadrado A and Nebreda AR. Mechanisms and functions of p38 MAPK signalling. Biochem J 2010; 429: 403-417.

Table S1. The 1557 protein molecules regulated by CDDO-Me in K562 cells

	Gene names	*Mol. weight [kDa]*	*Ratio H/L normalized*
1	*FANCI*	123.24	0.15118
2	*SRPK2*	77.526	0.30958
3	*XPO5*	136.31	0.34669
4	*HP1BP3*	61.206	0.39492
5	*NELFCD; TH1L*	65.478	0.39712
6	*HIST1H1C*	21.364	0.40766
7	*HMGA1*	10.679	0.4109
8	*ZC3HC1*	47.771	0.41357
9	*PCK2*	70.729	0.42607
10	*FDFT1*	48.115	0.43071
11	*STAT5A*	87.361	0.43188
12	*STAT5B*	89.865	0.43788
13	*CCNK*	41.293	0.46059
14	*DHCR7*	54.489	0.47687
15	*TRIP10*	52.699	0.47736
16	*HRC*	77.571	0.48875
17	*SKP1*	18.658	0.49059
18	*NOC3L*	92.547	0.50305
19	*NDUFA9*	42.509	0.50669
20	*EIF4G1*	158.52	0.53124
21	*TBRG4*	70.737	0.5313
22	*TTI1*	122.07	0.53455
23	*TNPO3*	102.54	0.53487
24	*DNAJA2*	45.745	0.54256
25	*SNCG*	13.331	0.54828
26	*UBE2L3*	17.861	0.55232
27	*ATP6V0A1*	95.755	0.55335
28	*NDUFA13; YJEFN3*	16.698	0.55542
29	*CAST*	63.665	0.55577
30	*DOHH*	24.385	0.56133
31	*NHP2*	17.201	0.56159
32	*KIAA1967*	103.14	0.56504
33	*STIM1*	77.422	0.56751
34	*NANS*	40.307	0.56844
35	*SLC1A5*	56.598	0.57504
36	*ATG7*	75.001	0.5833
37	*ZC3H4*	95.425	0.58401
38	*KPNB1*	97.169	0.58615
39	*FBXO6*	33.932	0.58652
40	*TFR2*	69.617	0.58668
41	*PSMB6*	25.357	0.59191
42	*HEMGN*	55.34	0.59293
43	*SAMSN1*	34.178	0.59459
44	*MCTS1*	19.228	0.59715
45	*FUS*	53.354	0.59841
46	*HADHB*	48.879	0.60323
47	*VAT1*	41.92	0.60628

48	*TPP1*	34.463	0.60675
49	*DDX23*	95.581	0.60972
50	*SMAP2*	37.697	0.61297
51	*TBK1*	83.641	0.617
52	*CISD2*	5.1441	0.61821
53	*PTDSS1*	34.579	0.6195
54	*RAC1*	21.45	0.61957
55	*SF1*	59.711	0.62157
56	*THOP1*	78.839	0.62235
57	*SNRNP70*	51.556	0.62246
58	*RPL19*	23.134	0.62433
59	*HMGA1*	11.676	0.62563
60	*DHX30*	129.44	0.6262
61	*IPO4*	118.71	0.63328
62	*PDHB*	37.2	0.63435
63	*SERPINB9*	42.403	0.63495
64	*TOR1AIP1*	52.406	0.63678
65	*AP1B1*	103.56	0.64032
66	*PRRC2A*	227.84	0.64068
67	*MYO1D*	49.768	0.64148
68	*FAM50A*	30.693	0.64243
69	*ELP3*	62.258	0.6471
70	*SLIRP*	12.122	0.64874
71	*BROX*	42.871	0.65133
72	*THOC6*	32.89	0.65142
73	*NOC4L*	58.467	0.65262
74	*TGM2*	77.328	0.6555
75	*MRPS9*	45.834	0.65615
76	*PICALM*	66.392	0.65682
77	*MRPS27*	41.329	0.65767
78	*NDUFS1*	66.921	0.65789
79	*DIS3*	63.616	0.65847
80	*CRYZ*	31.528	0.65891
81	*ECHS1*	31.387	0.65975
82	*PRRC2C*	295.73	0.65997
83	*HEATR2*	72.472	0.66048
84	*GPD2*	41.512	0.66074
85	*TCOF1*	144.31	0.66273
86	*APOA1BP*	20.43	0.66343
87	*TRMT1L*	81.746	0.66358
88	*ELOVL5*	30.742	0.66384
89	*HNRNPA3*	37.029	0.66744
90	*VAPA*	27.893	0.66793
91	*RAD23B*	43.171	0.66941
92	*WIBG*	22.704	0.67174
93	*NUPL1*	49.095	0.6728
94	*HBA1; HBA2*	15.257	0.67285
95	*NOL9*	79.322	0.6736
96	*RRP12*	132.71	0.67449

97	*MPST*	33.178	0.67802
98	*RAP2B*	20.504	0.67855
99	*UBE2N*	17.138	0.67933
100	*ATP6V1D*	21.921	0.67934
101	*PDXK*	30.638	0.67942
102	*FTO*	12.218	0.6801
103	*SAE1*	38.449	0.68067
104	*POLD1*	111.68	0.68325
105	*GCN1L1*	292.75	0.68354
106	*C2orf43; FLJ21820*	37.318	0.68503
107	*THOC5*	78.507	0.68528
108	*PDCD2*	35.29	0.68632
109	*PDS5A*	150.83	0.68656
110	*CSTF2; CSTF2T*	59.251	0.68706
111	*SORD*	38.324	0.68813
112	*BAZ1B*	170.45	0.68933
113	*MT-CO2*	25.565	0.69152
114	*SLC27A2*	70.311	0.69153
115	*ALDH16A1*	79.917	0.6928
116	*RCL1*	40.842	0.69373
117	*PAFAH1B3*	25.734	0.69561
118	*MRPL28*	30.156	0.69807
119	*PRKDC*	469.08	0.6982
120	*PPT1*	34.193	0.69835
121	*PDLIM5*	52.645	0.69844
122	*ZNF207*	49.692	0.70232
123	*CUTA*	16.832	0.70303
124	*SCCPDH*	47.151	0.70373
125	*SLC9A3R2*	17.803	0.70462
126	*TAF15*	61.557	0.70634
127	*FDXR*	53.836	0.70692
128	*AIMP1*	34.352	0.70727
129	*AK2*	25.614	0.70764
130	*KHSRP*	73.114	0.70779
131	*HDGF*	26.788	0.70985
132	*ATP6V1B2*	56.5	0.71011
133	*IARS2*	113.79	0.71023
134	*SEPT2*	36.94	0.71105
135	*CUL5*	90.954	0.71263
136	*CTCF*	82.785	0.71399
137	*CHAF1B*	61.492	0.715
138	*DCTN2*	34.258	0.71503
139	*VIM*	53.651	0.71506
140	*APOBEC3B*	45.924	0.71514
141	*DDB1*	126.97	0.71898
142	*ATP1A1*	113	0.71923
143	*UBAC1*	45.338	0.71967
144	*SRPK1*	72.383	0.71996
145	*RHOG*	21.308	0.72217

146	*NCBP1*	91.838	0.72292
147	*PTRF*	43.476	0.72549
148	*AIMP2*	35.348	0.72572
149	*CBX5*	22.225	0.72594
150	*EIF4H*	25.2	0.72744
151	*PPP2R1B*	52.213	0.72782
152	*PREP*	80.699	0.72848
153	*LYPLA2*	24.737	0.7314
154	*KDM1A*	92.902	0.73155
155	*BMS1*	145.81	0.73159
156	*HUWE1*	480.19	0.73385
157	*NTMT1*	15.896	0.73621
158	*FKBP8*	44.561	0.73686
159	*DNM2*	97.651	0.73716
160	*FLNB*	271.41	0.73747
161	*DPY30*	11.25	0.74076
162	*PRKAR2B*	46.302	0.74221
163	*ALDH1B1*	57.206	0.74282
164	*MRPL44*	37.535	0.74525
165	*DHX16*	119.26	0.74557
166	*FAM49B*	36.748	0.7461
167	*TK1*	25.468	0.74642
168	*TOMM40*	37.893	0.74652
169	*ECH1*	35.816	0.74802
170	*PYCR2*	25.868	0.74838
171	*HDAC2*	51.998	0.74894
172	*CNOT11*	14.248	0.74938
173	*DDX52*	67.497	0.75007
174	*PELP1*	119.7	0.75171
175	*SF3B2*	97.584	0.75223
176	*MYBBP1A*	140.13	0.75307
177	*DUT*	17.748	0.75378
178	*LAMTOR1*	17.745	0.75497
179	*SLC25A10; MRPL12*	48.099	0.75591
180	*DDX20*	92.239	0.75658
181	*NAP1L4*	42.823	0.75676
182	*PMPCA*	58.252	0.75697
183	*MSH6*	119.79	0.757
184	*RBM15*	99.7	0.75728
185	*LRPPRC*	157.9	0.75787
186	*SEC24C*	118.32	0.75874
187	*AIP*	37.636	0.75915
188	*SUGT1*	37.804	0.76124
189	*OPA1*	111.63	0.76199
190	*CSK*	50.704	0.76273
191	*ISOC1*	32.236	0.76344
192	*RRBP1*	84.325	0.7635
193	*EEF1A2*	50.47	0.76366
194	*SLC25A1*	34.012	0.76449

195	*CPSF1*	160.88	0.76456
196	*SNX9*	66.476	0.76501
197	*UBE2I*	15.516	0.76559
198	*MDN1*	632.81	0.76563
199	*XPOT*	109.96	0.76595
200	*COPG2*	97.621	0.76782
201	*UFD1L*	34.5	0.76916
202	*UQCRC2*	48.442	0.7697
203	*POLDIP2*	42.033	0.77032
204	*SEC16A*	228.87	0.77052
205	*SRRM2*	299.61	0.77172
206	*PSIP1*	60.103	0.77199
207	*GLOD4*	33.232	0.77221
208	*ARHGAP1*	50.435	0.77237
209	*UBA6*	117.97	0.77272
210	*NELFB*	65.697	0.77274
211	*CSE1L*	110.42	0.77401
212	*CTH*	39.505	0.77428
213	*PC*	129.63	0.77434
214	*MCFD2*	10.718	0.77649
215	*OGFOD1*	63.245	0.77826
216	*PDCD10*	24.701	0.77838
217	*CTNND1*	68.03	0.7784
218	*ACAT1*	45.199	0.77888
219	*CNDP2*	52.878	0.77906
220	*DECR1*	34.994	0.77947
221	*ETFA*	35.079	0.77967
222	*FEN1*	42.592	0.78016
223	*GTF3C4*	91.981	0.78166
224	*PLIN3*	45.803	0.78215
225	*SSSCA1*	20.916	0.78468
226	*NOB1*	46.674	0.78549
227	*C21orf33*	25.64	0.78557
228	*NHP2L1*	14.173	0.78623
229	*ATP5D*	17.49	0.78655
230	*PPP2R5D*	58.452	0.7866
231	*CLCC1*	62.022	0.78713
232	*PPM1F*	49.83	0.78732
233	*TACC3*	90.359	0.78755
234	*PTPN23*	178.97	0.78796
235	*HINT1*	13.802	0.78878
236	*DKC1*	57.673	0.78958
237	*STMN1*	17.302	0.79065
238	*NDC1*	63.572	0.79086
239	*HSD17B10*	26.923	0.79134
240	*ACADM*	42.426	0.79193
241	*RHOA; RHOC*	21.768	0.79229
242	*ASH2L*	55.324	0.79326
243	*GAPVD1*	157.46	0.79365

244	*POLR2E*	21.459	0.79392
245	*NQO2*	25.918	0.79468
246	*SNRPA*	31.279	0.79596
247	*MAPRE1*	29.999	0.79603
248	*GORASP2*	39.768	0.7961
249	*PARK7*	19.891	0.79616
250	*UBXN1*	32.913	0.79637
251	*IDH3A*	31.381	0.79715
252	*PAGE5*	11.777	0.79766
253	*RAE1*	40.968	0.79848
254	*DPM1*	29.634	0.79872
255	*MTX1*	35.777	0.79944
256	*PGAM1*	28.804	0.80062
257	*PANK4*	85.99	0.8008
258	*MTA2*	75.022	0.8019
259	*IK*	28.236	0.80223
260	*ECI1; DCI*	32.816	0.80276
261	*FECH*	47.862	0.80348
262	*VPS26A*	38.169	0.80356
263	*SHMT2*	53.454	0.80367
264	*ISYNA1*	47.146	0.80387
265	*BLMH*	52.562	0.80402
266	*VPS29*	20.505	0.80467
267	*YBX1*	35.924	0.80641
268	*ACAT2*	41.35	0.80724
269	*PDAP1*	20.63	0.80864
270	*UQCRFS1; UQCRFS1P1*	29.668	0.8088
271	*SDHA*	72.691	0.80895
272	*WARS*	53.165	0.81014
273	*SOD1*	15.936	0.81052
274	*TECR*	36.034	0.81102
275	*GATAD2A*	65.225	0.81199
276	*UBL4A*	17.776	0.81308
277	*RRP9*	51.84	0.81312
278	*UBE2V1; TMEM189; UBE2V2*	16.495	0.81319
279	*NDUFS2*	51.851	0.81441
280	*OTUB1*	31.284	0.81471
281	*PNP*	32.118	0.81474
282	*DDX6*	54.416	0.81482
283	*MAP4*	119.96	0.81512
284	*TRIP6*	50.287	0.81553
285	*RPS20*	13.373	0.81603
286	*PTMA*	11.758	0.81623
287	*TIMM50*	39.646	0.81693
288	*NUDCD1*	63.501	0.81701
289	*PGAM5*	28.02	0.81714
290	*SRSF7*	15.257	0.81726
291	*CBS*	60.586	0.81847
292	*PDLIM1*	36.071	0.81877

293	*AGPS*	72.911	0.81887
294	*LARP1*	116.46	0.81906
295	*AP2M1*	49.389	0.81939
296	*SKIV2L2*	117.8	0.81947
297	*CAPZB*	30.628	0.81964
298	*FERMT3*	75.429	0.81987
299	*CALB1*	30.025	0.82037
300	*ACTA1; ACTC1; ACTG2; ACTA2*	42.051	0.8229
301	*MST4; STK25*	37.77	0.82324
302	*FDPS*	40.532	0.82492
303	*EMC1*	109.42	0.82567
304	*UMPS*	52.221	0.82579
305	*EIF2B4*	57.557	0.82643
306	*VCP*	89.321	0.82652
307	*SLC25A24*	51.354	0.82655
308	*DDX47*	45.169	0.82674
309	*NUDT21*	26.227	0.82735
310	*VRK1*	45.476	0.82745
311	*DIABLO*	17.785	0.8285
312	*THUMPD1*	39.315	0.82907
313	*ILF2*	38.91	0.83016
314	*RCOR1; RCOR3*	53.027	0.8304
315	*CAPZA1*	32.922	0.83058
316	*ESYT1*	122.85	0.83058
317	*IPO11*	112.53	0.83074
318	*PGLS*	27.547	0.83104
319	*MOB1A; MOB1B*	25.079	0.83105
320	*AP2B1*	98.117	0.83109
321	*QPRT*	30.845	0.83113
322	*LYPLA1*	17.981	0.83135
323	*HSPA14*	54.794	0.83146
324	*PRDX3*	25.838	0.83148
325	*VARS*	140.47	0.83163
326	*PDCD11*	208.7	0.832
327	*HEATR3*	65.812	0.83253
328	*PRDX2*	21.892	0.83297
329	*MTCH2*	33.331	0.83323
330	*NDRG2*	30.495	0.83368
331	*RFC3*	34.756	0.83375
332	*CHCHD3*	26.152	0.83433
333	*PRMT5*	71.319	0.83454
334	*MACF1*	505.64	0.8348
335	*AHNAK*	629.09	0.83516
336	*TTLL12*	74.403	0.8356
337	*IDE*	117.97	0.8359
338	*GMPS*	76.715	0.83591
339	*TLN1*	269.76	0.83607
340	*NUDT5*	14.901	0.83621
341	*TUBA1C; TUBA1B*	49.895	0.83631

342	*PGPEP1*	23.138	0.83651
343	*PFN1*	15.054	0.83688
344	*CLIC1*	26.922	0.83723
345	*WDR12*	47.707	0.83793
346	*EPHX2*	58.855	0.83814
347	*PSAP*	58.112	0.83889
348	*TPRKB*	19.661	0.84007
349	*PPAT*	57.398	0.84066
350	*AP3B1*	116.19	0.84072
351	*YES1*	60.801	0.84077
352	*ANP32B*	22.276	0.84109
353	*MDH2*	35.503	0.84283
354	*ESD*	28.226	0.84315
355	*SUPT16H*	119.91	0.84391
356	*SNRPB2*	25.486	0.84397
357	*PSPC1*	45.57	0.84458
358	*DLST*	48.755	0.84467
359	*PSMD14*	34.577	0.84498
360	*PSMA5*	26.411	0.84509
361	*PPIA*	18.012	0.84593
362	*SMC3*	141.54	0.84621
363	*WASF2; WASF3*	31.979	0.8469
364	*GSTO1*	27.566	0.84729
365	*AKR1A1*	36.573	0.84763
366	*IGF2BP2*	54.721	0.84875
367	*RPS21*	8.85	0.849
368	*TMEM33*	25.223	0.84915
369	*TAGLN2*	22.391	0.84915
370	*LTN1*	200.55	0.84976
371	*IPO9*	115.96	0.84985
372	*CCAR1*	131.04	0.85067
373	*FAM98B*	37.19	0.85132
374	*LRRC47*	63.472	0.85138
375	*LSM3*	11.845	0.85146
376	*AIFM1*	66.294	0.85221
377	*SF3B1*	145.83	0.85237
378	*PRPF4*	58.32	0.85239
379	*MMS19*	108.38	0.85251
380	*DCTPP1*	18.681	0.85254
381	*CYCS*	11.333	0.85255
382	*VPS45*	22.994	0.85259
383	*CARM1*	63.459	0.85303
384	*RANBP1*	23.239	0.85311
385	*RRP1*	52.839	0.85336
386	*FKBP5*	51.212	0.85442
387	*SEPT11; SEPT6*	49.005	0.85513
388	*PPM1G*	59.271	0.85662
389	*TIA1*	31.624	0.85737
390	*LAGE3*	14.804	0.85748

391	*CMBL*	28.048	0.85753
392	*ACTL6A*	47.46	0.85796
393	*CUL2*	82.358	0.85844
394	*RBM8A*	19.889	0.85895
395	*SNRPF*	9.7251	0.85896
396	*ATP5O*	23.277	0.85901
397	*H2AFV; H2AFZ*	13.509	0.86051
398	*BSG*	17.36	0.86081
399	*CWC22*	85.576	0.86091
400	*CHRAC1*	6.2643	0.86103
401	*RAN*	24.423	0.86107
402	*CPNE1*	58.634	0.86108
403	*OCIAD1*	21.592	0.8612
404	*YTHDF2*	56.877	0.86178
405	*PSMA2*	25.898	0.86202
406	*EIF2S3; EIF2S3L*	51.109	0.86274
407	*HMGB3*	17.522	0.86323
408	*PRC1*	66.595	0.86415
409	*DENR*	17.77	0.8644
410	*AQR*	171.29	0.86511
411	*UCHL5*	36.079	0.86565
412	*ALDOC*	39.455	0.86579
413	*CDK2; CDK3*	27.164	0.86583
414	*RAP1B*	20.825	0.86594
415	*NASP*	85.237	0.86625
416	*BLVRA*	33.428	0.86731
417	*ALDOA*	39.42	0.8675
418	*TRIM25*	70.973	0.86771
419	*TOP2B*	182.66	0.86783
420	*POLR1C*	38.646	0.86802
421	*ATP1B3*	31.512	0.86806
422	*SUMO2; SUMO4; SUMO3*	8.1111	0.86838
423	*NUP153*	149.39	0.86874
424	*EIF6*	26.599	0.86974
425	*CLIC4*	28.772	0.87013
426	*GPS1*	53.371	0.87033
427	*DYNC1I2*	68.297	0.87067
428	*PCBP2*	34.917	0.87068
429	*EDF1*	15.48	0.87076
430	*EWSR1*	62.507	0.87087
431	*WDR36*	99.365	0.87109
432	*MEMO1*	31.307	0.87144
433	*GLUD1; GLUD2*	61.397	0.87162
434	*BCAS2*	26.131	0.87208
435	*CAP1*	51.901	0.87236
436	*SET*	32.103	0.87236
437	*MSH2*	97.321	0.87329
438	*HIST2H2AC; HIST2H2AA3*	13.988	0.87349
439	*DDX24*	91.48	0.87362

440	*IDH3B*	41.219	0.87492
441	*RPRD1B*	36.899	0.87523
442	*CS*	50.431	0.8753
443	*HTATSF1*	85.852	0.87566
444	*VCL*	116.72	0.8757
445	*RBBP4*	46.158	0.87578
446	*BLVRB*	22.119	0.87623
447	*SART1*	90.254	0.87632
448	*SLC16A1*	53.944	0.87637
449	*SF3B3*	135.58	0.87676
450	*IDI1*	26.319	0.87686
451	*ADSL*	54.889	0.87687
452	*MDH1*	36.426	0.87709
453	*SLC43A3*	36.797	0.87722
454	*UQCRC1*	52.645	0.87776
455	*PPIH*	15.8	0.87848
456	*ZYX*	61.277	0.87895
457	*ANP32E*	30.692	0.879
458	*NME1*	17.149	0.87968
459	*USP7*	126.27	0.87979
460	*ANP32A*	28.585	0.88108
461	*DPP3*	79.306	0.88137
462	*RPL22*	14.787	0.88155
463	*MTPN*	12.895	0.88236
464	*MAGOHB; MAGOH*	17.276	0.88246
465	*RCC2*	56.084	0.8826
466	*CANX*	67.567	0.8829
467	*PAICS*	47.079	0.88347
468	*NMNAT1*	31.932	0.88407
469	*HNRNPA0*	30.84	0.88408
470	*RPL23*	14.865	0.88457
471	*STAT1*	83.042	0.8848
472	*WDR1*	66.193	0.88482
473	*COPS3*	47.873	0.88513
474	*HADHA*	82.999	0.88523
475	*PRDX5*	17.031	0.886
476	*UROD*	40.786	0.8864
477	*SMARCA4*	181.26	0.88718
478	*PAIP1*	53.524	0.88735
479	*FLOT1*	47.355	0.88807
480	*FLNC*	287.28	0.88869
481	*ZNF598*	93.287	0.88879
482	*COMT*	24.449	0.88899
483	*PSMD5*	56.195	0.88905
484	*TCEA1*	33.969	0.88933
485	*PAK2; PAK3*	58.042	0.88944
486	*TUFM*	49.541	0.88959
487	*LCP1*	70.288	0.88961
488	*RAB11B; RAB11A*	24.488	0.89004

489	*IGF2BP1*	63.48	0.89024
490	*ELAC2*	70.106	0.89048
491	*PCMT1*	24.636	0.89114
492	*TUBB4B*	49.83	0.89128
493	*TYMS*	35.716	0.89304
494	*PRDX6*	25.035	0.89346
495	*BTF3*	22.168	0.89348
496	*SCFD1*	72.379	0.89364
497	*RPS2*	31.324	0.89369
498	*NONO*	54.231	0.89411
499	*PABPN1*	31.496	0.89434
500	*ATP2A2*	109.73	0.89443
501	*CRKL*	33.777	0.89451
502	*RIC8A*	58.942	0.89462
503	*THOC2*	182.77	0.89462
504	*PFDN5*	17.328	0.89464
505	*PEBP1*	21.057	0.89487
506	*PPIL1*	18.237	0.89544
507	*SNRPE*	10.803	0.89564
508	*CUL1*	87.387	0.89572
509	*XRCC6*	69.842	0.89598
510	*ARHGEF2*	108.24	0.896
511	*PRIM2*	58.805	0.89601
512	*LONP1*	95.179	0.89609
513	*HMBS*	35.761	0.89654
514	*NSUN2*	86.47	0.897
515	*PTGES2*	41.943	0.89704
516	*SLC29A1*	50.219	0.8974
517	*PPP2R1A*	65.308	0.89879
518	*G3BP2*	50.817	0.89882
519	*AFG3L2*	88.583	0.89896
520	*EPPK1*	555.61	0.89917
521	*PLEC*	512.6	0.8996
522	*KLC1*	62.506	0.90109
523	*RPS6KA3*	83.735	0.90122
524	*DRG1*	40.542	0.90148
525	*PRDX1*	22.11	0.9015
526	*RNPEP*	72.595	0.90182
527	*HNRNPM*	77.515	0.90215
528	*AP2A1*	105.36	0.90217
529	*UBTF*	84.936	0.90233
530	*FASN*	273.42	0.9024
531	*GNPDA1; GNPDA2*	32.668	0.90249
532	*ACLY*	119.77	0.90271
533	*CBX3*	20.811	0.90279
534	*GDI1*	50.582	0.90415
535	*GRHPR*	35.668	0.90425
536	*ATP5J2; PTCD1; ATP5J2-PTCD1*	5.7407	0.90463

537	*UTP20*	318.38	0.9047
538	*RAVER1*	77.843	0.90478
539	*MARS*	101.11	0.90502
540	*ABCE1*	67.314	0.90563
541	*ALDH18A1*	87.088	0.9058
542	*UBA1*	113.8	0.9059
543	*GALE*	38.281	0.90664
544	*SMCHD1*	215.74	0.90701
545	*GDI2*	50.663	0.90741
546	*RSU1*	31.54	0.90743
547	*MTHFD1*	101.56	0.9075
548	*RBM28*	85.737	0.90776
549	*AGK*	43.796	0.90822
550	*TSN*	26.183	0.90823
551	*HBD; HBB*	16.055	0.90849
552	*SMS*	41.268	0.90858
553	*SRRT*	100.15	0.90861
554	*PPIF*	22.04	0.90908
555	*PRPS2*	34.769	0.90914
556	*ACP1*	18.042	0.90938
557	*USP39*	56.358	0.91036
558	*SCAMP3*	38.287	0.91048
559	*SNRPD1*	13.281	0.9107
560	*RING1*	39.145	0.91099
561	*TUBG2; TUBG1*	51.091	0.91116
562	*CORO1C*	53.248	0.91122
563	*DHX38*	140.5	0.91131
564	*XPO7*	123.91	0.91137
565	*AASDHPPT*	35.776	0.9114
566	*RDX*	68.563	0.91147
567	*CYC1*	35.422	0.91149
568	*PSMD1*	102.26	0.91217
569	*PDIA6*	47.837	0.91239
570	*KIF2C*	81.312	0.9124
571	*SERPINB6*	42.621	0.91266
572	*H2AFY*	39.183	0.91358
573	*PTPN1*	49.966	0.91374
574	*MAT2B*	28.954	0.91412
575	*FIS1*	16.937	0.91441
576	*PEA15*	15.04	0.91455
577	*BZW1*	40.538	0.91461
578	*DNAJC2*	71.996	0.91507
579	*EIF3G*	35.611	0.91603
580	*SUMO1*	11.557	0.91612
581	*HNRNPF*	45.671	0.91621
582	*SAR1B;DKFZp434B2017*	22.41	0.91622
583	*USMG5*	6.4575	0.9165
584	*PGM2*	68.283	0.91657
585	*EEF1B2*	24.763	0.91694

586	*API5*	56.769	0.91702
587	*HAT1*	49.512	0.91731
588	*FBL*	33.784	0.91849
589	*IDH2*	45.179	0.91867
590	*UBQLN1*	59.219	0.91873
591	*HIST1H1E*	21.865	0.91878
592	*TBCD*	132.6	0.91945
593	*MRPS22*	36.805	0.91959
594	*ANK1*	197.75	0.91984
595	*PKLR*	61.829	0.9199
596	*PSMD7*	37.025	0.92053
597	*STAU1*	54.945	0.92074
598	*CYB5R3*	31.628	0.92088
599	*PSME3*	29.506	0.92107
600	*PFKL*	85.018	0.92141
601	*SFPQ*	76.149	0.92148
602	*DNAJC8*	29.841	0.92149
603	*SEPT9*	47.501	0.92221
604	*SNRPA1*	28.415	0.92262
605	*HNRNPAB*	30.302	0.92301
606	*NAA15*	101.2	0.92304
607	*UGP2*	55.676	0.92306
608	*TEX10*	103.91	0.92326
609	*PUS1*	41.729	0.92383
610	*EIF5A; EIF5AL1*	16.832	0.92431
611	*SARS*	58.777	0.92474
612	*TRMT10C*	47.346	0.92479
613	*RPL7L1*	28.661	0.92523
614	*SLC25A13*	74.175	0.92527
615	*UBQLN2*	65.695	0.92533
616	*MRTO4*	27.56	0.92621
617	*ACADVL*	68.058	0.92644
618	*GANAB*	106.87	0.92645
619	*RPS13*	17.222	0.92666
620	*CDC37*	44.468	0.92754
621	*TWF2*	39.548	0.92765
622	*FADD*	23.279	0.92775
623	*RAP2C*	13.512	0.9279
624	*SFXN1*	35.619	0.92839
625	*KPNA1*	60.221	0.9288
626	*SEPHS1*	35.62	0.92886
627	*TARDBP*	44.739	0.92898
628	*TBL3*	89.034	0.92937
629	*PTBP1*	57.221	0.92971
630	*GARS*	83.165	0.9302
631	*HDAC1*	55.102	0.93046
632	*SARNP*	23.671	0.93057
633	*SERPINB1*	42.741	0.93074
634	*ATXN10*	53.488	0.9314

635	*PRMT1*	37.709	0.93171
636	*RNH1*	49.973	0.93221
637	*KIF5B*	109.68	0.93289
638	*SF3A1*	88.885	0.93294
639	*TPI1*	26.669	0.93308
640	*CKB*	42.644	0.93384
641	*YWHAH*	28.218	0.93427
642	*CAPN1*	81.889	0.93429
643	*ADH5*	39.724	0.93457
644	*SEC23A*	82.968	0.93477
645	*SMC1A*	140.86	0.93627
646	*PFAS*	144.73	0.9367
647	*SYNCRIP*	62.656	0.93672
648	*FTH1*	21.225	0.93687
649	*DNTTIP2*	84.468	0.937
650	*PPP1CA*	37.512	0.93705
651	*CAT*	59.755	0.9379
652	*TRA2B*	21.935	0.93814
653	*CEBPZ*	114.16	0.93818
654	*THYN1*	25.697	0.93909
655	*TUBB*	47.766	0.93959
656	*DEK*	42.674	0.93974
657	*CPNE3; CPNE8; CPNE5; CPNE2; CPNE9; CPNE4; CPNE6; CPNE7*	60.13	0.93988
658	*XRCC5*	82.704	0.93992
659	*FH*	50.212	0.9404
660	*PSMB2*	22.836	0.94044
661	*ACAA1*	44.292	0.94053
662	*HADH*	34.293	0.94077
663	*PRPF40A*	105.93	0.94209
664	*NAT10*	115.73	0.94234
665	*CLIC2*	28.356	0.94235
666	*CLUH*	140.49	0.94235
667	*PUF60*	55.399	0.94246
668	*CDKN2AIP*	61.124	0.94264
669	*PHGDH*	56.65	0.94287
670	*APEX1*	35.554	0.94289
671	*HMGB2*	24.033	0.943
672	*ENY2*	10.984	0.94338
673	*NCL*	76.613	0.94395
674	*TES*	46.91	0.94423
675	*MAPK1*	41.389	0.94444
676	*UBR4*	571.85	0.94469
677	*ATAD3A; ATAD3B*	66.217	0.94502
678	*NDUFS8*	12.405	0.94531
679	*BCAT1*	42.837	0.94546
680	*DLAT*	68.996	0.94557
681	*TSNAX; DISC1*	33.112	0.94558
682	*GSTP1*	23.356	0.94605

683	*IMMT*	83.548	0.94617
684	*GOT1*	46.247	0.94623
685	*PCNA*	28.768	0.94636
686	*LMNA*	74.139	0.94701
687	*MPP1*	49.074	0.94716
688	*EXOSC2*	32.789	0.94764
689	*LIG1*	88.386	0.94768
690	*THRAP3*	108.66	0.94771
691	*HEATR1*	242.37	0.94791
692	*LBR*	70.702	0.94847
693	*PTPLAD1*	43.159	0.9492
694	*RPL23A*	17.695	0.94924
695	*UTP3*	54.557	0.94987
696	*ATP6V1H*	51.57	0.95004
697	*HIBCH*	38.012	0.95021
698	*TIMM13*	10.5	0.95037
699	*SRM*	33.824	0.95055
700	*PSMG1*	30.288	0.95069
701	*MSN*	67.819	0.95098
702	*FLNA*	278.22	0.95108
703	*MYL12A; MYL12B; MYL9*	19.794	0.95154
704	*ADSS*	50.097	0.95195
705	*XPNPEP1*	62.138	0.95223
706	*ABCF2*	71.289	0.95256
707	*EIF2B3*	44.803	0.95267
708	*OGDH*	115.51	0.95296
709	*CYFIP1*	145.18	0.95348
710	*RPS15*	17.04	0.95389
711	*HNRNPR; HNRPR*	70.942	0.95394
712	*RUVBL1*	50.227	0.95424
713	*PNO1*	27.924	0.95425
714	*EXOSC10*	98.088	0.95452
715	*UBA2*	71.223	0.95452
716	*CD2AP*	71.45	0.95453
717	*IPO8*	119.94	0.95461
718	*RTCA*	39.336	0.95518
719	*FAH*	46.374	0.95525
720	*KRT18*	48.057	0.95529
721	*ORC2*	65.971	0.95536
722	*APRT*	19.608	0.95548
723	*RAD50*	153.89	0.95591
724	*FUBP1*	67.56	0.95599
725	*WDR77*	36.724	0.95612
726	*FARSA*	54.157	0.95635
727	*TIMM44*	51.355	0.95656
728	*PCNP*	13.544	0.95696
729	*SRSF10*	20.117	0.95713
730	*ELAVL1*	36.091	0.95726
731	*PES1*	66.077	0.95773

732	*TKT*	67.877	0.9578
733	*ERP29*	28.993	0.95811
734	*PCBP1*	37.497	0.95819
735	*YARS*	59.143	0.95829
736	*MFAP1*	51.958	0.9586
737	*PBK*	36.085	0.95878
738	*HBG2*	16.126	0.95928
739	*GART*	107.77	0.95944
740	*DDX39B*	48.991	0.95995
741	*S100A11*	11.74	0.96025
742	*EEF1E1; hCG_2043275*	15.548	0.96036
743	*CCDC124*	25.835	0.96055
744	*CCDC6*	53.29	0.96113
745	*LMNA*	65.134	0.96117
746	*DDX17*	80.272	0.96203
747	*NOMO2; NOMO1; NOMO3*	122.06	0.96217
748	*LRRFIP1*	82.688	0.96266
749	*CLTC*	187.89	0.96295
750	*TUBB8*	49.775	0.96311
751	*PSMC5*	44.784	0.96314
752	*PSMC1*	49.184	0.96315
753	*KHDRBS1*	48.227	0.96316
754	*TXNDC17*	13.941	0.96377
755	*HNRNPA3*	39.594	0.96385
756	*SUB1*	14.395	0.96396
757	*RPLP1*	11.514	0.96423
758	*LDHB*	36.638	0.96431
759	*USP14*	56.068	0.96481
760	*RPN2*	67.723	0.96555
761	*COPS5*	37.578	0.96563
762	*H3F3B; H3F3A; HIST3H3; H3F3C*	14.914	0.96578
763	*RPS27A*	17.965	0.96605
764	*RMDN3*	34.038	0.96613
765	*MATR3*	94.622	0.96626
766	*TROVE2*	60.67	0.9663
767	*EFTUD2*	105.38	0.96656
768	*FARSB*	66.115	0.96726
769	*MYO18A*	226.69	0.96728
770	*CDK6*	36.938	0.96753
771	*AHCY*	47.716	0.96756
772	*ETFB*	27.843	0.96761
773	*C14orf166*	28.068	0.96827
774	*USP5*	93.307	0.96828
775	*HBE1*	16.203	0.96864
776	*CDK11A; CDK11B; CDC2L1*	45.229	0.96883
777	*PTGES3*	16.476	0.96911
778	*RPL8*	22.389	0.96924
779	*ADK*	38.703	0.96998
780	*HBZ*	15.637	0.97033

781	*IARS*	144.5	0.97051
782	*PSMA7*	27.887	0.97078
783	*G6PD*	59.256	0.97145
784	*NIP7*	20.462	0.97159
785	*COMMD9*	17.333	0.97168
786	*PDCD6IP*	96.022	0.97174
787	*PSME2*	27.401	0.97178
788	*HBS1L*	56.961	0.97191
789	*SF3A3*	58.848	0.97209
790	*GLRX3*	37.432	0.97228
791	*ILF3*	95.337	0.97277
792	*CALM1; CALM2; CALM3*	16.837	0.97287
793	*PSMA4*	29.483	0.97299
794	*NUP214*	212.57	0.97354
795	*IDH1*	46.659	0.97379
796	*TCEB1*	12.473	0.97432
797	*HNRNPL*	64.132	0.97491
798	*OGFR*	71.423	0.97545
799	*SPR*	28.048	0.97584
800	*MRE11A*	77.641	0.97591
801	*ACTN4*	104.85	0.97643
802	*RPL11*	20.252	0.97666
803	*RPL13*	24.261	0.97707
804	*PSME1*	28.723	0.97773
805	*KIAA1429*	201.05	0.97783
806	*EIF4A3*	46.871	0.97802
807	*DHX9*	140.96	0.97803
808	*NUP93*	93.487	0.97844
809	*MRPS34*	20.662	0.97855
810	*PSMC3*	47.352	0.97968
811	*STXBP3*	67.764	0.97981
812	*YWHAB*	27.85	0.98067
813	*PFKP*	85.595	0.9807
814	*DHX15*	90.932	0.98088
815	*SNRNP200*	244.5	0.98119
816	*NCAPG*	114.33	0.9813
817	*NNT*	113.89	0.98161
818	*STAT3*	83.125	0.9819
819	*RBM39*	58.656	0.9819
820	*ACOT7*	27.041	0.98243
821	*DAZAP1*	35.02	0.98284
822	*CUL3*	86.233	0.98305
823	*MCM5*	82.285	0.98342
824	*NUDC*	38.242	0.98378
825	*HNRNPK*	48.562	0.9841
826	*SLC25A3*	39.958	0.98418
827	*DNM1L*	78.099	0.98437
828	*NUP107*	106.37	0.98438
829	*TSTA3*	35.892	0.98498

830	*PPIL2*	58.823	0.98503
831	*HNRNPD*	23.811	0.98519
832	*ARPC4; ARPC4-TTLL3*	19.667	0.98546
833	*XPO1*	123.38	0.98671
834	*NPM3*	19.343	0.98689
835	*SSRP1*	81.074	0.98709
836	*DIAPH1*	138.91	0.98759
837	*DRAP1*	16.658	0.98769
838	*ACO1*	98.398	0.98776
839	*PSAT1*	40.422	0.98786
840	*MYL4*	21.564	0.98832
841	*CFL1*	18.502	0.98834
842	*RUVBL2*	51.156	0.98843
843	*PA2G4*	43.786	0.98871
844	*KARS*	68.047	0.98872
845	*DHPS*	36.582	0.98938
846	*GOT2*	47.517	0.98953
847	*QARS*	86.578	0.98974
848	*THOC3*	36.031	0.98988
849	*DBN1*	71.428	0.98989
850	*CAND1*	136.37	0.9903
851	*ACTB*	41.736	0.99033
852	*FSCN1*	54.529	0.99037
853	*LUC7L*	38.405	0.99072
854	*RAB5C*	23.482	0.99097
855	*U2AF2*	33.901	0.991
856	*LETM1*	83.353	0.99101
857	*BZW2*	46.913	0.99113
858	*FLOT2*	47.064	0.9912
859	*OAT*	48.534	0.99253
860	*RAB1B*	22.171	0.99277
861	*MCM3*	90.98	0.9928
862	*MYH9*	226.53	0.99303
863	*ACO2*	85.424	0.99312
864	*SLC3A2*	57.944	0.99316
865	*RPL17*	19.586	0.99362
866	*PARP1*	113.08	0.99369
867	*PSMD6*	45.531	0.99379
868	*TUBB6*	49.857	0.99385
869	*CDC73*	60.576	0.99398
870	*BID*	11.263	0.99446
871	*TUBB2A; TUBB2B*	49.906	0.99486
872	*ANAPC7*	60.002	0.9951
873	*UBE2K*	22.406	0.99543
874	*SPTBN1*	274.61	0.99551
875	*SPAG9*	144.68	0.99562
876	*CAPNS1*	28.315	0.99579
877	*SNRPD3*	13.291	0.99619
878	*VDAC1*	30.772	0.99647

879	*PAFAH1B2*	25.569	0.99659
880	*SRP72*	74.605	0.99685
881	*PSMB1*	26.489	0.99699
882	*CDK1*	34.095	0.99713
883	*DARS2*	73.562	0.99719
884	*TOMM22*	15.521	0.99725
885	*GNAI2; GNAI1; GNAI3*	40.45	0.99734
886	*RPL31*	14.463	0.99741
887	*MCM4*	96.557	0.99747
888	*WDR43*	74.89	0.99758
889	*RPL27A*	12.201	0.99796
890	*VPS35*	91.706	0.99796
891	*LYAR*	43.614	0.99825
892	*DDX5*	69.147	0.99841
893	*DDX46*	117.46	0.9988
894	*ALDH1A2*	56.723	0.99882
895	*PLRG1*	17.26	0.99906
896	*LSM1*	15.179	0.99916
897	*CCDC47*	55.317	0.99917
898	*SNAP29*	28.97	1.0002
899	*STOML2*	38.534	1.0003
900	*EIF5B*	138.83	1.0005
901	*RANBP3*	52.894	1.001
902	*HNRNPC*	32.238	1.0012
903	*PWP2*	102.45	1.0013
904	*PKM*	57.936	1.0015
905	*HPRT1*	24.579	1.0018
906	*HNRNPU*	90.583	1.002
907	*PIGS*	61.655	1.0023
908	*NOP2*	89.301	1.0023
909	*RPA2*	29.247	1.0024
910	*HMGN1*	9.5355	1.0026
911	*RPLP2*	11.665	1.0027
912	*NOP16*	21.188	1.0028
913	*UCHL3*	26.182	1.0031
914	*MAPRE2*	30.691	1.0033
915	*FKBP3*	25.177	1.0033
916	*UNC13D*	123.28	1.0033
917	*AAAS*	38.518	1.0037
918	*RPS3*	26.688	1.004
919	*NAP1L1*	24.366	1.0042
920	*STRAP*	38.438	1.0047
921	*EEF2*	95.337	1.0049
922	*PPP1R7*	25.593	1.005
923	*UAP1*	57.028	1.0052
924	*ARID3A*	62.888	1.0058
925	*RPS18*	17.718	1.0058
926	*NMT1*	56.806	1.0063
927	*MCM6*	92.888	1.0064

928	*PGRMC1*	21.671	1.0066
929	*NARS*	62.942	1.0071
930	*CPPED1*	35.548	1.009
931	*AARS*	106.81	1.0092
932	*ABCF1*	95.925	1.0093
933	*BUD31*	13.568	1.0094
934	*NME2; NME1-NME2; NME1*	30.137	1.0096
935	*PSMB4*	29.204	1.0097
936	*NUP155*	149.01	1.0098
937	*ATP5B*	56.559	1.0098
938	*IPO7*	119.52	1.0103
939	*NLN*	68.867	1.0107
940	*NUP160*	162.12	1.0107
941	*PHB2*	33.239	1.0107
942	*HIST1H3A*	15.404	1.011
943	*YWHAE*	29.174	1.011
944	*SEPT5*	34.672	1.0111
945	*NSDHL*	41.9	1.0118
946	*POLR2H*	16.996	1.012
947	*MDH1*	13.044	1.0128
948	*MOV10*	101.6	1.0128
949	*NUP205*	227.92	1.013
950	*PRPF8*	273.6	1.013
951	*ENOPH1*	23.364	1.0131
952	*DDX21*	87.343	1.0136
953	*TBCE*	59.345	1.0138
954	*LDHA*	36.688	1.0146
955	*FAF2*	52.623	1.0147
956	*DARS*	57.136	1.0152
957	*PSMB5*	28.48	1.0154
958	*CAB39*	39.869	1.0155
959	*PGD*	51.872	1.0162
960	*GAK*	134.46	1.0167
961	*NAA10*	24.783	1.0168
962	*HSPB11*	16.297	1.0169
963	*MCM7*	81.307	1.017
964	*EIF4B*	64.805	1.0173
965	*PSMA1*	29.555	1.0177
966	*PSMD2*	100.2	1.0178
967	*SUPV3L1*	87.99	1.0179
968	*RPS7*	22.127	1.0183
969	*RFC5*	36.104	1.0186
970	*MLEC*	32.233	1.0188
971	*TAOK3*	105.4	1.0189
972	*PSMA6*	27.399	1.0193
973	*MAT2A*	43.66	1.0195
974	*RPL6*	32.728	1.0195
975	*CKAP5*	218.52	1.0196
976	*RER1*	13.439	1.0212

977	*RBM14*	69.491	1.0212
978	*GEMIN5*	168.59	1.0213
979	*RPS28*	7.8409	1.0214
980	*NAA50*	14.886	1.0221
981	*HMGB1; HMGB1P1*	18.311	1.0222
982	*NUP50*	46.862	1.0224
983	*PGK1*	44.614	1.0224
984	*SSBP1*	17.259	1.0226
985	*SERBP1*	42.426	1.0236
986	*UFL1*	82.097	1.0237
987	*HNRNPA2B1*	37.429	1.0237
988	*RNPS1*	24.561	1.024
989	*NPM1*	29.464	1.0242
990	*MYH10*	229	1.0245
991	*MYL6*	14.436	1.0255
992	*PRPF6*	106.92	1.0256
993	*PTRH2*	19.193	1.0258
994	*ATIC*	64.615	1.0261
995	*TCERG1*	121.69	1.0264
996	*PRDX4*	30.54	1.0265
997	*ENO1*	47.168	1.0272
998	*ATP5F1*	28.908	1.0273
999	*HNRNPH1*	47.087	1.0274
1000	*SPC24*	19.001	1.028
1001	*RALY*	32.463	1.0281
1002	*ACTN1*	102.71	1.0281
1003	*CAD*	236.02	1.0289
1004	*EIF3J*	29.062	1.029
1005	*PHB*	29.804	1.0292
1006	*HNRNPA1; HNRNPA1L2*	29.386	1.0292
1007	*SMARCE1*	12.106	1.0299
1008	*RPL26; KRBA2; RPL26L1*	17.258	1.0299
1009	*TALDO1*	37.54	1.03
1010	*PSMA3*	27.647	1.0301
1011	*SNRPD2*	13.527	1.0305
1012	*EIF2B2*	38.989	1.0306
1013	*HSPD1*	61.054	1.0308
1014	*TIPRL*	20.214	1.0315
1015	*WDR75*	94.498	1.0318
1016	*BCCIP*	35.979	1.0327
1017	*SRRM1*	102.33	1.0327
1018	*PSMD8*	28.162	1.0327
1019	*GAPDH*	36.053	1.0327
1020	*MTDH*	63.836	1.0333
1021	*RPLP0; RPLP0P6*	34.273	1.0341
1022	*USP15*	109.3	1.0347
1023	*NUMA1*	236.51	1.0349
1024	*HSD17B4*	79.685	1.0354
1025	*RPL4*	47.697	1.0359

1026	*LRRC59*	34.93	1.0367
1027	*PRPF4B*	116.99	1.0369
1028	*SMC2*	124.92	1.0371
1029	*UBLCP1*	36.804	1.0376
1030	*GFM1*	66.034	1.0377
1031	*IPO5*	123.63	1.0382
1032	*SPC25*	26.152	1.0389
1033	*GPI*	63.146	1.0392
1034	*NOP56*	66.049	1.0397
1035	*PPP1R12A*	76.532	1.0398
1036	*RBM34*	24.079	1.0401
1037	*CCT4*	57.924	1.041
1038	*EZR*	69.412	1.0413
1039	*TNPO1*	101.31	1.0415
1040	*ZC3H15*	48.602	1.0416
1041	*PRKCSH*	59.177	1.0424
1042	*CALU*	37.106	1.0425
1043	*MBD3*	29.014	1.0429
1044	*MKI67*	358.62	1.0431
1045	*ATP5A1*	59.75	1.0431
1046	*HBG1*	16.14	1.0436
1047	*RPS15A*	14.839	1.0437
1048	*VASP*	39.829	1.0439
1049	*ATP6V1C1*	43.941	1.044
1050	*STT3A*	80.529	1.0451
1051	*LARS*	134.46	1.0459
1052	*ATP5H*	18.491	1.046
1053	*RARS*	75.378	1.0462
1054	*GSPT1*	68.6	1.0467
1055	*SON*	228.18	1.0468
1056	*SEPT7*	48.715	1.047
1057	*CARS*	82.845	1.047
1058	*SSB*	46.836	1.0472
1059	*RPS17L; RPS17*	15.55	1.0475
1060	*LGALS1*	14.716	1.0476
1061	*RPL18*	18.091	1.048
1062	*HNRPDL*	27.191	1.0481
1063	*RPS27*	9.461	1.0482
1064	*FTL*	20.019	1.0483
1065	*NRBP1*	59.844	1.0485
1066	*HSPA4*	94.33	1.0486
1067	*PNPT1*	85.95	1.0489
1068	*PPA1*	32.66	1.049
1069	*USP9X*	290.46	1.0505
1070	*YWHAZ*	27.745	1.0513
1071	*TRMT112*	14.199	1.052
1072	*RPS8*	24.205	1.0523
1073	*TRAP1*	74.267	1.0526
1074	*RPL10*	23.072	1.0529

1075	*THUMPD3*	57.002	1.0532
1076	*SRSF9*	25.542	1.0537
1077	*RPS11*	18.431	1.0537
1078	*RPL3*	46.108	1.0544
1079	*SLC2A14; SLC2A3*	44.891	1.0547
1080	*ATP6V1G1*	13.757	1.0549
1081	*NCAPD2*	157.18	1.0551
1082	*hCG_2044799; HNRNPUL2*	84.69	1.0559
1083	*C1QBP*	31.362	1.0564
1084	*LAP3*	52.771	1.0565
1085	*PSMC2*	48.633	1.0568
1086	*TUBA1B*	50.151	1.0571
1087	*PPP4R1*	105.19	1.0574
1088	*RPL14*	14.558	1.0578
1089	*RCC1*	39.584	1.0582
1090	*APOBEC3C*	22.826	1.0586
1091	*LMNB1*	66.408	1.0586
1092	*ARF1;ARF3*	20.697	1.0587
1093	*SND1*	102	1.0589
1094	*CPSF6*	52.325	1.0591
1095	*RPL27*	15.798	1.0591
1096	*GLO1*	19.043	1.0597
1097	*HIST2H3A*	15.388	1.0604
1098	*PSMD3*	60.977	1.0605
1099	*UTP14A*	82.004	1.0607
1100	*RPN1*	68.569	1.0607
1101	*VBP1*	22.658	1.0614
1102	*NUP37*	36.707	1.0618
1103	*NOLC1*	73.744	1.0626
1104	*KIF2A*	75.042	1.0626
1105	*RPSA; RPSAP58*	29.505	1.0631
1106	*SAFB*	95.18	1.0632
1107	*CTPS1*	66.69	1.0635
1108	*EEF1G*	50.118	1.0635
1109	*METAP2*	50.496	1.0638
1110	*EPRS*	170.59	1.0638
1111	*ALYREF*	26.888	1.0639
1112	*RAB14*	20.409	1.0639
1113	*ORC3*	82.253	1.0642
1114	*RPS4X*	29.597	1.0643
1115	*GNL3*	60.54	1.0645
1116	*BCLAF1*	83.231	1.0649
1117	*RPS26; RPS26P11*	13.015	1.0651
1118	*RBMX*	42.331	1.0651
1119	*CLTA*	17.687	1.0652
1120	*CUL4A*	76.82	1.0656
1121	*PRPF19*	55.18	1.0659
1122	*MCM2*	101.89	1.0659
1123	*RPS25*	13.742	1.0664

1124	*SF3B14*	14.585	1.0665
1125	*HARS*	54.846	1.0675
1126	*SMARCC1*	122.87	1.0676
1127	*EIF2S2*	38.388	1.0681
1128	*TRIM28*	88.549	1.0682
1129	*SLC25A11*	32.182	1.0684
1130	*CAPRIN1*	76.861	1.0688
1131	*PDCD6*	21.868	1.0691
1132	*SRP68*	70.729	1.0693
1133	*SNX2*	46.097	1.0694
1134	*CHD1; CHD2*	196.59	1.0697
1135	*U2AF1; U2AF1L4*	27.872	1.0698
1136	*RPS6*	28.68	1.0707
1137	*EPB41*	63.254	1.0709
1138	*SLC25A5*	32.852	1.0716
1139	*HK1*	101.08	1.0716
1140	*TARS*	83.434	1.0724
1141	*RPL21*	18.565	1.0728
1142	*BUB3*	31.703	1.0729
1143	*PSMD13*	42.945	1.0742
1144	*NEMF*	31.15	1.0746
1145	*SNRPN; SNRPB*	17.546	1.0746
1146	*CNOT1*	266.38	1.0746
1147	*CCT6A*	58.024	1.0752
1148	*RECQL*	11.077	1.0757
1149	*HYOU1*	111.33	1.0758
1150	*TMPO*	75.491	1.0759
1151	*RAB7A*	23.489	1.0766
1152	*TMPO*	50.67	1.0767
1153	*STUB1*	18.378	1.0773
1154	*PEPD*	49.69	1.0776
1155	*TCP1*	60.343	1.0777
1156	*GNB2L1*	35.076	1.0782
1157	*EEF1D*	31.121	1.0785
1158	*STT3B*	93.673	1.0789
1159	*ARL8B*	21.539	1.079
1160	*RAB10*	22.541	1.079
1161	*C20orf27*	19.291	1.0792
1162	*HSPBP1*	39.474	1.0793
1163	*SNRPG*	7.1013	1.0795
1164	*ARPC2*	34.333	1.0796
1165	*RPL12*	17.818	1.0797
1166	*CMPK1*	22.222	1.0799
1167	*NOP58*	59.578	1.0812
1168	*ARHGDIA*	21.614	1.0814
1169	*EBNA1BP2*	34.852	1.0815
1170	*IGF2BP3*	63.704	1.0818
1171	*TMED10*	24.976	1.0823
1172	*FKBP4*	51.804	1.0839

1173	*ANXA11*	51.242	1.084
1174	*LAMP2*	44.955	1.0844
1175	*PPIB*	23.742	1.0848
1176	*PRPF38B*	64.467	1.0857
1177	*ACTR1A; ACTR1B*	37.433	1.0858
1178	*SART3*	105.58	1.087
1179	*NACA*	15.016	1.0871
1180	*DYNC1H1*	532.4	1.0874
1181	*DLD*	54.177	1.0896
1182	*NUP85*	69.799	1.0905
1183	*NAMPT*	55.52	1.0907
1184	*NPEPPS*	102.99	1.0909
1185	*ETF1*	45.462	1.0914
1186	*BRIX1*	41.401	1.0917
1187	*MAP3K4*	163.01	1.0935
1188	*BAG6*	96.798	1.0939
1189	*HNRNPH2*	49.263	1.0944
1190	*SRPRB*	29.702	1.0945
1191	*TXNDC5*	36.177	1.0951
1192	*CCT8*	59.62	1.0951
1193	*PSMD12*	52.904	1.0956
1194	*RPL24*	14.369	1.0957
1195	*DNAJC7*	50.096	1.096
1196	*RPS5*	22.391	1.0969
1197	*RPS19*	16.06	1.0976
1198	*NDUFS3*	30.241	1.098
1199	*LAMP1*	44.882	1.0984
1200	*SMU1*	57.543	1.0996
1201	*PPP2CA; PPP2CB*	35.594	1.0996
1202	*TOMM70A*	67.454	1.1001
1203	*ATP6V1A*	64.735	1.1002
1204	*IQGAP1*	189.25	1.1002
1205	*PTPN11*	52.827	1.1017
1206	*PSMD4*	40.736	1.1018
1207	*PDIA3*	56.782	1.1021
1208	*DKFZp686J1372; TPM3*	26.42	1.103
1209	*ZMPSTE24*	54.812	1.1031
1210	*RRAGC; RRAGD*	44.223	1.1037
1211	*MPDU1; HBEBP2BPA*	10.978	1.1041
1212	*OLA1*	44.743	1.1045
1213	*RPL10A*	24.831	1.1055
1214	*EMD*	24.938	1.1063
1215	*SMC4*	144.45	1.1064
1216	*PSMC6*	44.172	1.1071
1217	*AATF*	63.132	1.1076
1218	*YWHAQ*	27.764	1.1079
1219	*STIP1*	62.639	1.1086
1220	*KCMF1*	41.945	1.1089
1221	*SCAF4*	123.64	1.1094

1222	*ARPC3*	20.546	1.1096
1223	*GIGYF2*	148.63	1.1099
1224	*VDAC3*	30.658	1.1108
1225	*COPS2*	51.596	1.1108
1226	*LMAN2*	36.543	1.1114
1227	*MRI1*	39.149	1.1118
1228	*KPNA4*	57.886	1.112
1229	*GRPEL1*	24.279	1.1123
1230	*YARS2*	53.198	1.1124
1231	*ACACA*	257.24	1.1127
1232	*HDLBP*	141.45	1.1132
1233	*MAP1LC3B; MAP1LC3B2; MAP1LC3A*	9.0115	1.1133
1234	*PABPC1*	70.67	1.1137
1235	*PYCR1*	33.34	1.1138
1236	*VAPB*	27.228	1.114
1237	*UBAP2L*	103.17	1.114
1238	*SRP54*	55.704	1.1141
1239	*TPD52L2*	22.237	1.1147
1240	*DDX3X; DDX3Y*	70.839	1.1147
1241	*DCUN1D5*	17.855	1.115
1242	*YME1L1*	75.981	1.1152
1243	*RPS12*	14.515	1.1161
1244	*ABHD14B*	19.756	1.117
1245	*COX4I1*	19.576	1.1177
1246	*DDOST*	49.019	1.1177
1247	*RPL7A*	29.995	1.1179
1248	*ARF4*	20.511	1.1182
1249	*CELF1*	50.13	1.1192
1250	*EIF2B1*	33.712	1.1192
1251	*NUP98*	187.2	1.1194
1252	*RPS10*	18.898	1.121
1253	*AGPAT1*	31.716	1.1211
1254	*CALR*	48.141	1.1213
1255	*HNRNPH3*	35.238	1.1216
1256	*DDX1*	82.431	1.1217
1257	*RBBP7*	46.938	1.122
1258	*EIF2S1*	36.112	1.1221
1259	*BYSL*	49.601	1.1225
1260	*SRSF2*	15.156	1.1226
1261	*EIF4E*	25.097	1.1226
1262	*NUP210*	205.11	1.1229
1263	*ACIN1*	145.44	1.1231
1264	*MAPK14*	32.357	1.1235
1265	*WDR26*	70.459	1.1242
1266	*ARPC1B*	40.949	1.1243
1267	*DYNLT1*	10.2	1.1246
1268	*AGL*	174.76	1.1248
1269	*HK2*	98.972	1.1251
1270	*PSMB3*	22.949	1.1267

1271	*CCT5*	59.67	1.1274
1272	*RPL38*	8.2178	1.1277
1273	*CTNNBL1*	61.97	1.1277
1274	*PSMC4*	47.366	1.128
1275	*ST13; ST13P5; ST13P4*	41.331	1.1284
1276	*TRNT1*	47.828	1.1285
1277	*HSPE1*	10.932	1.1289
1278	*SEC13*	35.54	1.1291
1279	*RBM12*	97.394	1.1303
1280	*NRD1*	131.14	1.1315
1281	*RANGAP1*	63.541	1.1327
1282	*G3BP1*	52.164	1.1345
1283	*RSL1D1*	54.972	1.1363
1284	*IKBKAP*	150.25	1.1366
1285	*CSNK2A2*	41.213	1.1374
1286	*CCT3*	60.533	1.1378
1287	*CHORDC1*	37.489	1.1389
1288	*IMPDH2*	55.804	1.1389
1289	*RPS9*	22.591	1.1392
1290	*PPAN*	23.108	1.1394
1291	*WDR3*	106.1	1.1395
1292	*EIF3K*	25.059	1.1408
1293	*DNMT1*	183.16	1.1408
1294	*ZC3HAV1*	77.902	1.141
1295	*TXN*	9.4519	1.1411
1296	*ANXA2; ANXA2P2*	38.604	1.1412
1297	*EIF1*	12.732	1.1419
1298	*PITHD1*	24.121	1.1431
1299	*FTSJ3*	96.557	1.1433
1300	*LUC7L2*	46.513	1.1449
1301	*RPS24*	15.069	1.1456
1302	*CLASP2*	138.86	1.1473
1303	*DYNC1LI1*	56.578	1.1474
1304	*CPSF7*	41.265	1.1489
1305	*DDX54*	98.594	1.15
1306	*LUC7L3*	51.466	1.1502
1307	*SAR1A*	22.367	1.1506
1308	*UBXN7*	54.862	1.1506
1309	*NOL11*	81.123	1.1512
1310	*PGM3*	59.851	1.1512
1311	*KIAA0020*	73.584	1.1515
1312	*VDAC2*	30.348	1.1516
1313	*ASNA1*	37.119	1.1526
1314	*RFC2*	39.157	1.1529
1315	*PNN*	81.613	1.1529
1316	*SBDS*	28.763	1.1529
1317	*DNAJC9*	29.909	1.153
1318	*PRPF3*	77.528	1.1552
1319	*EHD1*	60.626	1.1553

1320	*CYB5B*	15.716	1.156
1321	*UCK2*	29.299	1.1563
1322	*EIF3B*	92.48	1.1565
1323	*CSNK2A1; CSNK2A3*	45.31	1.1566
1324	*RTN4*	37.144	1.1576
1325	*LMNB2*	67.688	1.1579
1326	*SPATA5L1*	66.111	1.1585
1327	*HMGCS1*	57.293	1.1601
1328	*HCFC1*	208.73	1.1601
1329	*TPR*	267.29	1.1604
1330	*ABCB10*	79.147	1.1614
1331	*UBR5*	309.22	1.1622
1332	*SMARCA5*	121.9	1.1633
1333	*RPS3A*	29.945	1.1635
1334	*HSPA9*	73.68	1.1637
1335	*ADRM1*	42.153	1.1638
1336	*COPB2*	99.045	1.1645
1337	*NSFL1C*	40.572	1.1654
1338	*GSS*	52.384	1.1657
1339	*CNBP*	18.742	1.1668
1340	*ADAR*	103.64	1.1668
1341	*RRM1*	90.069	1.167
1342	*SRSF1*	27.744	1.1676
1343	*LRRC40*	68.249	1.1684
1344	*U2SURP*	118.23	1.1698
1345	*UTP15*	56.355	1.17
1346	*AK1*	21.635	1.1709
1347	*ACOT13*	12.366	1.1721
1348	*GSTK1*	25.497	1.1725
1349	*OXSR1*	58.022	1.1726
1350	*KPNA2*	57.861	1.1726
1351	*AP3D1*	136.65	1.1736
1352	*PEF1*	30.381	1.1737
1353	*ARHGEF1*	102.43	1.1742
1354	*HNRNPUL1*	84.793	1.1744
1355	*AHSA1*	38.274	1.1748
1356	*PRKCB; PRKCA*	77.011	1.1759
1357	*MORC3*	107.11	1.176
1358	*COPB1*	107.14	1.1766
1359	*EIF4A1*	46.153	1.1773
1360	*PPP2R2A*	51.691	1.1781
1361	*RPL9*	20.874	1.1791
1362	*ACTR3*	47.371	1.1793
1363	*CHD4*	217.1	1.1794
1364	*NSF*	71.583	1.1798
1365	*CDV3*	22.079	1.18
1366	*CCT2*	57.488	1.181
1367	*ANXA7*	50.315	1.1813
1368	*ECM29; KIAA0368*	204.29	1.182

1369	*PFDN6*	14.582	1.1826
1370	*UPF1*	123.03	1.1828
1371	*SLC25A6*	32.866	1.1852
1372	*TUBB3*	50.432	1.1858
1373	*RPL7*	29.225	1.186
1374	*COLGALT1*	71.635	1.1864
1375	*RBM25*	100.18	1.1866
1376	*PPME1*	42.315	1.1876
1377	*DDX18*	75.406	1.188
1378	*NCKAP1*	128.79	1.1894
1379	*CSDE1*	74.583	1.1904
1380	*TPT1*	19.595	1.1905
1381	*ATL3*	58.772	1.191
1382	*COPE*	34.51	1.1914
1383	*USO1*	107.89	1.1915
1384	*CIRBP*	18.648	1.192
1385	*NOL6*	127.32	1.192
1386	*EIF3I*	36.501	1.1933
1387	*MAGEB2*	35.277	1.1935
1388	*PABPC4*	69.578	1.1947
1389	*PRKAG1*	31.905	1.1958
1390	*NUP62*	53.254	1.1958
1391	*EIF3M*	42.502	1.1969
1392	*RAB1A*	22.677	1.1988
1393	*CACYBP*	21.228	1.2002
1394	*HSP90B1*	92.468	1.2002
1395	*CYB5R1*	34.094	1.2004
1396	*TOP1*	90.725	1.2006
1397	*SPTA1*	279.67	1.2011
1398	*RAB8A*	23.668	1.2013
1399	*GNB1*	18.34	1.2029
1400	*HDDC2*	19.55	1.2034
1401	*SRSF3*	14.203	1.2035
1402	*HIST2H2BE; HIST1H2BB; HIST1H2BO; HIST1H2BJ; HIST3H2BB*	13.92	1.2038
1403	*TOMM5*	6.0352	1.2047
1404	*RPL30*	12.656	1.2068
1405	*CCT7*	59.366	1.2071
1406	*UNC45A*	101.67	1.2079
1407	*TMX2*	29.642	1.2081
1408	*ATP6V1E1*	26.145	1.2082
1409	*TSR1*	91.809	1.2087
1410	*RPL18A*	16.714	1.2088
1411	*SEH1L*	29.541	1.209
1412	*YWHAG*	28.302	1.2119
1413	*AMPD2*	88.197	1.2128
1414	*MAP1B*	270.63	1.2142
1415	*EEF1A1; EEF1A1P5*	50.14	1.2146
1416	*SURF4*	17.97	1.2155
1417	*HSPB1*	22.782	1.2155

1418	*NUP43*	42.15	1.2158
1419	*PAFAH1B1*	46.637	1.216
1420	*NUP133*	128.98	1.2176
1421	*AKR1C1; AKR1C3*	36.788	1.2183
1422	*GTPBP4*	73.964	1.2186
1423	*GAR1*	20.834	1.2189
1424	*MLLT4*	182	1.222
1425	*ANXA1*	38.714	1.222
1426	*MKI67IP*	34.222	1.2222
1427	*ECI2*	39.609	1.2249
1428	*SOD2*	24.722	1.2255
1429	*HSP90AA1*	84.659	1.226
1430	*RANBP2*	358.2	1.2273
1431	*COPS4*	40.196	1.2288
1432	*ATP5C1*	32.996	1.2315
1433	*RFC4*	39.681	1.2317
1434	*SRSF5*	31.263	1.2354
1435	*SSR4*	18.998	1.2354
1436	*RPS16*	14.419	1.2357
1437	*EIF3F*	37.563	1.2363
1438	*ZC3H18*	84.099	1.2367
1439	*RPF2*	35.582	1.2371
1440	*ANXA5*	35.936	1.2381
1441	*COASY*	62.328	1.2402
1442	*TFRC*	84.87	1.2417
1443	*EIF4G2*	102.36	1.2423
1444	*GRB2*	20.557	1.2431
1445	*RPL15*	24.146	1.2432
1446	*SEC31A*	117.67	1.2439
1447	*CBR1; CBR3*	18.762	1.2454
1448	*RFC1*	128.18	1.2471
1449	*C22orf28*	55.21	1.2475
1450	*SACM1L*	66.966	1.2477
1451	*SRSF6*	38.418	1.2478
1452	*RAB21*	24.347	1.2505
1453	*FXR1*	50.99	1.2522
1454	*POR*	76.689	1.2545
1455	*TOP2A*	174.38	1.2546
1456	*RAB3GAP2*	155.98	1.255
1457	*ERP44*	46.971	1.2555
1458	*HIST1H4A*	11.367	1.2588
1459	*KIF11*	119.16	1.2593
1460	*EIF3A*	166.57	1.2596
1461	*RPL36*	12.254	1.26
1462	*DNAJB1*	27.016	1.2604
1463	*RPL13A; RPL13a*	23.577	1.262
1464	*RPL37A*	7.624	1.265
1465	*ELP4*	46.587	1.2678
1466	*AKR1D1*	32.747	1.272

1467	*RPL5*	34.362	1.2761
1468	*SNX6*	33.57	1.2788
1469	*RRP15*	31.484	1.2809
1470	*RAB2A; DKFZp313C1541;RAB2B*	23.545	1.2809
1471	*ACTR2*	44.76	1.2816
1472	*ASNS*	62.168	1.2824
1473	*PDCD5*	14.285	1.2828
1474	*SPAG5*	134.42	1.2835
1475	*HSPA5*	72.332	1.2856
1476	*PSMD11*	47.463	1.286
1477	*PSMB7*	29.965	1.2868
1478	*EIF2A*	62.288	1.2872
1479	*SEC23B*	86.478	1.2883
1480	*SEC11A*	18.651	1.2894
1481	*RAB6A; RAB6B*	23.548	1.2915
1482	*PPWD1*	55.699	1.2921
1483	*DNAJA1*	37.044	1.2931
1484	*P4HB*	57.116	1.2958
1485	*TBL2*	45.935	1.296
1486	*SNX1*	51.812	1.298
1487	*RPL34*	13.293	1.2982
1488	*MAGEC1*	123.64	1.2983
1489	*HSPA8*	70.897	1.3004
1490	*NAPA;NAPB*	29.163	1.3019
1491	*COPG1*	97.717	1.302
1492	*AP1G1*	91.35	1.3021
1493	*DDRGK1*	35.61	1.3027
1494	*RRS1*	41.193	1.3037
1495	*HIST1H2BL; HIST1H2BM; HIST1H2BN; HIST1H2BH; HIST2H-2BF; HIST1H2BC; HIST1H2BD; H2BFS; HIST1H2BK*	13.952	1.3062
1496	*DUSP12*	37.687	1.316
1497	*EIF3E*	52.22	1.3163
1498	*RPL32*	15.616	1.3184
1499	*PRPF31*	54.766	1.3242
1500	*EIF2AK2*	57.39	1.326
1501	*AKR1C2*	36.735	1.3266
1502	*COPA*	138.34	1.3266
1503	*SGTA*	34.063	1.3304
1504	*SSR1*	29.373	1.3349
1505	*TMX1*	31.791	1.3407
1506	*EIF3H; EIF3S3*	39.93	1.342
1507	*SLC2A1*	54.083	1.3426
1508	*CTSD*	44.552	1.3431
1509	*GSR*	51.7	1.3437
1510	*SRPR*	66.558	1.346
1511	*PDIA4*	72.932	1.35
1512	*EDC4*	151.66	1.3551
1513	*HSP90AB1*	83.263	1.3708
1514	*MAGED2*	55.795	1.373

1515	*EIF5*	49.222	1.3751
1516	*PGRMC2*	23.818	1.3776
1517	*HSBP1*	8.5435	1.3779
1518	*TXNRD1*	53.166	1.3832
1519	*EIF3C; EIF3CL*	105.34	1.3832
1520	*CUL4B*	84.016	1.3878
1521	*GALNT2*	64.732	1.3901
1522	*TBC1D15*	77.394	1.3901
1523	*BAG2*	23.772	1.3902
1524	*BPNT1*	29.188	1.3937
1525	*HSPA6; HSPA7*	71.027	1.3938
1526	*NUSAP1*	42.351	1.3954
1527	*GFPT1*	76.758	1.4012
1528	*FLII*	138.49	1.4021
1529	*RTN3*	25.609	1.4131
1530	*HIST2H3PS2*	15.43	1.4184
1531	*TMED9*	27.277	1.4271
1532	*ARL1*	18.565	1.4331
1533	*EPHX1*	52.948	1.435
1534	*TTC1*	33.526	1.4468
1535	*SERPINH1*	46.44	1.4559
1536	*HSPH1*	92.115	1.4576
1537	*IGF2R*	274.37	1.4604
1538	*EIF3L*	61.013	1.4619
1539	*CRTAP*	41.432	1.4714
1540	*GOLGB1*	367.42	1.4779
1541	*PELO*	43.359	1.479
1542	*TIMM23; TIMM23B*	21.943	1.485
1543	*HSP90AB4P*	58.264	1.4985
1544	*SNAP23*	23.354	1.5985
1545	*ANKRD28*	112.96	1.631
1546	*PFKM*	81.775	1.6316
1547	*UBE2S*	23.845	1.6677
1548	*ACBD3*	60.593	1.6762
1549	*RQCD1*	33.631	1.7068
1550	*DDX27*	86.604	1.7197
1551	*CCNB1*	44.932	1.7377
1552	*MDC1*	195.98	1.7546
1553	*DNAJA3*	49.611	1.8783
1554	*GCLM*	30.727	2.1669
1555	*NQO1*	22.793	2.8478

Table S2. The ingenuity canonical pathways regulated by CDDO-Me in K562 cells

	Ingenuity Canonical Pathways	*-log (p-value)*	*Ratio*	*z-score*	*Molecules*
1	EIF2 signaling	5.45E01	3.72E-01	1.414	RPL11, RPL22, RPLP2, EIF2A, RPS11, RPS7, RPL13, EIF3B, RPS20, RPS13, EIF5, RPS2, PPP1CA, RPL32, PABPC1, RPL3, RPS8, RPL12, EIF3E, RPL37A, EIF2S2, RPL10A, EIF3M, RPL9, RPS6, RPL15, RPL8, EIF4A3, RPL10, RPL6, RPS15A, RPS25, RPL24, RPLP1, RPS3A, RPS18, RPL7A, EIF2S1, EIF4G1, RPL7, RPS4X, RPS28, RPL27A, RPL14, RPL18A, RPS9, EIF3A, RPS5, RPS3, RPS12, RPL18, RPS24, RPS19, RPL4, RPL17, RPS10, RPL30, EIF3J, RPS21, RPL23, RPL27, EIF3F, RPS15, RPS16, EIF4A1, EIF2B1, RPS27A, RPL5, EIF3L, & RPL38
2	Regulation of eIF4 and p70S6K signaling	2.48E01	2.67E-01	NaN	RPS3A, RPS18, EIF4G1, EIF2S1, EIF2A, RPS11, RPS4X, RPS7, RPS28, EIF3B, RPS20, RPS13, RPS9, EIF3A, RPS2, RPS12, RPS3, RPS5, RPS24, PABPC1, RPS19, RPS8, RPS10, EIF3J, RPS21, EIF3E, EIF2S2, EIF3M, RPS6, PPP2R1A, EIF3F, RPS15, RPS16, EIF4A3, EIF4A1, EIF2B1, RPS27A, RPS25, RPS15A, & EIF3L
3	Protein ubiquitination pathway	2.48E01	1.97E-01	NaN	USP5, PSMA7, SKP1, HSPA5, PSMC5, HSPA4, DNAJC8, PSMC2, PSMA2, PSMA6, PSMB5, DNAJC9, HSPA9, PSMD5, PSMD6, PSMD3, HSPA8, PSMD11, PSMB7, UBE2L3, PSMB2, PSMA5, PSMD12, PSMB1, PSMA4, HSP90AA1, PSMD1, PSMD4, HSPB1, PSMB3, USP14, PSMD7, CUL1, DNAJA1, HSP90B1, HSP90AB1, PSMC6, HSPE1, PSMD14, PSMA3, USP15, PSMD13, HSPH1, PSMA1, HSPD1, PSMB6, PSMD8, PSMC1, PSMD2, UBA1, & DNAJC7
4	mTOR signaling	1.76E01	1.91E-01	NaN	RPS3A, RPS18, EIF4G1, RPS11, RPS4X, RPS7, RPS28, RHOG, RPS20, EIF3B, RPS13, RPS9, EIF3A, RPS2, RPS12, RPS3, RPS5, EIF4B, RPS24, RPS19, RPS8, RPS10, EIF3J, RPS21, EIF3E, EIF3M, RPS6, PPP2R1A, EIF3F, RPS15, RPS16, EIF4A3, EIF4A1, RPS27A, RPS25, RPS15A, & EIF3L
5	RAN signaling	1.33E01	6.32E-01	NaN	KPNB1, KPNA4, RANBP2, RCC1, CSE1L, TNPO1, RANGAP1, RAN, XPO1, RANBP1, KPNA2, & IPO5
6	tRNA charging	1.19E01	2.44E-01	NaN	CARS, GARS, HARS, TARS, MARS, QARS, EPRS, FARSB, FARSA, NARS, LARS, WARS, RARS, YARS, KARS, DARS, AARS, VARS, SARS, & IARS
7	Glycolysis I	8.38E00	2.93E-01	NaN	PGK1, ENO1, GPI, PKLR, TPI1, PGAM1, PKM, ALDOA, GAPDH, PFKL, PFKM, & ALDOC
8	Nrf2-mediated oxidative stress response	7E00	1.22E-01	0.577	USP14, DNAJC9, PPIB, PRDX1, ACTB, SOD1, DNAJA1, GSTO1, TXNRD1, GSR, ERP29, STIP1, DNAJC8, CAT, VCP, CCT7, TXN, GCLM, FKBP5, GSTP1, DNAJC7, & GSTK1
9	Mitochondrial dysfunction	6.66E00	1.17E-01	NaN	HSD17B10, SDHA, ATP5A1, ATP5O, ACO2, VDAC2, GSR, ATP5C1, PRDX3, PARK7, ATP5B, CAT, UQCRC2, CYC1, NDUFS2, CYCS, VDAC1, UQCRC1, NDUFS3, ATP5F1, COX4I1, & AIFM1
10	Remodeling of epithelial adherens junctions	6.62E00	1.91E-01	0.000	TUBA1B, NME1, RAB5C, TUBB4B, MAPRE1, ACTB, RAB7A, TUBB, IQGAP1, TUBB8, VCL, ACTN4, & DNM1L
11	Cell cycle:G_2/M DNA damage checkpoint regulation	6.43E00	2.24E-01	1.134	YWHAQ, PRKDC, YWHAG, YWHAE, YWHAH, YWHAB, CUL1, YWHAZ, TOP2A, SKP1, & CDK1
12	Unfolded protein response	5.98E00	2.04E-01	NaN	HSPA8, HSPA4, CALR, P4HB, HSP90B1, HSPH1, HSPA9, VCP, CANX, HSPA5, & EIF2A
13	Gluconeogenesis I	4.84E00	1.96E-01	NaN	PGK1, ENO1, GPI, PGAM1, ALDOA, GAPDH, MDH1, MDH2, & ALDOC
14	Aldosterone signaling in epithelial cells	4.66E00	1.05E-01	NaN	DNAJC9, PDIA3, HSPH1, HSPA9, HSPD1, DNAJA1, HSPA5, HSPA8, HSPA4, HSP90B1, HSP90AB1, DNAJC8, HSPE1, HSP90AA1, DNAJC7, HSPB1, AHCY
15	DNA double-strand break repair by non-homologous end joining	4.25E00	3.57E-01	NaN	PRKDC, XRCC6, XRCC5, RAD50, & PARP1
16	Phagosome maturation	4.17E00	1.1E-01	NaN	DYNC1H1, CALR, TUBA1B, RAB5C, TUBB8, TUBB4B, PRDX1, RAB7A, CANX, ATP6V1G1, TUBB, ATP6V1A, PRDX6, & PRDX2
17	Glutaryl-CoA degradation	4.14E00	2.61E-01	NaN	HSD17B10, ACAT2, HADHB, HSD17B4, HADHA, & HADH
18	Granzyme B signaling	3.94E00	3.12E-01	-0.447	PRKDC, NUMA1, CYCS, LMNB1, & PARP1
19	14-3-3-mediated signaling	3.88E00	1.09E-01	0.707	TUBA1B, YWHAG, YWHAE, YWHAH, TUBB4B, PDIA3, YWHAB, YWHAZ, VIM, TUBB, YWHAQ, TUBB8, & PDCD6IP
20	Oxidative phosphorylation	3.88E00	1.09E-01	NaN	SDHA, ATP5C1, ATP5B, ATP5A1, CYC1, UQCRC2, ATP5O, NDUFS2, CYCS, NDUFS3, UQCRC1, ATP5F1, & COX4I1
21	Cell cycle control of chromosomal replication	3.72E00	2.22E-01	NaN	MCM5, MCM3, MCM6, MCM2, MCM4, & MCM7
22	TCA cycle II (eukaryotic)	3.5E00	1.71E-01	NaN	SDHA, CS, ACO2, DLD, MDH1, FH, & MDH2

23	Purine nucleotides *de novo* biosynthesis II	3.5E00	1.71E-01	NaN	ADSS, ADSL, GMPS, IMPDH2, PAICS, ATIC, & GART
24	Granzyme A signaling	3.43E00	2.5E-01	NaN	ANP32A, SET, NME1, HIST1H1E, & APEX1
25	HIPPO signaling	3.29E00	1.15E-01	-0.378	YWHAQ, PPP2R1A, YWHAG, YWHAE, YWHAH, YWHAB, CUL1, YWHAZ, SKP1, & PPP1CA
26	BER pathway	3.2E00	3.08E-01	NaN	PCNA, FEN1, APEX1, & PARP1
27	Aspartate degradation II	3.07E00	2.86E-01	NaN	GOT1, MDH1, MDH2, & GOT2
28	Telomere extension by telomerase	2.95E00	2.67E-01	NaN	XRCC6, HNRNPA2B1, XRCC5, & RAD50
29	Superpathway of methionine degradation	2.89E00	1.21E-01	NaN	CBS/CBSL, PRMT5, DLD, GOT1, MAT2A, GOT2, PRMT1, & AHCY
30	Lipid antigen presentation by CD1	2.88E00	1.92E-01	NaN	CALR, AP2A1, PDIA3, AP2B1, & CANX
31	Isoleucine degradation I	2.66E00	1.72E-01	NaN	HSD17B10, ACAT2, DLD, HADHB, & HADHA
32	Ketogenesis	2.63E00	2.22E-01	NaN	ACAT2, HADHB, HMGCS1, & HADHA
33	Caveolar-mediated endocytosis signaling	2.6E00	1.1E-01	NaN	RAB5C, FLNA, FLNC, ACTB, COPA, COPB2, COPB1, & COPG1
34	Myc mediated apoptosis signaling	2.58E00	1.21E-01	NaN	YWHAQ, YWHAG, YWHAE, YWHAH, YWHAB, YWHAZ, & CYCS
35	Aryl hydrocarbon receptor signaling	2.53E00	8.22E-02	NaN	TGM2, HSP90B1, HSP90AB1, ALDH1A2, HSP90AA1, GSTP1, PTGES3, GSTO1, SMARCA4, GSTK1, HSPB1, & MCM7
36	PI3K/AKT signaling	2.51E00	8.59E-02	1.508	YWHAQ, HSP90B1, CDC37, PPP2R1A, YWHAG, YWHAE, YWHAH, HSP90AB1, YWHAB, YWHAZ, & HSP90AA1
37	Fatty acid β-oxidation I	2.5E00	1.33E-01	NaN	HSD17B10, HADHB, HSD17B4, ACADM, HADHA, & HADH
38	Epithelial adherens junction signaling	2.48E00	8.11E-02	NaN	RAP1B, MYH10, TUBA1B, MYH9, TUBB8, TUBB4B, ACTB, MYL4, VCL, ACTN4, TUBB, & IQGAP1
39	Cysteine biosynthesis III (mammalia)	2.46E00	1.56E-01	NaN	CBS/CBSL, PRMT5, MAT2A, PRMT1, & AHCY
40	DNA methylation and transcriptional repression signaling	2.45E00	2E-01	NaN	CHD4, HDAC1, DNMT1, & RBBP4
41	Tryptophan degradation III (eukaryotic)	2.45E00	1.3E-01	NaN	HSD17B10, ACAT2, HADHB, HSD17B4, HADHA, & HADH
42	Endoplasmic reticulum stress pathway	2.37E00	1.9E-01	NaN	CALR, HSP90B1, EIF2S1, & HSPA5
43	Cell cycle:G_1/S checkpoint regulation	2.34E00	1.09E-01	1.000	RPL11, PA2G4, CUL1, HDAC1, RPL5, GNL3, & SKP1
44	Vitamin-C transport	2.3E00	1.82E-01	NaN	SLC2A1, TXN, TXNRD1, & GSTO1
45	Pentose phosphate pathway	2.22E00	1.74E-01	NaN	PGD, TKT, TALDO1, & G6PD
46	Antigen presentation pathway	2.18E00	1.35E-01	NaN	CALR, PSMB5, PDIA3, CANX, & PSMB6
47	p70S6K signaling	2.12E00	8E-02	1.000	YWHAQ, RPS6, PPP2R1A, YWHAG, YWHAE, YWHAH, PDIA3, YWHAB, EEF2, & YWHAZ
48	Methionine degradation I (to homocysteine)	2.09E00	1.6E-01	NaN	PRMT5, MAT2A, PRMT1, & AHCY
49	Tight junction signaling	2.07E00	7.19E-02	NaN	MYH10, EPB41, PPP2R1A, MYH9, NUDT21, ACTB, VAPA, MYL4, ARHGEF2, SAFB, VCL, & VASP
50	ILK signaling	2.06E00	6.91E-02	1.155	MYH10, MYH9, CFL1, ACTB, VIM, PPP2R1A, RHOG, FLNA, FLNC, MYL4, KRT18, ACTN4, & VCL
51	Antiproliferative role of TOB in T cell signaling	2.03E00	1.54E-01	NaN	PABPC1, PABPC4, CUL1, & SKP1
52	Huntington's disease signaling	1.99E00	6.38E-02	NaN	SDHA, GNB2L1, HSPA9, CLTC, HDAC1, HSPA5, TGM2, GNB1, HSPA8, HSPA4, ATP5B, CAPN1, TCERG1, CYCS, & DNM1L
53	Mevalonate pathway I	1.97E00	1.48E-01	NaN	ACAT2, HADHB, HMGCS1, & HADHA
54	Regulation of cellular mechanics by calpain protease	1.95E00	1.03E-01	NaN	EZR, CAPN1, TLN1, VCL, ACTN4, & CDK1
55	AMPK signaling	1.92E00	6.63E-02	1.633	CAB39, PPP2R1A, SLC2A1, EEF2, FASN, ACTB, SMARCC1, PFKL, AK2, SMARCA4, PPM1G, ELAVL1, & PFKM
56	Systemic lupus erythematosus signaling	1.9E00	6.39E-02	NaN	SNRPA, PRPF19, PRPF8, HNRNPA2B1, SNRPE, EFTUD2, SNRNP70, SNRNP200, PRPF6, SNU13, SNRPD3, HNRNPC, PRPF31, & SNRPA1
57	Actin cytoskeleton signaling	1.87E00	6.33E-02	-0.535	MYH10, PFN1, MYH9, CFL1, ACTB, TLN1, IQGAP1, DIAPH1, FLNA, EZR, MYL4, VCL, ACTN4, & MSN
58	Inosine-5'-phosphate biosynthesis II	1.86E00	1.88E-01	NaN	ADSL, PAICS, & ATIC
59	VEGF signaling	1.84E00	8.16E-02	NaN	YWHAE, ACTB, EIF2B1, VCL, ACTN4, EIF2S1, ELAVL1, & EIF2S2

60	ERK5 signaling	1.76E00	9.38E-02	NaN	YWHAQ, YWHAG, YWHAE, YWHAH, YWHAB, & YWHAZ
61	Hypoxia signaling in the cardiovascular system	1.73E00	9.23E-02	NaN	P4HB, HSP90B1, UBE2L3, HSP90AB1, HSP90AA1, & LDHA
62	Mismatch repair in eukaryotes	1.71E00	1.67E-01	NaN	PCNA, MSH2, & FEN1
63	Ketolysis	1.71E00	1.67E-01	NaN	ACAT2, HADHB, & HADHA
64	Aspartate biosynthesis	1.7E00	2.86E-01	NaN	GOT1 & GOT2
65	Mitotic roles of Polo-like kinase	1.7E00	9.09E-02	NaN	HSP90B1, PPP2R1A, HSP90AB1, CAPN1, HSP90AA1, & CDK1
66	Superpathway of serine and glycine biosynthesis I	1.65E00	1.58E-01	NaN	PSAT1, PHGDH, & SHMT2
67	Sucrose degradation V (mammalian)	1.65E00	1.58E-01	NaN	TPI1, ALDOA, & ALDOC
68	Apoptosis signaling	1.59E00	7.87E-02	-1.134	ACIN1, CAPN1, LMNA, CYCS, CDK1, PARP1, & AIFM1
69	Thioredoxin pathway	1.59E00	2.5E-01	NaN	TXN & TXNRD1
70	Glutathione redox reactions II	1.59E00	2.5E-01	NaN	GSR & PDIA3
71	Formaldehyde oxidation II (glutathione-dependent)	1.59E00	2.5E-01	NaN	ADH5 & ESD
72	Superpathway of geranylgeranyldiphosphate biosynthesis I (via mevalonate)	1.58E00	1.14E-01	NaN	ACAT2, HADHB, HMGCS1, & HADHA
73	Death receptor signaling	1.52E00	7.61E-02	0.378	ACIN1, ACTB, ZC3HAV1, LMNA, CYCS, HSPB1, & PARP1
74	RhoGDI signaling	1.49E00	6.15E-02	-0.333	GNB1, RHOG, CFL1, EZR, ACTB, GNB2L1, GDI2, MYL4, ARHGEF2, ARHGDIA, & MSN
75	Guanine and guanosine salvage I	1.49E00	2.22E-01	NaN	PNP & HPRT1
76	Adenine and adenosine salvage I	1.49E00	2.22E-01	NaN	PNP & APRT
77	Oxidized GTP and dGTP detoxification	1.49E00	2.22E-01	NaN	DDX6 & RUVBL2
78	Glutamate degradation II	1.49E00	2.22E-01	NaN	GOT1 & GOT2
79	Virus entry via endocytic pathways	1.46E00	7.37E-02	NaN	AP2A1, FLNA, FLNC, ACTB, AP2B1, CLTC, & TFRC
80	Pyruvate fermentation to lactate	1.4E00	2E-01	NaN	LDHA & LDHB
81	Tetrahydrofolate salvage from 5,10-methenyltetra-hydrofolate	1.4E00	2E-01	NaN	MTHFD1 & GART
82	Superoxide radicals degradation	1.4E00	2E-01	NaN	CAT & SOD1
83	Germ cell-Sertoli cell junction signaling	1.39E00	6.13E-02	NaN	TUBA1B, RHOG, CFL1, TUBB8, TUBB4B, ACTB, VCL, ACTN4, TUBB, & IQGAP1
84	Cyclins and cell cycle regulation	1.39E00	7.69E-02	NaN	PPP2R1A, PA2G4, CUL1, HDAC1, SKP1, & CDK1
85	UDP-*N*-acetyl-D-galactosamine biosynthesis II	1.38E00	1.25E-01	NaN	HK1, GPI, & UAP1
86	Telomerase signaling	1.37E00	7.07E-02	1.342	HSP90B1, PPP2R1A, HSP90AB1, DKC1, HDAC1, HSP90AA1, & PTGES3
87	Mechanisms of viral exit from host cells	1.36E00	9.76E-02	NaN	ACTB, XPO1, PDCD6IP, & LMNB1
88	Clathrin-mediated endocytosis signaling	1.36E00	5.85E-02	NaN	HSPA8, CD2AP, AP2A1, RAB5C, PICALM, ACTB, AP2B1, CLTC, RAB7A, TFRC, & DNM1L
89	Induction of apoptosis by HIV1	1.35E00	8.33E-02	1.342	SLC25A13, SLC25A6, SLC25A3, CYCS, & SLC25A5
90	Pentose phosphate pathway (oxidative branch)	1.32E00	1.82E-01	NaN	PGD & G6PD
91	Heme degradation	1.32E00	1.82E-01	NaN	BLVRA & BLVRB
92	L-cysteine degradation I	1.32E00	1.82E-01	NaN	GOT1 & GOT2
93	Glutathione redox reactions I	1.29E00	1.15E-01	NaN	GSR, PRDX6, & GSTK1
94	Cleavage and polyadenylation of pre-mRNA	1.25E00	1.67E-01	NaN	NUDT21 & PABPN1
95	Acetyl-CoA biosynthesis I (pyruvate dehydrogenase complex)	1.25E00	1.67E-01	NaN	DLAT & DLD
96	Breast cancer regulation by stathmin1	1.24E00	5.58E-02	NaN	GNB1, STMN1, TUBA1B, PPP2R1A, TUBB8, TUBB4B, GNB2L1, ARHGEF2, TUBB, PPP1CA, & CDK1
97	Protein kinase A signaling	1.21E00	4.77E-02	0.535	RAP1B, MYH10, YWHAG, YWHAH, YWHAE, YWHAB, PDIA3, GNB2L1, YWHAZ, TIMM50, YWHAQ, GNB1, HIST1H1E, FLNC, FLNA, MYL4, PPP1CA, APEX1, & VASP

98	Spliceosomal cycle	1.19E00	5E-01	NaN	& U2AF2
99	Hereditary breast cancer signaling	1.19E00	6.11E-02	NaN	NPM1, MSH2, ACTB, HDAC1, SMARCC1, CDK1, RAD50, & SMARCA4
100	Pentose phosphate pathway (non-oxidative branch)	1.19E00	1.54E-01	NaN	TKT & TALDO1
101	Serine biosynthesis	1.13E00	1.43E-01	NaN	PSAT1 & PHGDH
102	Calcium transport I	1.13E00	1.43E-01	NaN	ANXA5 & ATP2A2
103	Glucocorticoid receptor signaling	1.12E00	4.98E-02	NaN	YWHAH, ACTB, HSPA9, HSPA5, PTGES3, SMARCA4, HSPA8, HSPA4, HSP90B1, HSP90AB1, ANXA1, HSP90AA1, SMARCC1, & FKBP5
104	Regulation of actin-based motility by Rho	1.09E00	6.45E-02	-1.342	RHOG, PFN1, CFL1, ACTB, MYL4, & ARHGDIA
105	Signaling by Rho family GTPases	1.07E00	5.08E-02	0.333	GNB1, STMN1, RHOG, CFL1, EZR, ACTB, GNB2L1, MYL4, VIM, ARHGEF2, IQGAP1, & MSN
106	Arsenate Detoxification I (Glutaredoxin)	1.03E00	1.25E-01	NaN	PNP & GSTO1
107	Arginine Degradation VI (Arginase 2 Pathway)	1.03E00	1.25E-01	NaN	OAT & PYCR1
108	Parkinson's Signaling	1.03E00	1.25E-01	NaN	PARK7 & CYCS
109	ERK/MAPK Signaling	1.03E00	5.24E-02	0.447	RAP1B, YWHAQ, PPP2R1A, YWHAG, YWHAH, YWHAB, YWHAZ, TLN1, PPP1CA, & HSPB1
110	Ephrin B Signaling	1.01E00	6.67E-02	NaN	GNB1, CFL1, GNB2L1, CAP1, & HNRNPK
111	Role of CHK Proteins in Cell Cycle Checkpoint Control	9.87E-01	7.27E-02	NaN	PCNA, PPP2R1A, CDK1, & RAD50
112	Noradrenaline and Adrenaline Degradation	9.87E-01	7.27E-02	NaN	ADH5, HSD17B10, COMT, & ALDH1A2
113	IGF-1 Signaling	9.86E-01	6.06E-02	NaN	YWHAQ, YWHAG, YWHAE, YWHAH, YWHAB, & YWHAZ
114	UDP-*N*-acetyl-D-glucosamine Biosynthesis II	9.83E-01	1.18E-01	NaN	GFPT1 & UAP1
115	Adenine and Adenosine Salvage III	9.83E-01	1.18E-01	NaN	PNP & HPRT1
116	Valine Degradation I	9.83E-01	8.57E-02	NaN	DLD, HADHB, & HADHA
117	Role of BRCA1 in DNA damage response	9.6E-01	6.41E-02	NaN	MSH2, ACTB, SMARCC1, RAD50, & SMARCA4
118	Folate polyglutamylation	9.41E-01	1.11E-01	NaN	MTHFD1 & SHMT2
119	Acyl carrier protein metabolism	9.08E-01	2.5E-01	NaN	AASDHPPT
120	ATM signaling	9.04E-01	6.78E-02	NaN	SMC2, TRIM28, CDK1, & RAD50
121	GADD45 signaling	9.02E-01	1.05E-01	NaN	PCNA & CDK1
122	Proline biosynthesis II (from arginine)	9.02E-01	1.05E-01	NaN	OAT & PYCR1
123	Antioxidant action of vitamin C	8.97E-01	5.71E-02	NaN	SLC2A1, PDIA3, TXN, TXNRD1, GSTO1, & PRDX6
124	Superpathway of cholesterol biosynthesis	8.77E-01	6.02E-02	NaN	NSDHL, ACAT2, HADHB, HMGCS1, & HADHA
125	Pyrimidine deoxyribonucleotides *de novo* biosynthesis I	8.55E-01	7.5E-02	NaN	DUT, NME1, & RRM1
126	Glutathione-mediated detoxification	8.55E-01	7.5E-02	NaN	GSTP1, GSTO1, & GSTK1
127	Prostate cancer signaling	8.31E-01	5.81E-02	NaN	HSP90B1, PA2G4, HSP90AB1, HSP90AA1, & GSTP1
128	Sorbitol degradation I	8.18E-01	2E-01	NaN	SORD
129	Adenine and adenosine salvage VI	8.18E-01	2E-01	NaN	ADK
130	CTLA4 signaling in cytotoxic T lymphocytes	8.01E-01	5.68E-02	NaN	AP2A1, PPP2R1A, AP2B1, CLTC, & AP1G1
131	Urate biosynthesis/inosine 5'-phosphate degradation	7.68E-01	8.7E-02	NaN	IMPDH2 & PNP
132	Heme biosynthesis II	7.68E-01	8.7E-02	NaN	UROD & HMBS
133	Ethanol degradation II	7.47E-01	6.67E-02	NaN	ADH5, HSD17B10, & ALDH1A2
134	Glycine biosynthesis I	7.45E-01	1.67E-01	NaN	SHMT2
135	Tumoricidal function of hepatic natural killer cells	7.39E-01	8.33E-02	NaN	CYCS & AIFM1

136	Xenobiotic metabolism signaling	7.39E-01	4.38E-02	NaN	HSP90B1, PPP2R1A, HSP90AB1, ALDH1A2, CAT, HSP90AA1, DNAJC7, GSTP1, PTGES3, GSTO1, GSTK1, & ESD
137	Role of OCT4 in mammalian embryonic stem cell pluripotency	7.27E-01	6.52E-02	NaN	PHB, IGF2BP1, & PARP1
138	Maturity onset diabetes of young (MODY) signaling	6.86E-01	7.69E-02	NaN	PKLR & GAPDH
139	Spermidine biosynthesis I	6.85E-01	1.43E-01	NaN	SRM
140	Fatty acid biosynthesis initiation II	6.85E-01	1.43E-01	NaN	FASN
141	Integrin signaling	6.82E-01	4.48E-02	-2.333	RAP1B, RHOG, ARF4, ACTB, CAPN1, TLN1, VCL, ACTN4, & VASP
142	RhoA signaling	6.65E-01	4.84E-02	0.000	PFN1, CFL1, EZR, ACTB, MYL4, & MSN
143	Folate transformations I	6.38E-01	7.14E-02	NaN	MTHFD1 & SHMT2
144	Estrogen receptor signaling	6.35E-01	4.72E-02	NaN	PRKDC, DDX5, THRAP3, PHB2, HNRNPD, & SMARCA4
145	Trehalose degradation II (trehalase)	6.34E-01	1.25E-01	NaN	HK1
146	NADH repair	6.34E-01	1.25E-01	NaN	GAPDH
147	Methylglyoxal degradation I	6.34E-01	1.25E-01	NaN	GLO1
148	Acetyl-CoA biosynthesis III (from citrate)	6.34E-01	1.25E-01	NaN	ACLY
149	Myo-inositol biosynthesis	6.34E-01	1.25E-01	NaN	ISYNA1
150	Xanthine and xanthosine salvage	6.34E-01	1.25E-01	NaN	PNP
151	Cysteine biosynthesis/homocysteine degradation	6.34E-01	1.25E-01	NaN	CBS/CBSL
152	Asparagine biosynthesis I	6.34E-01	1.25E-01	NaN	ASNS
153	S-adenosyl-L-methionine biosynthesis	6.34E-01	1.25E-01	NaN	MAT2A
154	eNOS signaling	6.2E-01	4.52E-02	-2.000	HSPA8, HSPA4, HSP90B1, HSP90AB1, HSPA9, HSP90AA1, & HSPA5
155	Pyrimidine ribonucleotides *de novo* biosynthesis	6.07E-01	5.66E-02	NaN	NME1, CAD, & CTPS1
156	HIF1a signaling	6.03E-01	4.81E-02	NaN	SLC2A1, HSP90AA1, LDHA, APEX1, & LDHB
157	PPARα/RXRa activation	6.03E-01	4.35E-02	-2.236	CAND1, HSP90B1, HSP90AB1, PDIA3, FASN, CKAP5, HSP90AA1, & GOT2
158	Role of p14/p19ARF in tumor suppression	5.94E-01	6.67E-02	NaN	NPM1 & SF3A1
159	Creatine-phosphate biosynthesis	5.9E-01	1.11E-01	NaN	CKB
160	2-Ketoglutarate dehydrogenase complex	5.9E-01	1.11E-01	NaN	DLD
161	Branched-chain a-keto acid dehydrogenase complex	5.9E-01	1.11E-01	NaN	DLD
162	L-cysteine degradation III	5.9E-01	1.11E-01	NaN	GOT1
163	Sertoli cell-Sertoli cell junction signaling	5.87E-01	4.3E-02	NaN	EPB41, TUBA1B, TUBB8, TUBB4B, ACTB, VCL, ACTN4, & TUBB
164	Calcium signaling	5.87E-01	4.3E-02	NaN	RAP1B, MYH10, CALR, LETM1, MYH9, HDAC1, MYL4, & ATP2A2
165	Amyotrophic lateral sclerosis signaling	5.72E-01	4.67E-02	NaN	RAB5C, CAPN1, CAT, CYCS, & SOD1
166	Phenylalanine degradation IV (mammalian, *via* side chain)	5.55E-01	6.25E-02	NaN	GOT1 & GOT2
167	Ethanol degradation IV	5.36E-01	6.06E-02	NaN	ALDH1A2 & CAT
168	Heme biosynthesis from uroporphyrinogen-III I	5.16E-01	9.09E-02	NaN	UROD
169	Glutathione biosynthesis	5.16E-01	9.09E-02	NaN	GCLM
170	Rapoport-Luebering glycolytic shunt	5.16E-01	9.09E-02	NaN	PGAM1
171	Cardiac β-adrenergic signaling	5.1E-01	4.26E-02	0.000	GNB1, PPP2R1A, GNB2L1, PPP1CA, ATP2A2, & APEX1
172	RAR activation	5.08E-01	4.06E-02	NaN	ACTB, ALDH1A2, SMARCC1, RPL7A, PSMC5, SMARCA4, PARP1, & PRMT1

173	Androgen signaling	5.06E-01	4.39E-02	NaN	GNB1, HSPA4, CALR, GNB2L1, & HSP90AA1
174	Cellular effects of sildenafil (Viagra)	5.02E-01	4.23E-02	NaN	MYH10, MYH9, PABPC4, PDIA3, ACTB, & MYL4
175	Cell cycle regulation by BTG family proteins	5.01E-01	5.71E-02	NaN	PPP2R1A & PRMT1
176	Diphthamide biosynthesis	4.85E-01	8.33E-02	NaN	EEF2
177	Palmitate biosynthesis I (animals)	4.85E-01	8.33E-02	NaN	FASN
178	Ascorbate recycling (cytosolic)	4.85E-01	8.33E-02	NaN	GSTO1
179	NAD biosynthesis III	4.85E-01	8.33E-02	NaN	NAMPT
180	G protein signaling mediated by Tubby	4.85E-01	5.56E-02	NaN	GNB1 & GNB2L1
181	UVA-induced MAPK signaling	4.85E-01	4.49E-02	2.000	PDIA3, ZC3HAV1, CYCS, & PARP1
182	FAK signaling	4.75E-01	4.44E-02	NaN	ACTB, CAPN1, TLN1, & VCL
183	Purine nucleotides degradation II (aerobic)	4.7E-01	5.41E-02	NaN	IMPDH2 & PNP
184	Assembly of RNA polymerase III complex	4.57E-01	7.69E-02	NaN	SF3A1
185	Tetrapyrrole biosynthesis II	4.57E-01	7.69E-02	NaN	HMBS
186	L-DOPA degradation	4.57E-01	7.69E-02	NaN	COMT
187	Glycine cleavage complex	4.57E-01	7.69E-02	NaN	DLD
188	Arginine degradation I (arginase pathway)	4.57E-01	7.69E-02	NaN	OAT
189	GDP-mannose biosynthesis	4.57E-01	7.69E-02	NaN	GPI
190	Retinoic acid mediated apoptosis signaling	4.51E-01	4.62E-02	NaN	ZC3HAV1, CYCS, & PARP1
191	Neuregulin signaling	4.47E-01	4.3E-02	NaN	RPS6, HSP90B1, HSP90AB1, & HSP90AA1
192	DNA double-strand break repair by homologous recombination	4.32E-01	7.14E-02	NaN	RAD50
193	Proline biosynthesis I	4.32E-01	7.14E-02	NaN	PYCR1
194	dTMP *de novo* biosynthesis	4.32E-01	7.14E-02	NaN	SHMT2
195	Antiproliferative role of somatostatin receptor 2	4.3E-01	4.48E-02	NaN	RAP1B, GNB1, & GNB2L1
196	Role of PKR in interferon induction and antiviral response	4.26E-01	5E-02	NaN	CYCS & EIF2S1
197	Pyrimidine ribonucleotides interconversion	4.26E-01	5E-02	NaN	NME1 & CTPS1
198	Dopamine degradation	4.13E-01	4.88E-02	NaN	COMT & ALDH1A2
199	Prostanoid biosynthesis	4.08E-01	6.67E-02	NaN	PTGES3
200	p53 signaling	4.04E-01	4.08E-02	NaN	PRKDC, PCNA, HDAC1, & GNL3
201	Phospholipase C signaling	3.97E-01	3.67E-02	NaN	RAP1B, TGM2, PEBP1, GNB1, RHOG, GNB2L1, HDAC1, MYL4, & ARHGEF2
202	Fcγ receptor-mediated phagocytosis in macrophages and monocytes	3.96E-01	4.04E-02	-1.000	EZR, ACTB, TLN1, & VASP
203	Selenocysteine biosynthesis II (archaea and eukaryotes)	3.87E-01	6.25E-02	NaN	SARS
204	GDP-glucose biosynthesis	3.87E-01	6.25E-02	NaN	HK1
205	Paxillin signaling	3.81E-01	3.96E-02	-2.000	ACTB, TLN1, VCL, & ACTN4
206	GABA receptor signaling	3.72E-01	4.11E-02	NaN	AP2A1, UBQLN1, & AP2B1
207	Lysine degradation II	3.67E-01	5.88E-02	NaN	AASDHPPT
208	2-Oxobutanoate degradation I	3.67E-01	5.88E-02	NaN	DLD
209	5-Aminoimidazole ribonucleotide biosynthesis I	3.49E-01	5.56E-02	NaN	GART

210	Histidine degradation III	3.49E-01	5.56E-02	NaN	MTHFD1
211	D-myo-inositol (1,4,5,6)-tetrakisphosphate biosynthesis	3.43E-01	3.68E-02	NaN	SET, ATP1A1, PPP4R1, PPP1CA, & SACM1L
212	D-myo-inositol (3,4,5,6)-tetrakisphosphate biosynthesis	3.43E-01	3.68E-02	NaN	SET, ATP1A1, PPP4R1, PPP1CA, & SACM1L
213	Estrogen biosynthesis	3.43E-01	4.26E-02	NaN	HSD17B10 & HSD17B4
214	Axonal guidance signaling	3.36E-01	3.41E-02	NaN	GNB1, RAP1B, KLC1, TUBA1B, PFN1, CFL1, TUBB8, PDIA3, TUBB4B, GNB2L1, RTN4, MYL4, PSMD14, TUBB, & VASP
215	Gap junction signaling	3.33E-01	3.57E-02	NaN	TUBA1B, TUBB8, TUBB4B, PDIA3, ACTB, & TUBB
216	Uridine-5'-phosphate biosynthesis	3.32E-01	5.26E-02	NaN	CAD
217	DNA damage-induced 14-3-3σ signaling	3.32E-01	5.26E-02	NaN	CDK1
218	VDR/RXR activation	3.23E-01	3.8E-02	NaN	SERPINB1, CALB1, & PSMC5
219	Cardiac hypertrophy signaling	3.17E-01	3.45E-02	1.134	ADSS, GNB1, RHOG, PDIA3, GNB2L1, EIF2B1, MYL4, & HSPB1
220	Glucose and glucose-1-phosphate degradation	3.16E-01	5E-02	NaN	HK1
221	Purine ribonucleosides degradation to ribose-1-phosphate	3.16E-01	5E-02	NaN	PNP
222	Leukocyte extravasation signaling	3.05E-01	3.43E-02	0.000	RAP1B, EZR, ACTB, VCL, ACTN4, VASP, & MSN
223	Nitric oxide signaling in the cardiovascular system	2.99E-01	3.54E-02	2.000	HSP90B1, HSP90AB1, HSP90AA1, & ATP2A2
224	nNOS signaling in neurons	2.95E-01	3.85E-02	NaN	CAPN1 & PFKM
225	Serotonin degradation	2.87E-01	3.57E-02	NaN	ADH5, HSD17B10, & ALDH1A2
226	Zymosterol biosynthesis	2.87E-01	4.55E-02	NaN	NSDHL
227	Fatty acid a-oxidation	2.87E-01	4.55E-02	NaN	ALDH1A2
228	Semaphorin signaling in neurons	2.86E-01	3.77E-02	NaN	RHOG & CFL1
229	Lysine degradation V	2.74E-01	4.35E-02	NaN	AASDHPPT
230	Guanosine nucleotides degradation III	2.74E-01	4.35E-02	NaN	PNP
231	Glycine betaine degradation	2.74E-01	4.35E-02	NaN	SHMT2
232	Actin nucleation by ARP-WASP complex	2.62E-01	3.57E-02	NaN	RHOG & VASP
233	Estrogen-mediated S phase entry	2.62E-01	4.17E-02	NaN	CDK1
234	Arginine biosynthesis IV	2.62E-01	4.17E-02	NaN	OAT
235	D-myo-inositol-5-phosphate metabolism	2.54E-01	3.27E-02	NaN	SET, ATP1A1, PPP4R1, PPP1CA, & SACM1L
236	Crosstalk between dendritic cells and natural killer cells	2.49E-01	3.33E-02	NaN	FSCN1, ACTB, & TLN1
237	Nur77 signaling in T lymphocytes	2.47E-01	3.45E-02	NaN	HDAC1 & CYCS
238	Citrulline biosynthesis	2.39E-01	3.85E-02	NaN	OAT
239	Leucine degradation I	2.39E-01	3.85E-02	NaN	ACADM
240	TR/RXR activation	2.38E-01	3.26E-02	NaN	ENO1, SLC2A1, & FASN
241	Dopamine receptor signaling	2.38E-01	3.26E-02	NaN	PPP2R1A, COMT, & PPP1CA
242	g-Glutamyl cycle	2.19E-01	3.57E-02	NaN	GCLM
243	Adenosine nucleotides degradation II	2.19E-01	3.57E-02	NaN	PNP
244	Triacylglycerol degradation	2.01E-01	3.33E-02	NaN	PRDX6
245	Histamine degradation	2.01E-01	3.33E-02	NaN	ALDH1A2
246	Oxidative ethanol degradation III	2.01E-01	3.33E-02	NaN	ALDH1A2

Table S3. The functional networks regulated by CDDO-Me in K562 cells

ID	*Molecules in Network*	*Score*	*Focus Molecules*	*Top Diseases and Functions*
1	CAND1, IGF2BP1, LYPLA1, PA2G4, Ras, RPL3, RPL4, RPL6, RPL8, RPL11, RPL12, RPL23, RPL30, RPL7A, RPLP1, RPLP2, RPS2, RPS3, RPS5, RPS6, RPS8, RPS10, RPS11, RPS12, RPS13, RPS15, RPS16, RPS18, RPS20, RPS21, RPS24, RPS28, RPS15A, RPS3A, & VARS	55	34	RNA post-transcriptional modification, protein synthesis, & cancer
2	ABCE1, BRIX1, CARS, CUL1, cyclin B, DARS, DAZAP1, DKC1, EBNA1BP2, ECH1, EEF1G, EIF3F, EIF3L, EIF3M, EIF5B, EPRS, FARSA, G3BP1, GARS, IARS, KARS, LARS, MARS, NHP2, OLA1, QARS, RARS, Ras homolog, RBM28, RNA polymerase I, RRP12, SND1, SUPT16H, VPS35, & WDR3	49	32	Protein synthesis, gene expression, & RNA post-transcriptional modification
3	ABCF1, ARHGDIA, EIF6, ERP44, EZR, FBL, FLNC, GDI2, GNL3, HEMGN, HNRNPA3, IMPDH2, MIR124, MSN, NAT10, NOP58, NPM1, NUDC, PABPC4, PES1, PPM1G, RAB5, RAB10, RAB11, RAB5C, RAB7A, RAB8A, RAC, RCC2, Rho-GDI, RHOG, TBL3, UBA1, WDR36, & YARS	44	30	RNA post-transcriptional modification, cell morphology, & cellular assembly and organization
4	26S Proteasome, ACTB, ANXA7, estrogen receptor, FUBP1, GNB2L1, HNRNPA2B1, HSP90AA1, HSP90AB1, IGH (family), IQGAP1, KHDRBS1, MYH10, NCL, NRD1, PDGFR, PRPF19, PRPF31, RPS7, RPS9, RPS25, RTN4, SERPINB6, SLC25A3, SON, TAGLN2, trypsin, TSN, UBQLN1, VCP, VIM, YWHAB, YWHAE, YWHAG, & YWHAH	44	30	Connective tissue disorders, developmental disorder, & hereditary disorder
5	60S ribosomal subunit, ADSL, ATIC, BZW1, BZW2, CMBL, eIF, EIF2, EIF5, EIF2A, EIF2B1, EIF2S2, EIF3E, GART, HNRNPL, IGF2BP3, MAPK, PAICS, PUF60, ribosomal 40s subunit, RPL5, RPL9, RPL10, RPL13, RPL14, RPL15, RPL17, RPL18, RPL24, RPL32, RPL38, RPL10A, RPL27A, RPL37A, & SF3A3	43	30	Gene expression, protein synthesis, & amino acid metabolism
6	ABCF2, ACO2, aconitase, ALDO, ALDOA, ALDOC, AP2 a, AP2A1, AP2B1, CKB, CLTC, DDX1, DPP3, dynamin, EDC4, EHD1, FUS, G6PD, JNK, KIF2A, KLC1, LDHB, MAP1LC3, NONO, PDS5A, PGK1, PICALM, RBMX, RTCB, SERBP1, SFPQ, SRRM2, SYNCRIP, TALDO1, & TARS	42	29	Cardiovascular disease, cell death and survival, & connective tissue disorders
7	ACIN1, ALYREF, API5, CLIC1, DDX39B, EIF3, EIF3A, EIF3B, EIF3J, EIF4A, EIF4A1, EIF4A3, EIF4B, EIF4F, EIF4G, EIF4G1, EIF4H, ERK, ETF1, GSPT1, LUC7L2, NASP, NCBP1, PABPC1, PPME1, RBM39, RBM8A, SAFB, SRRT, SRSF1, SRSF3, SRSF6, SRSF7, U2AF2, & UPF1	41	30	RNA post-transcriptional modification, molecular transport, & RNA trafficking
8	ARF, ARF4, ARL1, CCDC47, COPI, COPA, COPB1, COPB2, COPG1, DDOST, DHX30, dolichyl-diphosphooligosaccharide-protein glycotransferase, DRG1, glutathione transferase, GST, GSTK1, GSTO1, GTPBP4, LUC7L3, NF-κB (complex), RAB1B, RPN2, SACM1L, SAR1A, SEC23, SEC23B, SEC24C, SEC31A, SFXN1, SRP54, SRP68, SRP72, STAU1, STT3A, & ZC3H15	40	28	Infectious diseases, post-translational modification, & developmental disorder
9	CALB1, CAPZB, CAT, CD2AP, DHX15, EFTUD2, glutathione peroxidase, GSR, HNRNPK, HSPH1, LDH (complex), MATR3, MTPN, PCBP1, PCBP2, PFKL, PFKM, phosphofructokinase, PRPF6, PRPF8, PTBP1, PTPase, SBDS, SF3A1, SF3B1, SF3B2, SF3B3, snRNP, SNRNP200, SNRPA, SNRPA1, SNRPE, SOD, SRC (family), & TCERG1	40	28	RNA post-transcriptional modification, infectious diseases, & organismal injury and abnormalities
10	AASDHPPT, AIFM1, BCLAF1, BSG, calpain, CAPN1, casein, CK1, CSDE1, FLNA, HBE1, HBG1, HBZ, hemoglobin, HNRNPD, LRRC47, methyltransferase, MMP, MPP1, NMT1, NUP93, NUP205, peroxidase (miscellaneous), PHB2, PLEC, PNN, PPIA, PRDX1, PRDX2, PRDX6, PRMT1, PRMT5, PYCR1, SLC3A2, & TPR	40	28	Connective tissue disorders, hematological disease, & organismal injury and abnormalities
11	Apoptosome, BAZ1B, CAB39, CEBPZ, cytokeratin, DDX5, DDX21, DDX46, ESD, hnRNP H, HNRNPA0, HNRNPF, HNRNPH1, HNRNPH3, HNRNPUL1, lamin b, LMNA, LMNB1, MI2, MTA, MTCH2, MYBBP1A, NuRD, OXSR1, PDAP1, & PI3K (complex), RALY, RSL1D1, SMARCA5, SMC4, SNU13, TARDBP, TOP2A, U2SURP, & YTHDF2	37	27	RNA post-transcriptional modification, cellular assembly and organization, & cell morphology
12	a-Tubulin, AP1G1, ARHGEF2, BAG2, b-tubulin, CCT2, CCT3, CCT4, CCT5, CCT7, CCT8, CCT6A, CKAP5, cytoplasmic dynein, DYNC1H1, dynein, EPB41, g-tubulin, GCN1, LRRC59, MAP1B, N-cadherin, NUMA1, p38 MAPK, PARK7, PPP2R1A, PPP4R1, TCP1, TUBA1B, TUBB, TUBB8, TUBB4B, tubulin (complex), tubulin (family), & VAPA	35	26	Cellular assembly and organization, cell-to-cell signaling and interaction, & reproductive system development and function
13	ANP32A, APEX1, DDX6, DHX9, EEF2, FKBP5, HIST1H1E, HIST1H4A, ILF2, ILF3, KU, LARP1, MCM, MCM2, MCM3, MCM4, MCM5, MCM6, MCM7, MIRLET7, NOP56, PABPN1, PRKDC, RAD50, RNR, RPA, RPS4X, RUVBL2, SET complex, SSRP1, TIP60, TOP1, VEGF, XRCC5, & XRCC6	35	27	DNA replication, recombination, and repair, protein synthesis, & cellular response to therapeutics
14	14-3-3 (β, ε, ζ), 14-3-3 (β, γ, θ, η, ζ), 14-3-3 (η, θ, ζ), CORO1C, ENO1, ESYT1, FEN1, GANAB, GAPDH, GNRH, GOT2, GPI, histone, HMGN1, HNRNPAB, IL-1, JINK1/2, LDHA, NAP1L1, NDUFS2, NDUFS3, PARP1, PCNA, PGAM1, PHB, PNP, POLb-POLe-POLg-XRCC1-LIGI-PARP1-PCNA-FEN1, PSMA3, RBM14, SET, SHMT2, SSBP1, TPI1, YWHAQ, & YWHAZ	35	27	Carbohydrate metabolism, hereditary disorder, & neurological disease

15	ADSS, AFG3L2, AK2, APRT, ARMT1, CRYZ, EIF5, GMPS, HNF4A, IKBKE, ISYNA1, LRPPRC, MAPRE1, MRPS14, OGFR, PELO, PPP4R1, RBM28, RNF2, RPS19, RPS19BP1, RPS27A, RPS4Y1, RRP1, RRP8, SEC11A, SFXN1, SLIRP, SMCHD1, SRP68, TCF, TIMM50, TMX2, TTLL12, & ZC3H15	33	25	Nucleic acid metabolism, small molecule biochemistry, & developmental disorder
16	AChR, ACLY, ARL8B, ASNS, ATP5A1, ATPase, C1q, calmodulin, chymotrypsin, COX4I1, HEATR1, IgG1, IgG3, IMMT, KIF5B, LCP1, LONP1, MSH2, MYH9, P-glycoprotein, PEBP1, PELO, PSAT1, PSMC1, PSMC5, PSMD2, PSMD3, PSMD4, PSMD11, secretase g, SERPINB1, SLC25A13, ubiquitin, UBR4, & USP14	33	25	Cellular assembly and organization, cellular function and maintenance, & cellular movement
17	AARS, adenosine tetraphosphatase, ADK, Akt, ANT, ATP synthase, ATP5B, ATP5C1, ATP5F1, ATP5O, ATP6V1G1, BLVRB, CS, EEF1B2, ETFB, F1 ATPase, FH, H^+-transporting two-sector ATPase, HARS, hexokinase, HK1, LETM1, malate dehydrogenase, MDH1, MDH2, MRE11, PDGF (family), SLC25A6, TIMM44, TKT, TOMM70A, VDAC, VDAC1, VDAC2, & WARS	31	24	Nucleic acid metabolism, small molecule biochemistry, & cellular function and maintenance
18	CBX3, CHD4, DDX17, DEK, DLAT, DLD, DNMT1, HAT, HDAC1, HDAC1/2, HIST1H3A, histone deacetylase, histone H4, HNRNPC, HNRNPM, HNRNPU, IPO4, MAT2A, N-COR, NAA15, NAA50, p85 (PIK3r), PCMT1, RAR, RBBP4, RNA polymerase III, RXR, SLIRP, SMARCC1, SNRNP70, T3-TR-RXR, thymidine kinase, thyroid hormone receptor, TMPO, & ZC3HAV1	29	23	Cancer, cellular development, & organismal injury and abnormalities
19	14-3-3, ADCY, ADRB, ANXA1, ANXA5, ATP2A2, CALU, collagen α1, FGF, FSH, GCLM, GOT1, H2AFY, HMBS, HMGCS1, HSPA4, KPNA2, KRT18, LGALS1, LH, MKI67, MRTO4, NADPH oxidase, NSDHL, PLC, RAB14, Raf, RRM1, SAPK, SRM, STIP1, TRIM28, tyrosine kinase, UBE2L3, & UROD	29	23	Dermatological diseases and conditions, cell-to-cell signaling and interaction, & cellular movement
20	AHCY, AHSA1, CALR, CANX, CCAR1, CCAR2, CD1, CD1D-CANX-CALR-ERp57, COMT, DNAJC, DNAJC7, DNAJC8, DNAJC9, EEF1D, ENaC, GADD45, HLA-B27, HSP, HSP22/HSP40/HSP90, HSP90B1, HSPA5, HYOU1, LFA-1, MHC Class I (complex), NPEPPS, P4HB, PDIA3, PDIA4, PDIA6, peptidylprolyl isomerase, PKC(s), PPIB, PTGES3, RPN1, & SUB1	29	23	Post-translational modification, protein folding, & developmental disorder
21	ACADM, ACTN4, ATP6V1A, CACYBP, caspase, CBS/CBSL, CDC37, creatine kinase, CUL4A, CYCS, DNAJA1, DNM1L, ETFA, GOT, HCFC1, HDAC, HSP27, HSP70, HSP90, HSPA8, HSPA9, HSPB1, HSPD1, IKB, IKK (complex), NAMPT, NOS, PARP, PPA1, RPL22, RSK, SKP1, SOD1, TFRC, & TXN	29	23	Post-translational modification, protein folding, & nucleic acid metabolism
22	19S proteasome, 20s proteasome, GSK3, immunoproteasome Pa28/20s, MHC CLASS I (family), MTORC2, NF-κB (family), proteasome PA700/20s, PSMA, PSMA1, PSMA2, PSMA4, PSMA5, PSMA6, PSMA7, PSMB, PSMB1, PSMB2, PSMB3, PSMB5, PSMB6, PSMB7, PSMC, PSMC2, PSMC6, PSMD, PSMD1, PSMD5, PSMD6, PSMD7, PSMD8, PSMD12, PSMD13, PSMD14, & PSMG1	28	23	Endocrine system disorders, gastrointestinal disease, & metabolic disease
23	CSE1L, ERK1/2, ERP29, ESR1-ESR1-estrogen-estrogen, histone H1, importin-a, importin-b, IPO5, IPO7, karyopherin-b, KPNA4, KPNB1, nucleoporin, NUP153, NUP160, NUP214, RAN, RAN-GTP, RANBP1, RANBP2, RANGAP1, RANGAP1-RANBP1-RANBP2-RAN-GTP, RCC1, RPL7, RPL27, RPL18A, TAP, THRAP3, TNPO1, transportin, TRAP/media, UBA2, VRK1, XPO1, & XPOT	28	23	Molecular transport, protein trafficking, & RNA trafficking
24	3-Hydroxyacyl-CoA dehydrogenase, ACAT2, acetyl-CoA C-acetyltransferase, ADH5, alcohol dehydrogenase, C1QBP, CTPS1, CYC1, cytochrome b_{c1}, cytochrome C, cytochrome-c oxidase, DECR1, GCN5L, GLO1, HADH, HADHA, HADHB, HSD17B4, HSD17B10, HSPE1, long-chain-enoyl-CoA hydratase, mediator, mitochondrial complex 1, nuclear factor 1, PKA, PKLR, PRDX3, RNH1, SKIV2L2, SLC25A5, SRPR, SWI-SNF, TUFM, UQCRC1, & UQCRC2	27	22	Energy production, lipid metabolism, & small molecule biochemistry
25	Adaptor protein 2, ATP1A1, CD3, CDK1, Cg, Ck2, clathrin, DCTPP1, DDB1, ELAVL1, GSTP1, HIST2H3A, histone H3, HPRT1, ISOC1, KHSRP, KIAA0430, MAP4, MYL4, NME1, PHGDH, PPP1CA, RAB21, RNA polymerase II, RUVBL1, SKIDA1, SMARCA4, SMC2, SNRPD3, SSB, TCR, TNF (family), TSPAN9, UAP1, & ZCRB1	27	22	DNA replication, recombination, and repair, energy production, & nucleic acid metabolism

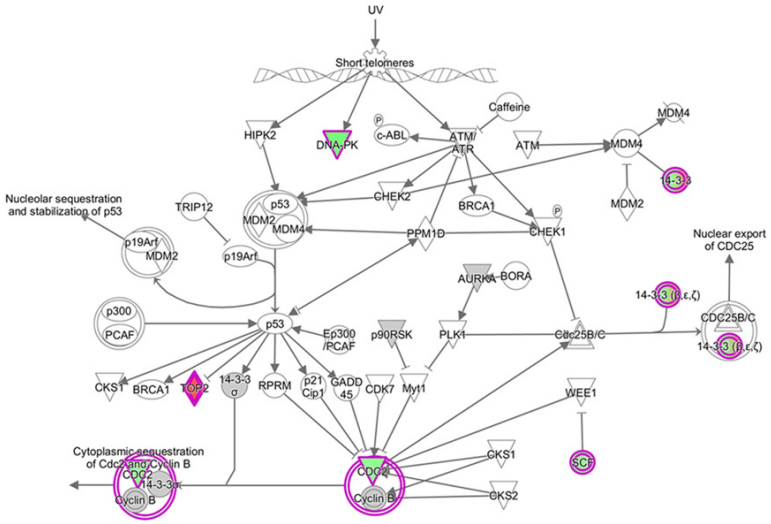

Figure S1. Cell cycle: G_2/M DNA damage checkpoint regulation signaling pathway was regulated by CDDO-Me in K562 cells. K562 cells were incubated with 0.5 μM CDDO-Me for 24 h and evaluated using the SILAC-based proteomics analysis. Red indicates an up-regulation and green indicates a down-regulation. The intensity of green and red molecule colors indicates the degree of down or up-regulation, respectively. Solid arrow indicates direct interaction and dashed arrow indicates indirect interaction.

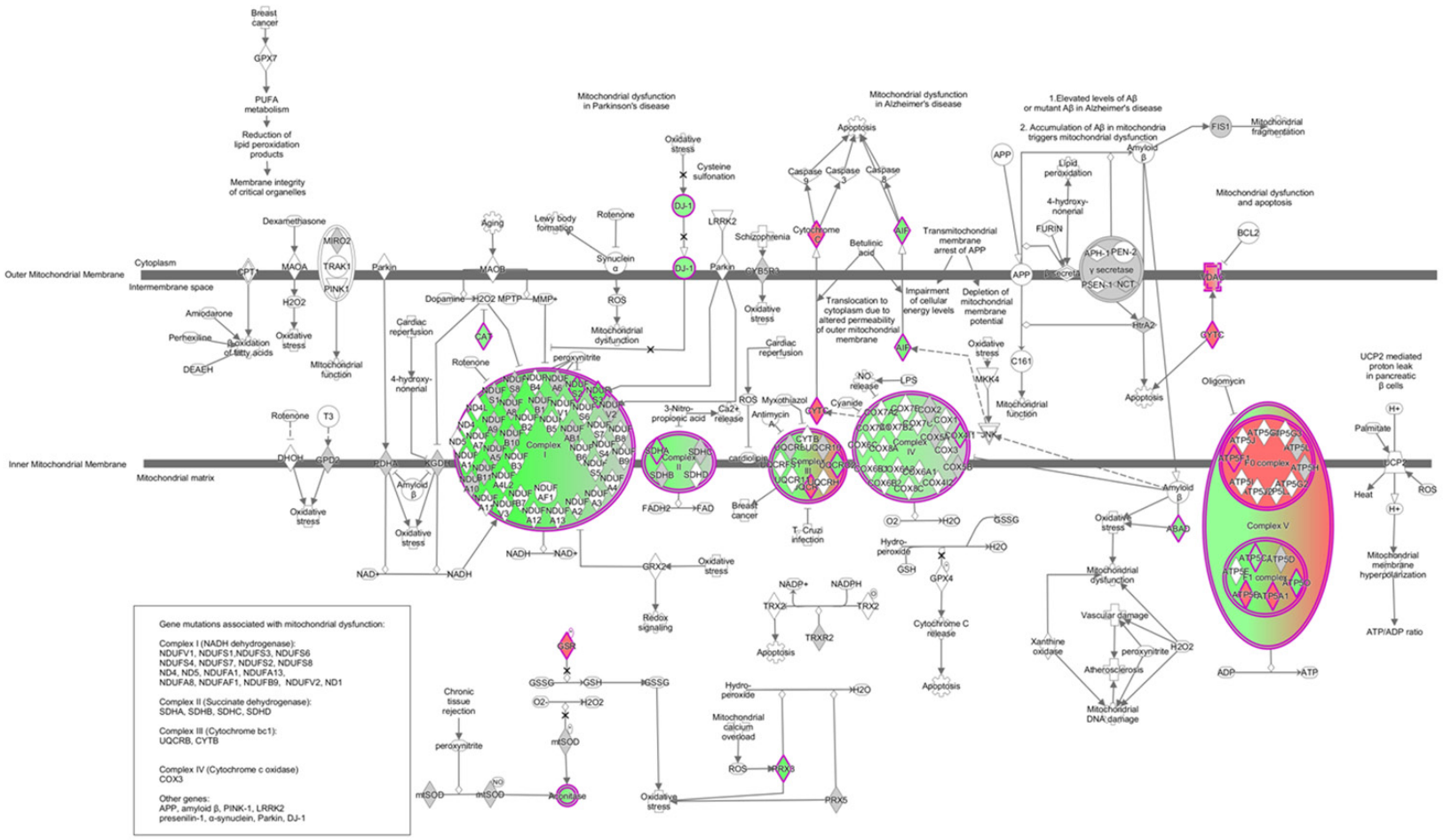

Figure S2. Mitochondrial dysfunction signaling pathway was regulated by CDDO-Me in K562 cells. K562 cells were incubated with 0.5 μM CDDO-Me for 24 h and evaluated using the SILAC-based proteomics analysis. Red indicates an up-regulation and green indicates a down-regulation. The intensity of green and red molecule colors indicates the degree of down or up-regulation, respectively. Solid arrow indicates direct interaction and dashed arrow indicates indirect interaction.

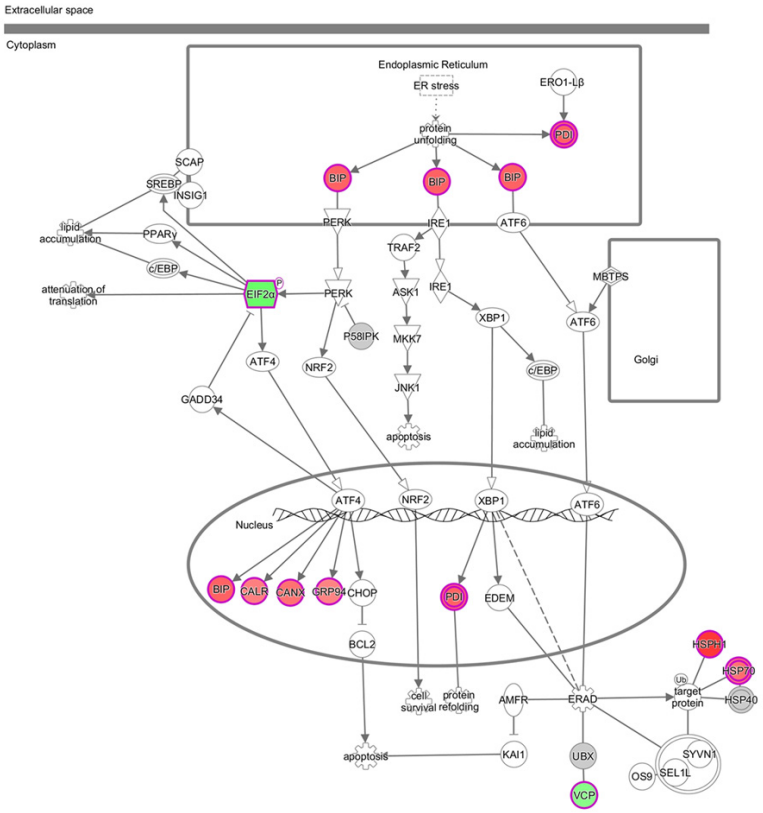

Figure S3. UPR signaling pathway was regulated by CDDO-Me in K562 cells. K562 cells were incubated with 0.5 μM CDDO-Me for 24 h and evaluated using the SILAC-based proteomics analysis. Red indicates an up-regulation and green indicates a down-regulation. The intensity of green and red molecule colors indicates the degree of down or up-regulation, respectively. Solid arrow indicates direct interaction and dashed arrow indicates indirect interaction.

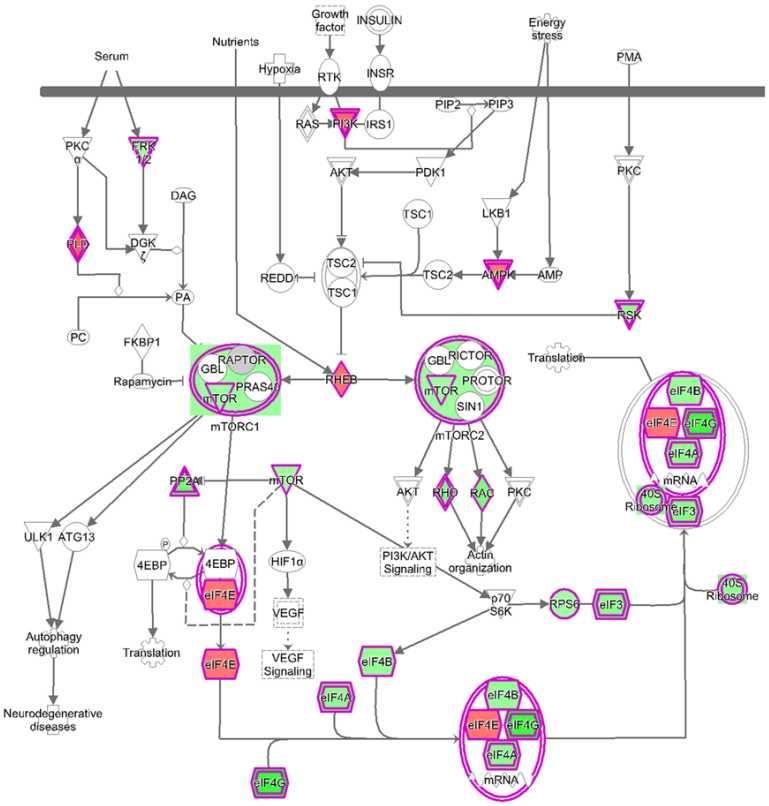

Figure S4. mTOR signaling pathway was regulated by CDDO-Me in K562 cells. K562 cells were incubated with 0.5 μM CDDO-Me for 24 h and evaluated using the SILAC-based proteomics analysis. Red indicates an up-regulation and green indicates a down-regulation. The intensity of green and red molecule colors indicates the degree of down or up-regulation, respectively. Solid arrow indicates direct interaction and dashed arrow indicates indirect interaction.